OAK RIDGE NATIONAL LABORATORY
operated by
UNION CARBIDE CORPORATION
NUCLEAR DIVISION
for the
U.S. ATOMIC ENERGY COMMISSION

HC 3.00
MF .65

ORNL - TM - 1594
COPY NO. - 259
DATE - Dec. 7, 1966

Neutron Physics Division

CALCULATIONS OF THE RADIATION HAZARD DUE TO EXPOSURE OF SUPERSONIC AIRCRAFT TO SOLAR FLARE PROTONS*

M. Leimdorfer
R. G. Alsmiller, Jr.
R. T. Boughner

ABSTRACT

Monte Carlo transport calculations have been carried out to estimate the dose which travelers in supersonic aircraft will receive from a typical spectrum of solar flare protons. This dose, from both primary protons and secondary particles, as a function of depth in a tissue slab placed at various depths in the atmosphere has been obtained. The incident spectrum is broken into eight energy regions and the dose from the incident protons in each of these regions is presented.

NOTE:

This Work Supported by
NATIONAL AERONAUTICS AND SPACE ADMINISTRATION
Under Order R-104(1)

*This paper, without App. B, will be published in Nuclear Science and Engineering.

TABLE OF CONTENTS

I. INTRODUCTION

Travelers and operating personnel in future supersonic aircraft will, at least when traveling polar routes, be subjected to a radiation hazard from solar protons and from the secondary particles produced in the atmosphere, in the aircraft, and in tissue by these protons (1). Estimates of the radiation dose at various depths in the atmosphere from primary flare protons have been given by Schaefer (2) and by Foelsche (3). Estimates of the dose from primary protons and from the low-energy secondary particles produced in the atmosphere by these protons have been given by Flamm and Lingenfelter (4).

In this paper dose results based on Monte Carlo transport calculations are presented. The calculations include contributions from the high-energy as well as the low-energy secondary neutrons and protons. The dose from primary and secondary particles has been obtained, both in rads and rems, at various depths in the atmosphere for a typical solar flare proton spectrum incident isotropically on the top of the atmopshere. Because of the lack of data on particle production at high energies, only incident protons having energies less than 450 MeV are considered. The incident spectrum has been broken into eight energy regions, and calculations have been performed separately for each of these regions in order to determine the importance of the various incident energies for producing secondary particles.

In section II various details of the calculations, such as the geometry used and the incident spectrum considered, are discussed. The results are given in section III.

II. CALCULATIONAL DETAILS

The geometry has been simplified to the case of multilayered slabs. Starting at the top of the atmosphere, we consider a slab of air Z_A g/cm^2 thick,[a] a slab of iron Z_{Fe} g/cm^2 thick, a slab of tissue 30 cm thick, a slab of iron Z_{Fe} g/cm^2 thick, and an infinite layer of air. The iron and tissue are, of course, intended to simulate the aircraft and the passengers, respectively.

The time- and energy-integrated proton flare spectrum, assumed to be incident isotropically on the top of the atmosphere, was taken to be exponential in rigidity; that is, the number of incident protons per cm^2 with energy greater than E, $P_{io}(>E)$, was expressed as

$$P_{io}(>E) = Ke^{-P(E)/P_o} , \tag{2.1}$$

$$P(E) = \frac{1}{e} [E(E + 2M)]^{\frac{1}{2}} , \tag{2.2}$$

where

E = kinetic energy,

M = proton rest energy,

e = electronic charge,

P_o,K = constants which characterize a particular flare.

In the calculation reported here, P_o was taken to be 100 MV and K was chosen so that there was one incident particle per cm^2 with energy greater than 30 MeV. With this normalization, Eq. 2.1 becomes

a. The atmospheric density is a varying function of depth. It may easily be shown from the transport equations that if depth is measured in g/cm^2, the calculations carried out here are independent of the density variations.

$$P_{io}(>E) = e^{P(30)/P_o} e^{-P(E)/P_o} . \qquad (2.3)$$

In some of the work, the number of incident particles between two definite energies is of interest. For future reference, we note that the number of incident particles per cm^2 with energy between E_1 and E_2 is

$$e^{P(30)/P_o} \left[e^{-P(E_1)/P_o} - e^{-P(E_2)/P_o} \right] . \qquad (2.4)$$

The calculations were carried out using the nucleon transport code written by Kinney (5). In this code the nonelastic cross section for nucleon-nucleus collisions and the energy and angular distribution of secondary nucleons from such collisions when the incident energy is greater than 50 MeV are taken from the intranuclear cascade calculations of Bertini (6,7). Elastic nucleon-nucleus collisions at energy greater than 50 MeV are neglected. In hydrogenous media, neutron and proton elastic collisions with hydrogen at energies greater than 50 MeV are treated using experimental data.[b]

Protons with energy less than 50 MeV are assumed to slow down and stop without undergoing nuclear collision. Neutrons with energy less than 50 MeV are transported using the neutron transport code written by Irving et al. (8,5). Elastic neutron collisions below 50 MeV are treated using

---

b. The data used are the same as those used in the Bertini calculations (6).

primarily experimental data[c] and nonelastic neutron collisions are treated using a slightly modified version of the evaporation code written by Dresner (9,5).

In the calculations reported here, only incident protons in the energy range 50 to 450 MeV are considered. For the cases considered, the low-energy (<50-MeV) incident protons are stopped in the air layer and therefore do not contribute to the dose in the tissue. The dose contribution of the secondary neutrons produced by these low-energy incident protons is small and may be neglected (12). The restriction to incident particles of less than 450 MeV arises because of the lack of data on particle production from nucleon-nucleus collisions at the higher energies. A discussion of the validity of neglecting the higher energy (>450 MeV) incident particles is given in the next section of this paper.

The dose calculations are carried out in the manner described in the work of Zerby and Kinney (13). In particular, the quality factors used here are the same as those used in this previous work.

---

c. The master cross-section tape compiled by D. C. Irving for use in the neutron transport code, together with references to the data used, is available on request from the Radiation Shielding Information Center, Oak Ridge National Laboratory. In the case of iron, this master tape contains cross-section values only for energies of less than 18 MeV. In the calculations reported here, the cross sections for iron at the higher energies were taken from reference 10, and the angular distributions from neutron-iron elastic collisions were obtained from optical model calculations (11).

III. RESULTS AND CONCLUSIONS

Calculations have been carried out for Z_A values of 22, 36, and 58 g/cm^2,[d] and for a Z_{Fe} value of 1 g/cm^2.[e] The dose as a function of depth in tissue from the primary particles, as well as from the several varieties of secondary particles, has been obtained in each case. The calculations were performed by breaking the incident spectrum into 50-MeV intervals and treating each of these energy groups separately, so the dose as a function of depth in the tissue from each of these energy groups has been obtained. The detailed information is too extensive to be presented here and will be published elsewhere (14). In this paper only the more general results will be given.

In Tables I, II, and III, the rad and rem dose averaged over 30 cm of tissue at three atmospheric depths are given for various energy ranges of the incident protons. The primary proton ionization dose is defined to be the energy deposited per gram of tissue by incident protons that have not undergone nuclear collision, and the secondary particle dose is defined to be the energy deposited per gram of tissue by all particles produced by both elastic and nonelastic nuclear collisions. The total dose from each energy group is, of course, the sum of the primary proton ionization dose and the secondary particle dose. The calculations were carried out using the spectrum given by Eq. 2.3, and within each energy group the normalization given by Eq. 2.4 was used so the values in a given

---

d. These Z_A values correspond approximately to altitudes of 85,000, 75,000, and 65,000 ft, respectively.

e. In one special case, discussed in Appendix A, a Z_{Fe} value of 5 g/cm^2 was used.

Table I. Dose Averaged Over 30 cm of Tissue for $Z_A = 22$ g/cm^2 and $Z_{Fe} = 1$ g/cm^2

(One proton per cm^2 with energy >30 MeV isotropically incident on top of the atmosphere.)

Incident Proton Energy Interval (MeV)	Rad Dose			Rem Dose		
	Primary Protons Ionization	Secondary Particles	Total	Primary Protons Ionization	Secondary Particles	Total
50-100	0.00	7.75×10^{-12}	7.75×10^{-12}	0.00	2.69×10^{-11}	2.69×10^{-11}
100-150	0.00	1.24×10^{-11}	1.24×10^{-11}	0.00	6.88×10^{-11}	6.88×10^{-11}
150-200	1.18×10^{-11}	1.25×10^{-11}	2.43×10^{-11}	1.55×10^{-11}	5.50×10^{-11}	7.05×10^{-11}
200-250	1.00×10^{-10}	1.53×10^{-11}	1.15×10^{-10}	1.18×10^{-10}	5.48×10^{-11}	1.73×10^{-10}
250-300	7.76×10^{-11}	1.73×10^{-11}	9.49×10^{-11}	8.59×10^{-11}	5.54×10^{-11}	1.41×10^{-10}
300-350	4.39×10^{-11}	1.56×10^{-11}	5.95×10^{-11}	4.65×10^{-11}	4.20×10^{-11}	8.85×10^{-11}
350-400	1.96×10^{-11}	1.05×10^{-11}	3.01×10^{-11}	2.02×10^{-11}	2.67×10^{-11}	4.69×10^{-11}
400-450	8.84×10^{-12}	6.54×10^{-12}	1.54×10^{-11}	9.01×10^{-12}	1.55×10^{-11}	2.45×10^{-11}
50-450	2.62×10^{-10}	9.79×10^{-11}	3.60×10^{-10}	2.95×10^{-10}	3.45×10^{-10}	6.40×10^{-10}

Table II. Dose Averaged Over 30 cm of Tissue for $Z_A = 36$ g/cm^2 and $Z_{Fe} = 1$ g/cm^2

(One proton per cm^2 with energy >30 MeV isotropically incident on top of the atmosphere.)

Incident Proton Energy Interval (MeV)	Rad Dose			Rem Dose		
	Primary Protons Ionization	Secondary Particles	Total	Primary Protons Ionization	Secondary Particles	Total
50-100	0.00	4.28×10^{-12}	4.28×10^{-12}	0.00	1.84×10^{-11}	1.84×10^{-11}
100-150	0.00	7.76×10^{-12}	7.76×10^{-12}	0.00	3.94×10^{-11}	3.94×10^{-11}
150-200	0.00	7.97×10^{-12}	7.97×10^{-12}	0.00	3.76×10^{-11}	3.76×10^{-11}
200-250	1.53×10^{-12}	6.16×10^{-12}	7.69×10^{-12}	1.99×10^{-12}	2.59×10^{-11}	2.79×10^{-11}
250-300	2.56×10^{-11}	6.51×10^{-12}	3.21×10^{-11}	3.01×10^{-11}	2.49×10^{-11}	5.50×10^{-11}
300-350	2.49×10^{-11}	7.81×10^{-12}	3.27×10^{-11}	2.76×10^{-11}	2.40×10^{-11}	5.16×10^{-11}
350-400	1.52×10^{-11}	7.27×10^{-12}	2.25×10^{-11}	1.60×10^{-11}	1.87×10^{-11}	3.47×10^{-11}
400-450	7.09×10^{-12}	4.76×10^{-12}	1.19×10^{-11}	7.30×10^{-12}	1.22×10^{-11}	1.95×10^{-11}
50-450	7.43×10^{-11}	5.25×10^{-11}	1.27×10^{-10}	8.30×10^{-11}	2.01×10^{-10}	2.84×10^{-10}

Table III. Dose Averaged Over 30 cm of Tissue for $Z_A = 58$ g/cm^2 and $Z_{Fe} = 1$ g/cm^2

(One proton per cm^2 with energy >30 MeV isotropically incident on top of the atmosphere.)

Incident Proton Energy Interval (MeV)	Rad Dose			Rem Dose		
	Primary Protons Ionization	Secondary Particles	Total	Primary Protons Ionization	Secondary Particles	Total
50-100	0.00	3.24×10^{-12}	3.24×10^{-12}	0.00	1.34×10^{-11}	1.34×10^{-11}
100-150	0.00	5.07×10^{-12}	5.07×10^{-12}	0.00	2.43×10^{-11}	2.43×10^{-11}
150-200	0.00	5.30×10^{-12}	5.30×10^{-12}	0.00	2.18×10^{-11}	2.18×10^{-11}
200-250	0.00	4.54×10^{-12}	4.54×10^{-12}	0.00	1.95×10^{-11}	1.95×10^{-11}
250-300	0.00	3.03×10^{-12}	3.03×10^{-12}	0.00	1.34×10^{-11}	1.34×10^{-11}
300-350	2.64×10^{-12}	2.65×10^{-12}	5.29×10^{-12}	3.23×10^{-12}	1.07×10^{-11}	1.39×10^{-11}
350-400	5.86×10^{-12}	2.50×10^{-12}	8.40×10^{-12}	6.60×10^{-12}	7.85×10^{-12}	1.44×10^{-11}
400-450	4.43×10^{-12}	2.38×10^{-12}	6.81×10^{-12}	4.76×10^{-12}	6.45×10^{-12}	1.12×10^{-11}
50-450	1.29×10^{-11}	2.87×10^{-11}	4.16×10^{-11}	1.46×10^{-11}	1.17×10^{-10}	1.32×10^{-10}

column are additive.[f] At the bottom of each column the sum over all energy groups is given.

The doses summed over all energy groups and multiplied by the number of incident protons per cm^2 may be taken as an estimate of the doses from the incident flare. A rough estimate of the error introduced by neglecting the incident particles with energy greater than 450 MeV may be obtained by assuming that a higher energy particle will contribute approximately the same amount as a particle in the energy interval 400 to 450 MeV. Thus, if one takes the total dose contribution in rads or rems given in the tables for the energy interval 400 to 450 MeV and multiplies by the factor

$$\frac{e^{P(30)/100}\, e^{-P(450)/100}}{e^{P(30)/100}\left[e^{-P(400)/100} - e^{P(450)/100}\right]},$$

one obtains an estimate of the contribution of the neglected higher energy particles. This factor has a value of approximately unity and therefore

f. Strictly speaking, the values in the tables are valid only for an incident spectrum with P_o equal to 100 MV. However, if one assumes that the shape of the spectrum within a 50-MeV interval is not crucial, then approximate dose values for other P_o values may be obtained by renormalization. To obtain approximate values for an incident spectrum with a characteristic rigidity P_o', one multiplies the values in the table by

$$\frac{e^{P(30)/P_o'}\left[e^{-P(E_1)/P_o'} - e^{-P(E_2)/P_o'}\right]}{e^{P(30)/P_o}\left[e^{-P(E_1)/P_o} - e^{-P(E_2)/P_o}\right]},$$

where P_o equals 100 MV and E_1 and E_2 are the lower and upper limits, respectively, of the energy intervals in the tables.

the dose contribution of the particles in the energy interval 400 to 450 MeV may be taken as a rough estimate of the dose contribution of the incident particles with energy greater than 450 MeV. On the basis of this estimate, the contribution of the higher energy particles is not negligible but is probably not as significant as the contribution of the low-energy incident particles, at least for the shield thicknesses considered here. It is to be noted that the contribution of the higher energy particles becomes more appreciable as the shield thickness increases.

The doses summed over all energy intervals, given in the tables as well as later in this paper, may be taken as estimates of the dose that passengers will receive when a supersonic aircraft is traveling in the vicinity of the earth's magnetic poles where the earth's magnetic field does not prevent the low-energy protons from entering the atmosphere. Some information on the doses at other latitudes may be obtained by omitting the appropriate low-energy contributions shown in the tables. When this is done, however, the high-energy contribution that has been neglected becomes more significant, and thus only a very limited amount of information can be obtained.

In Fig. 1 the rad doses for Z_A = 36 g/cm^2 are given as a function of depth in the tissue, while in Figs. 2, 3, and 4 the rem doses are given as a function of depth in the tissue for Z_A = 22, 36, and 58 g/cm^2, respectively. For comparison purposes, the dose is broken into a large number of constituent parts. A primary proton is defined to be an incident proton which has undergone ionization stopping but neither elastic nor nonelastic nuclear collision. All particles produced by either elastic or nonelastic nuclear collision of the incident protons are considered

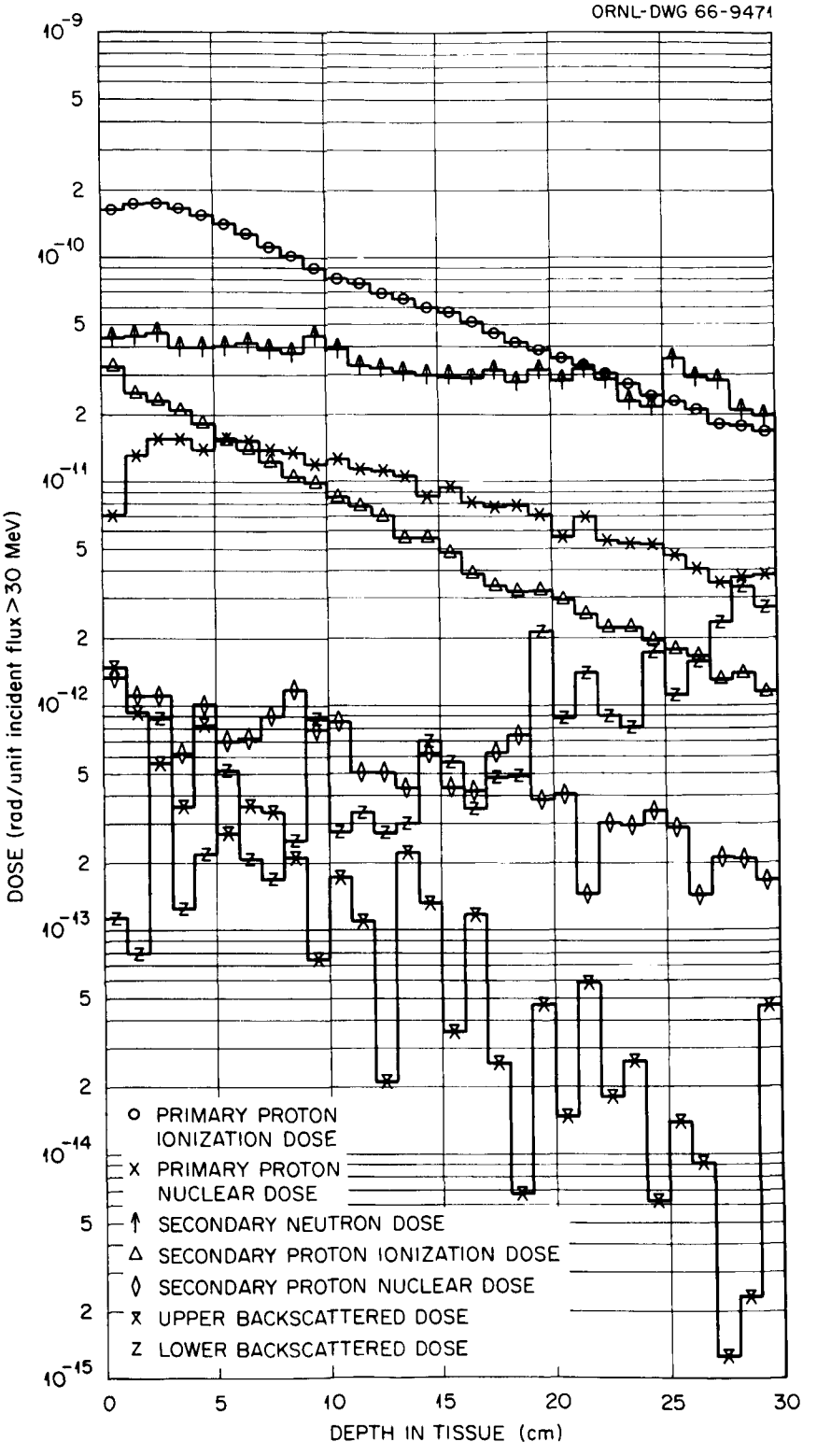

Fig. 1. Rad Dose vs Depth in Tissue for Atmospheric Depth of 36 g/cm^2 (~ 75,000 ft).

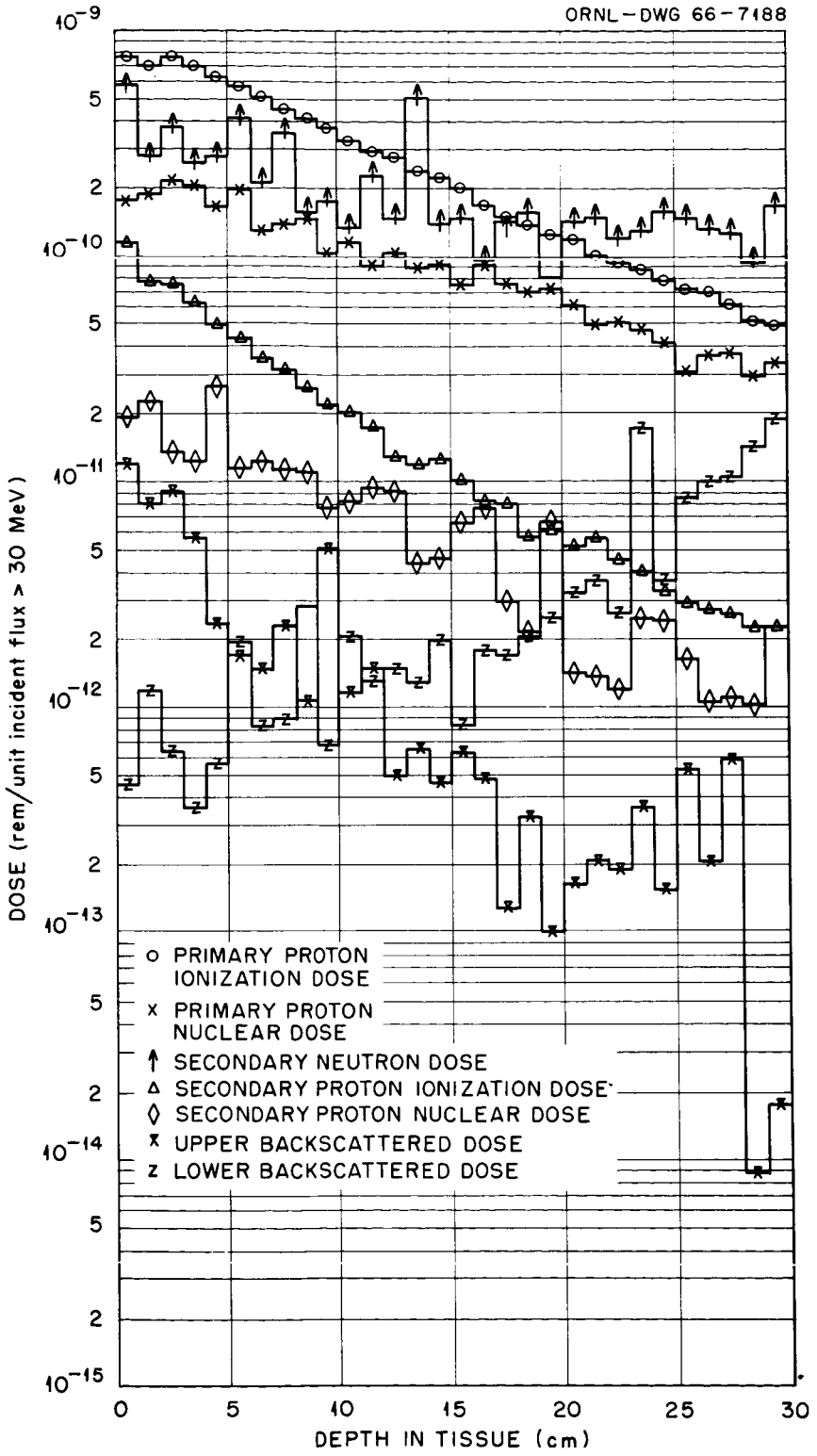

Fig. 2. Rem Dose vs Depth in Tissue for Atmospheric Depth of 22 g/cm^2 (~ 85,000 ft).

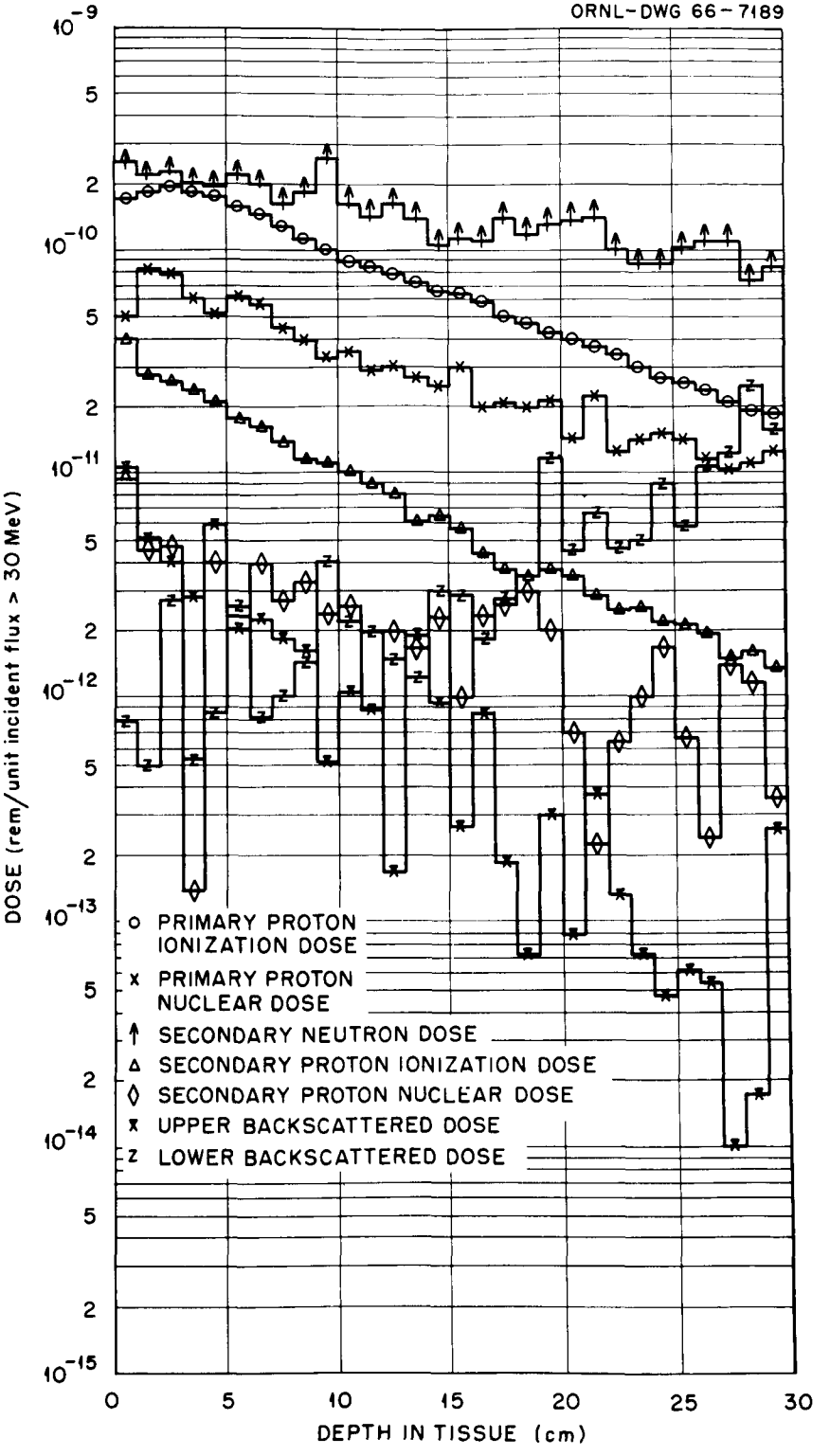

Fig. 3. Rem Dose vs Depth in Tissue for Atmospheric Depth of 36 g/cm^2 (~ 75,000 ft).

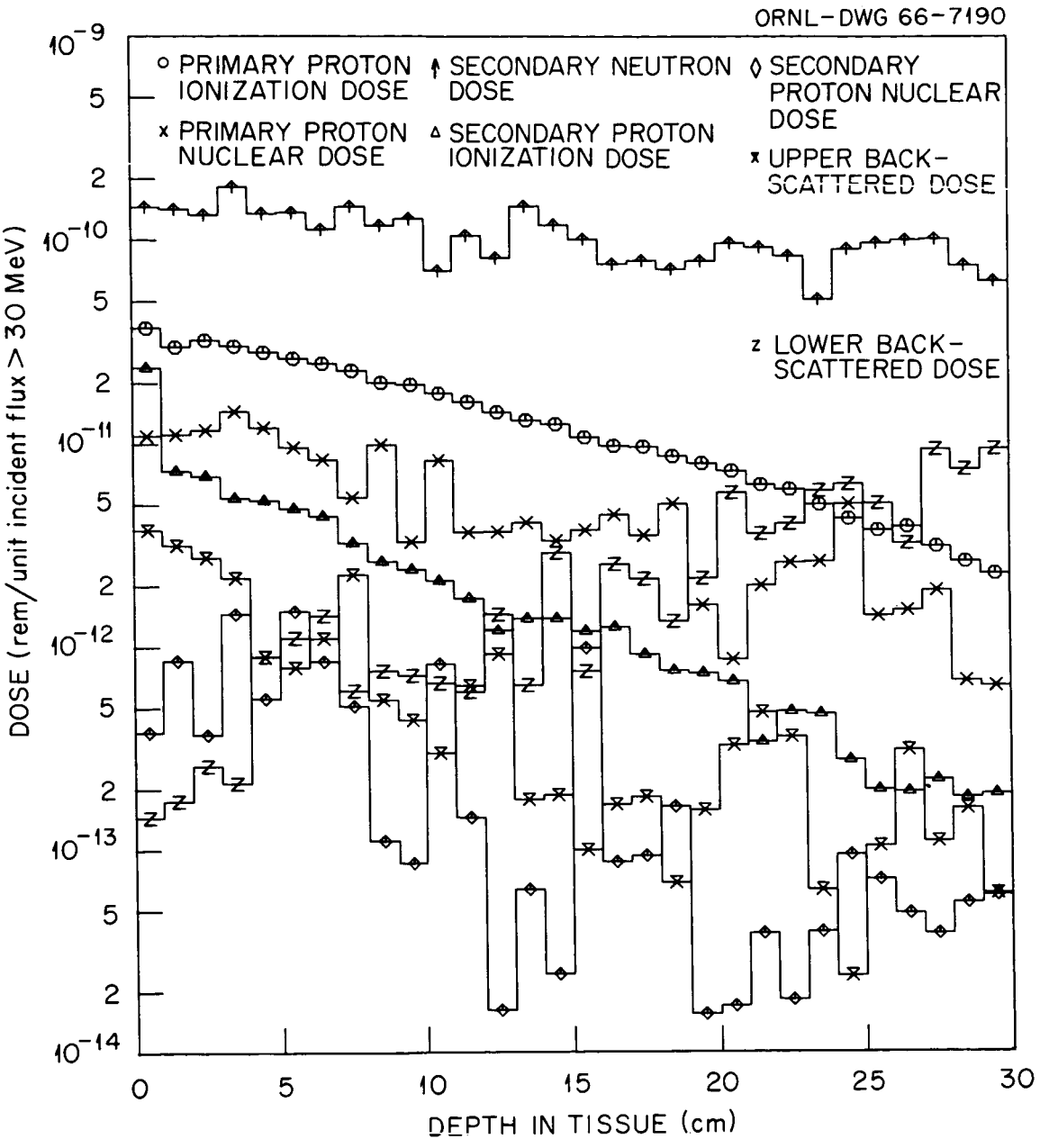

Fig. 4. Rem Dose vs Depth in Tissue for Atmospheric Depth of 58 g/cm^2 (~ 65,000 ft).

to be secondary particles. The primary proton, the secondary proton, and the secondary neutron fluxes are defined to be those which would exist at the upper iron-tissue interface if the tissue and the material below the tissue were replaced by vacuum. The primary proton ionization dose is the energy deposition per gram of tissue due to the ionization and excitation of tissue atoms by primary protons. The primary proton nuclear dose is the energy deposited per gram of tissue by all particles produced in the tissue by the nuclear collision of primary protons. The secondary proton ionization dose and nuclear dose are defined in the same manner as the corresponding primary proton quantities. The upper backscattered dose is the energy deposited per gram of tissue by all particles which cross from the tissue into the upper layer of iron. The lower backscattered dose is the energy deposited per gram of tissue by all particles which cross from the lower layer of iron into the tissue. The total dose is, of course, obtained by summing all seven histograms in each figure.

In Fig. 1, where the rad dose is considered, the primary proton ionization dose constitutes the major part of the dose over most of the tissue depth. The secondary neutron dose is the next most important contribution and is notable because it is essentially flat. The secondary proton ionization dose is not negligible in the first few centimeters of tissue but rapidly becomes so as one goes to the larger tissue depths. The secondary proton nuclear dose, the upper backscattered dose, and the lower backscattered dose are negligible.

It is interesting to compare Figs. 1 and 3, where the rad and rem doses, respectively, are given for the same geometry. The primary proton ionization dose is essentially the same in rads and rems while the neu-

tron dose is appreciably higher in rems. As a consequence, the secondary neutrons contribute appreciably to the total rem dose. It should also be noted that the primary proton nuclear dose is considerably larger in rems than in rads.

In proceeding from Fig. 2 to Fig. 4, one considers progressively thicker air shields and finds that the secondary neutron contribution becomes increasingly more significant. In Fig. 2 the primary proton ionization dose, the primary proton nuclear dose, and the secondary neutron dose all contribute appreciably to the total dose. In Fig. 4 the secondary neutrons contribute a large fraction of the total dose and the primary protons contribute only a small amount. In all three figures, the secondary proton doses and the upper and lower backscattered doses are small.

REFERENCES

1. A report of the ICRP Task Group, "Radiobiological Aspects of the Supersonic Transport," Health Phys., 12, 209 (1966).

2. H. J. SCHAEFER, "Depth of Penetration of Solar Protons into the Atmosphere and Related Radiation Exposure in Supersonic Transport," Aerospace Medicine, 34, 1-4 (1963).

3. T. FOELSCHE, "Radiation Exposure in Supersonic Transports," Langley Research Center, NASA, TND-1383 (1962).

4. E. J. FLAMM and R. E. LINGENFELTER, "Neutron and Proton Dosages in the Upper Atmosphere from Solar Flare Radiation," Science, 144, 1566-1569 (1964).

5. W. E. KINNEY, "The Nucleon Transport Code, NTC," ORNL-3610, Oak Ridge National Laboratory (1964).

6. H. W. BERTINI, "Low-Energy Intranuclear Cascade Calculations," Phys. Rev., 131, 1801 (1963), with erratum Phys. Rev., 138, AB2 (1965).

7. H. W. BERTINI, "Results from Low-Energy Intranuclear Cascade Calculations," ORNL-TM-1225, Oak Ridge National Laboratory (1965).

8. D. C. IRVING et al., "05R, A General Purpose Monte Carlo Neutron Transport Code," ORNL-3622, Oak Ridge National Laboratory (1965).

9. L. DRESNER, "EVAP - A Fortran Program for Calculating the Evaporation of Various Particles from Excited Compound Nuclei," ORNL-TM-196, Oak Ridge National Laboratory (1961).

10. D. J. HUGHES and R. B. SCHWARTZ, "Neutron Cross Sections," BNL-325, 2nd ed., Brookhaven National Laboratory (1958).

11. D. C. IRVING, personal communication (1966).

12. D. C. IRVING et al., "The Secondary Particle Contribution to the Dose from Solar Flare Protons Incident Isotropically on Slab Shields," Nucl. Sci. Eng., 25, 373 (1966).

13. C. D. ZERBY and W. E. KINNEY, "Calculated Tissue Current-to-Dose Conversion Factors for Nucleons Below 400 MeV," Nucl. Instr. and Methods, 36, 125 (1965).

14. M. LEIMDORFER, R. G. ALSMILLER, Jr., and R. T. BOUGHNER, "Calculations of the Radiation Hazard Due to Exposure of Supersonic Aircraft to Solar Flare Protons," ORNL-TM-1594, Oak Ridge National Laboratory (to be published).

APPENDIX A.

In all of the calculations discussed in the body of the paper, the same thicknesses of iron were used, and no attempt was made to determine whether the iron layers had an appreciable effect on the results. The two iron slabs are, of course, a very crude approximation to an actual aircraft which will have a very uneven mass distribution and will contain, at least in some regions, very large masses of iron. In order to get at least a partial answer to the question of whether or not large masses of iron will change the results, one calculation has been performed using $Z_A = 32$ g/cm^2 and $Z_{Fe} = 5$ g/cm^2.

In this calculation only particles in the energy range 350 to 400 MeV are considered. The portion of the spectrum given in Eq. 2.3 between 350 and 400 MeV was taken to be incident isotropically on the top of the atmosphere. For these incident particles the rem doses, averaged over 30 cm of tissue, for the case $Z_A = 32$ g/cm^2, $Z_{Fe} = 5$ g/cm^2, and for the case $Z_A = 36$ g/cm^2, $Z_{Fe} = 1$ g/cm^2, are shown in Table A1. The various doses in the table have the same definition as before. These two cases are comparable in the sense that they both have the same total amount of material in g/cm^2 above the tissue.

The results for the two cases are very similar. In almost all cases, the differences are sufficiently small that they may be ascribed to statistical fluctuations. The difference in the secondary neutron doses may be real and not statistical but these differences are too small to be of significance in the total dose. For this very special case at least, the difference between iron and air has a negligible effect on the dose.

Table A1. Rem Dose Averaged Over 30 cm of Tissue from Incident Protons in the Energy Interval 350-400 MeV for Z_A = 32 g/cm^2 and Z_{Fe} = 5 and 1 g/cm^2

(One proton per cm^2 with energy >30 MeV isotropically incident on top of the atmosphere.)

Dose Component	Rem Dose	
	Z_{Fe} = 5 g/cm^2	Z_{Fe} = 1 g/cm^2
Primary Proton Ionization Dose	1.56×10^{-11}	1.60×10^{-11}
Primary Proton Nuclear Dose	9.34×10^{-12}	9.51×10^{-12}
Secondary Proton Ionization Dose	2.92×10^{-12}	3.08×10^{-12}
Secondary Proton Nuclear Dose	7.57×10^{-13}	7.51×10^{-13}
Secondary Neutron Dose	5.59×10^{-14}	5.02×10^{-12}
Upper Backscattered Dose	3.98×10^{-14}	6.35×10^{-14}
Lower Backscattered Dose	7.24×10^{-14}	2.98×10^{-13}
Total	3.43×10^{-11}	3.47×10^{-11}

APPENDIX B.

In this appendix the detailed results obtained by breaking the incident flare spectrum into eight 50-MeV intervals are given. In all of the calculations, the incident spectrum given in Eq. 2.3 was used with P_o = 100 MV. The normalization within each energy interval, therefore, is that given in Eq. 2.4.

The results are given in Figs. B.1 to B.48. In Figs. B.1 to B.8 the rad doses for the case Z_A = 22 g/cm^2, Z_{Fe} = 1 g/cm^2 are given, while in Figs. B.9 to B.16 the rem doses for this case are given. In Figs. B.17 to B.24 the rad doses for the case Z_A = 36 g/cm^2, Z_{Fe} = 1 g/cm^2 are given, while in Figs. B.25 to B.32 the rem doses, respectively, are given for the case Z_A = 36 g/cm^2, Z_{Fe} = 1 g/cm^2.

The various doses have, of course, the same definitions as in the body of the paper. The legend is the same for all graphis and is as follows:

= Primary proton ionization dose,

X = Primary proton nuclear dose;

= Secondary neutron dose;

= Secondary proton ionization dose;

= Secondary proton nuclear dose;

X = Upper backscattered dose;

Z = Lower backscattered dose.

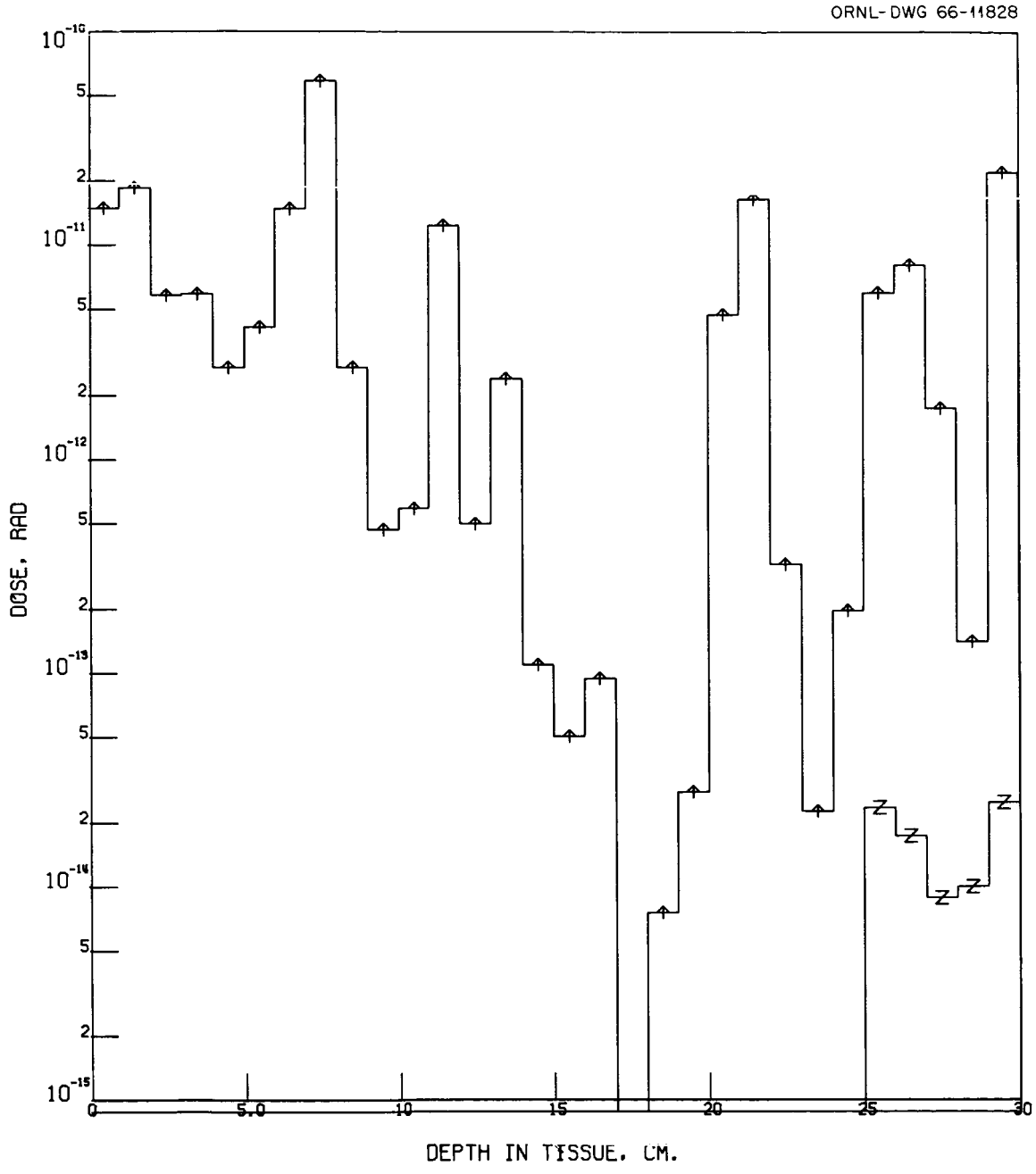

Fig. B1. Rad Dose Due to 50- to 100-MeV Incident Protons as a Function of Depth in Tissue for Z_A = 22 g/cm^2 and Z_{Fe} = 1 g/cm^2.

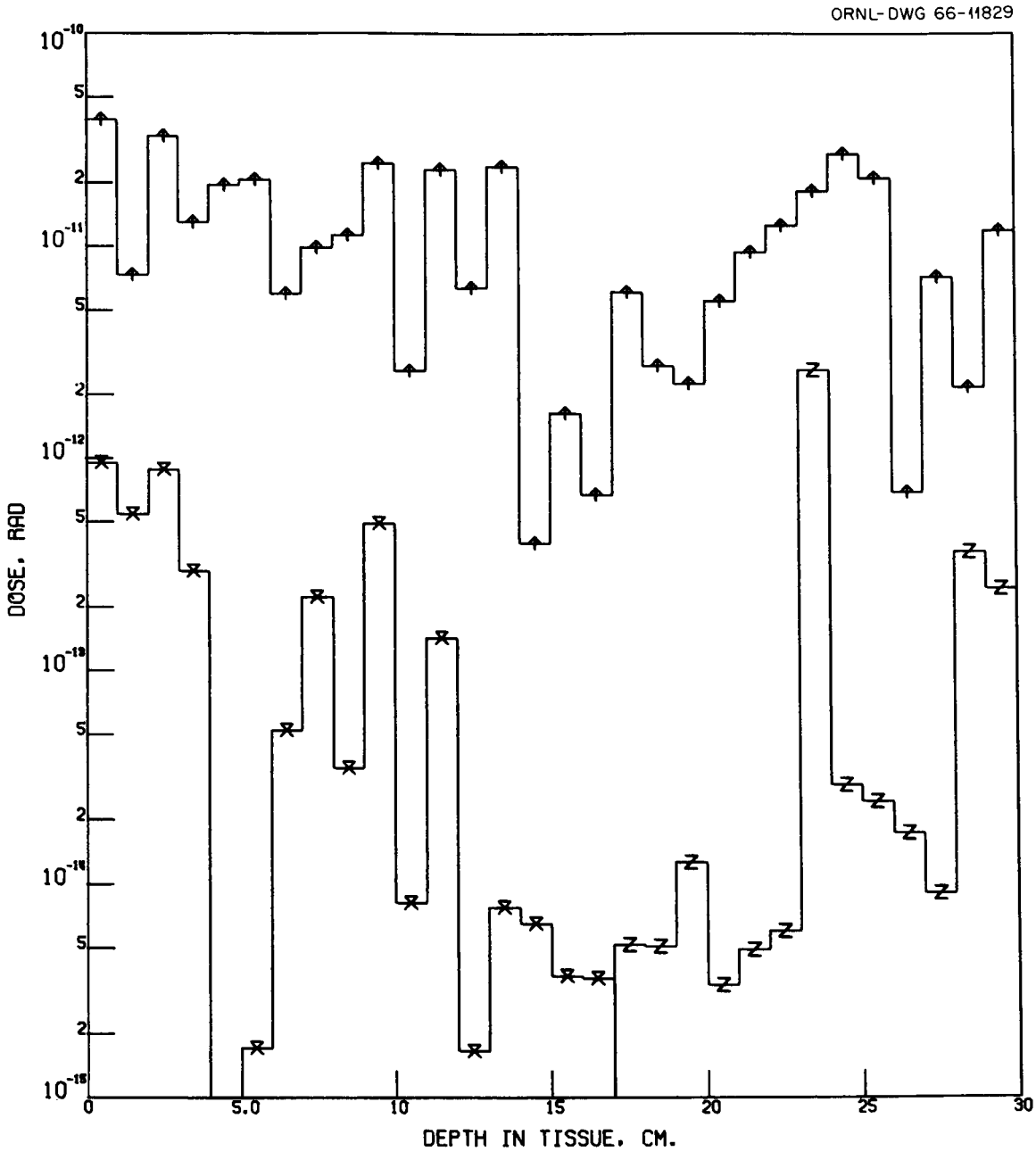

Fig. B2. Rad Dose Due to 100- to 150-MeV Incident Protons as a Function of Depth in Tissue for Z_A = 22 g/cm^2 and Z_{Fe} = 1 g/cm^2.

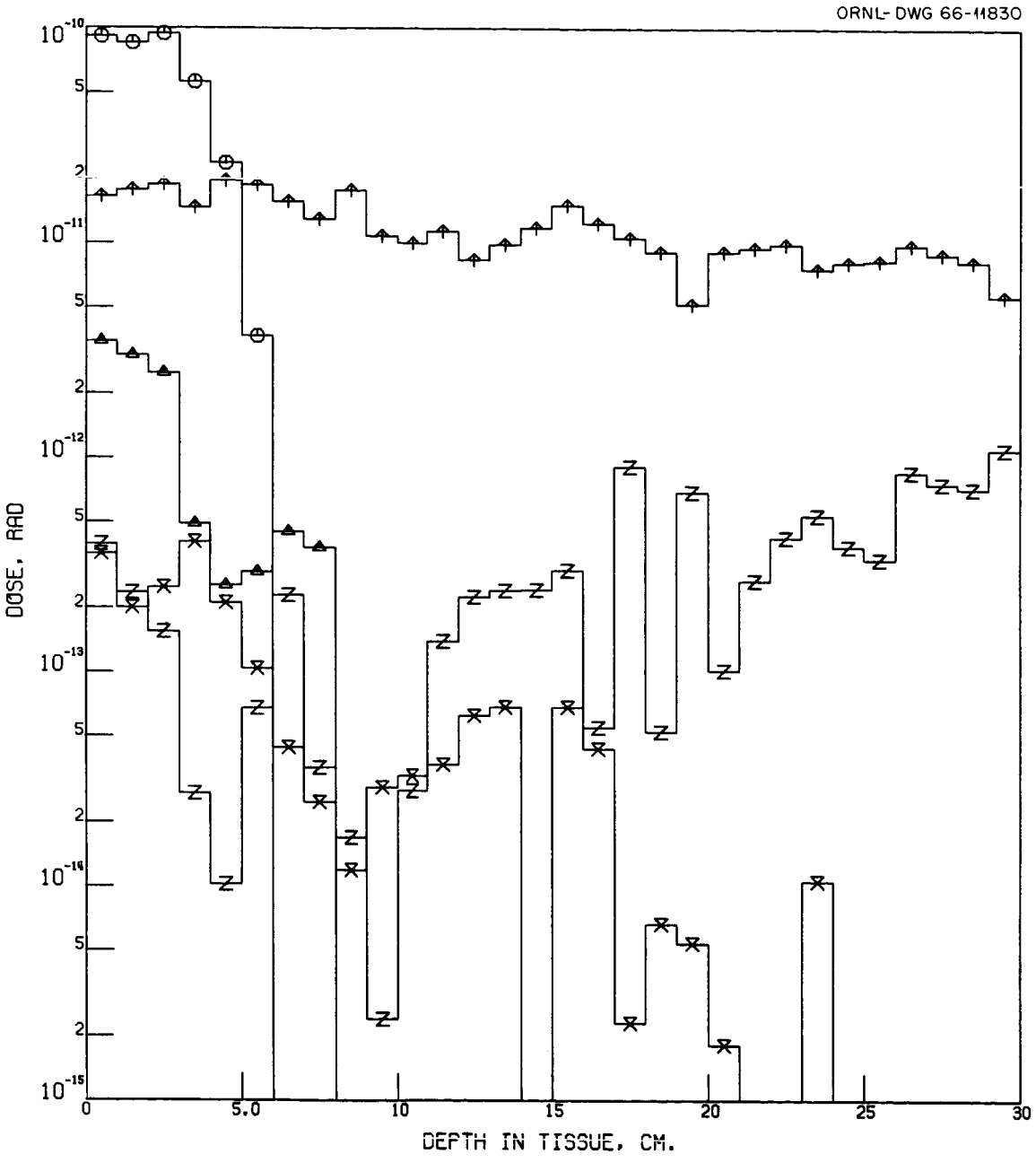

Fig. B3. Rad Dose Due to 150- to 200-MeV Incident Protons as a Function of Depth in Tissue for Z_A = 22 g/cm^2 and Z_{Fe} = 1 g/cm^2.

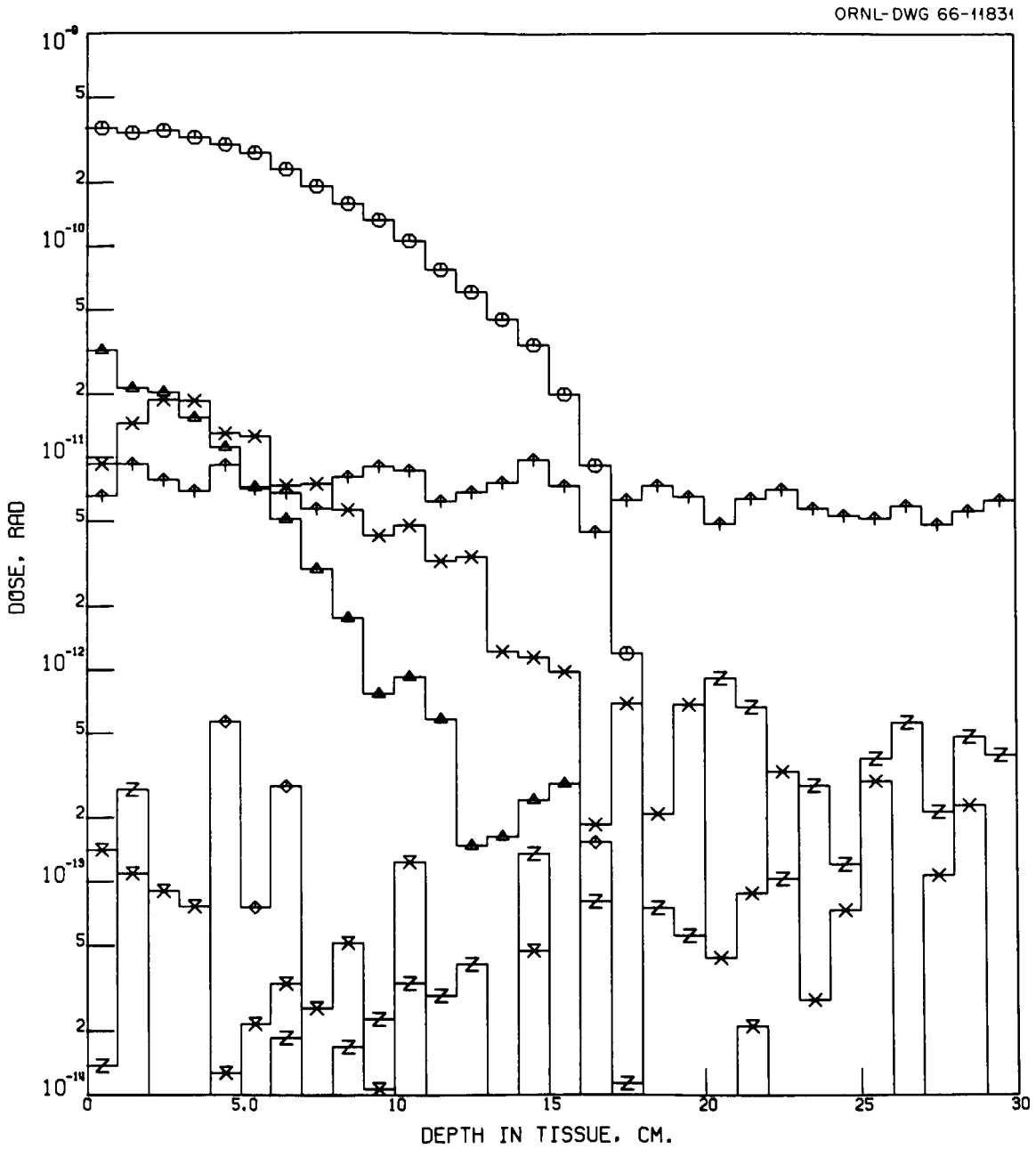

Fig. B4. Rad Dose Due to 200- to 250-MeV Incident Protons as a Function of Depth in Tissue for Z_A = 22 g/cm^2 and Z_{Fe} = 1 g/cm^2.

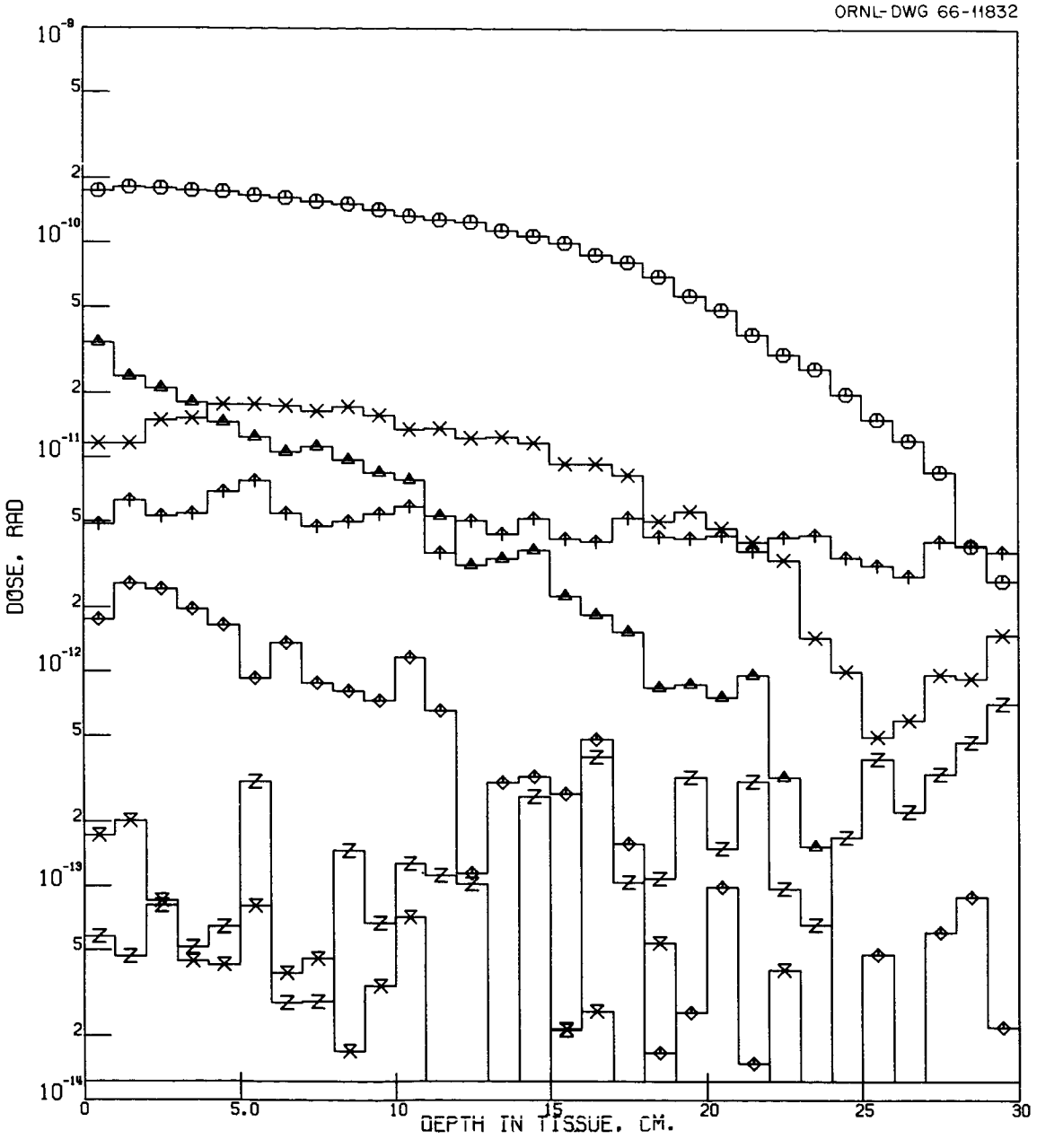

Fig. B5. Rad Dose Due to 250- to 300-MeV Incident Protons as a Function of Depth in Tissue for Z_A = 22 g/cm^2 and Z_{Fe} = 1 g/cm^2.

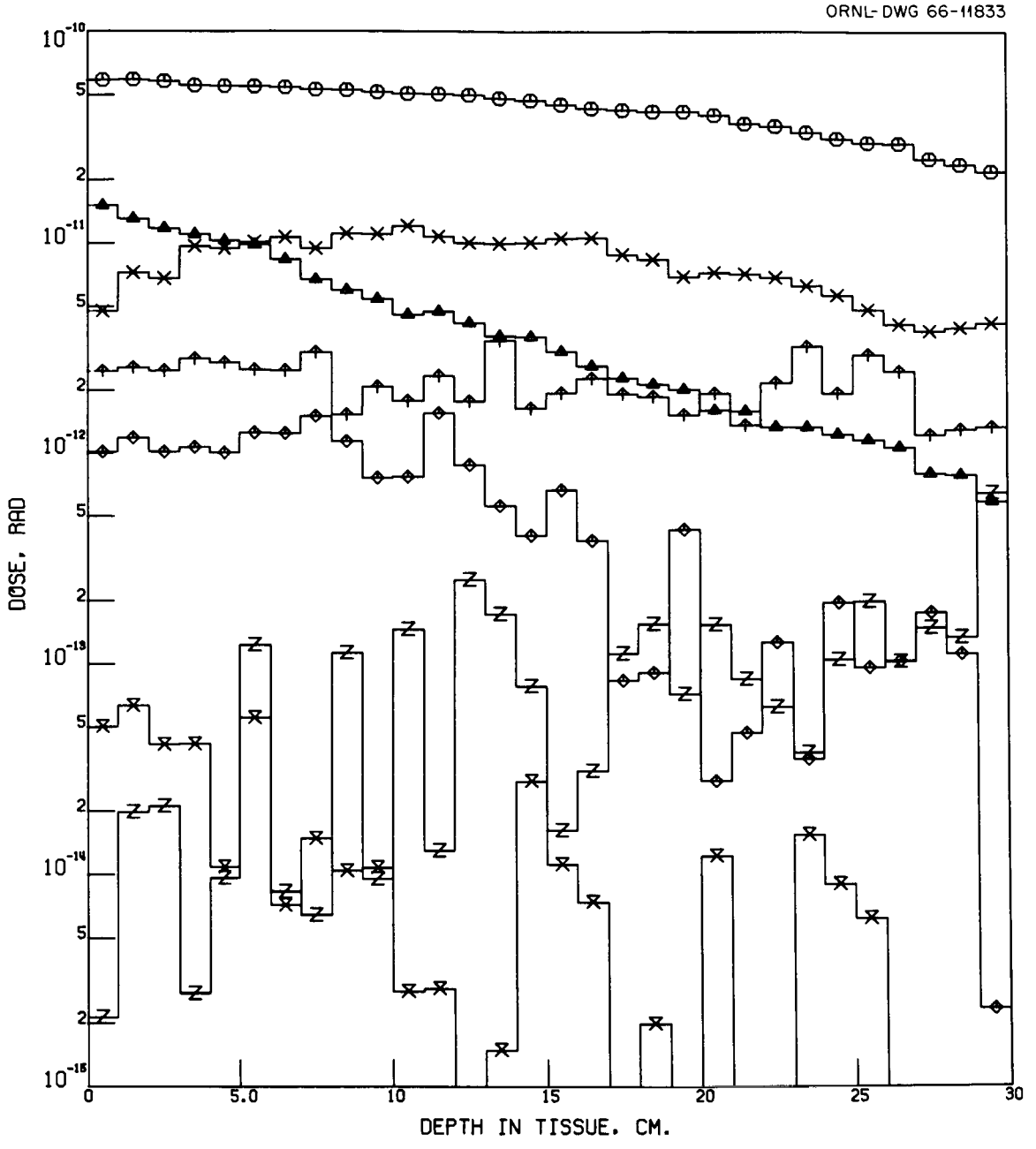

Fig. B6. Rad Dose Due to 300- to 350-MeV Incident Protons as a Function of Depth in Tissue for Z_A = 22 g/cm^2 and Z_{Fe} = 1 g/cm^2.

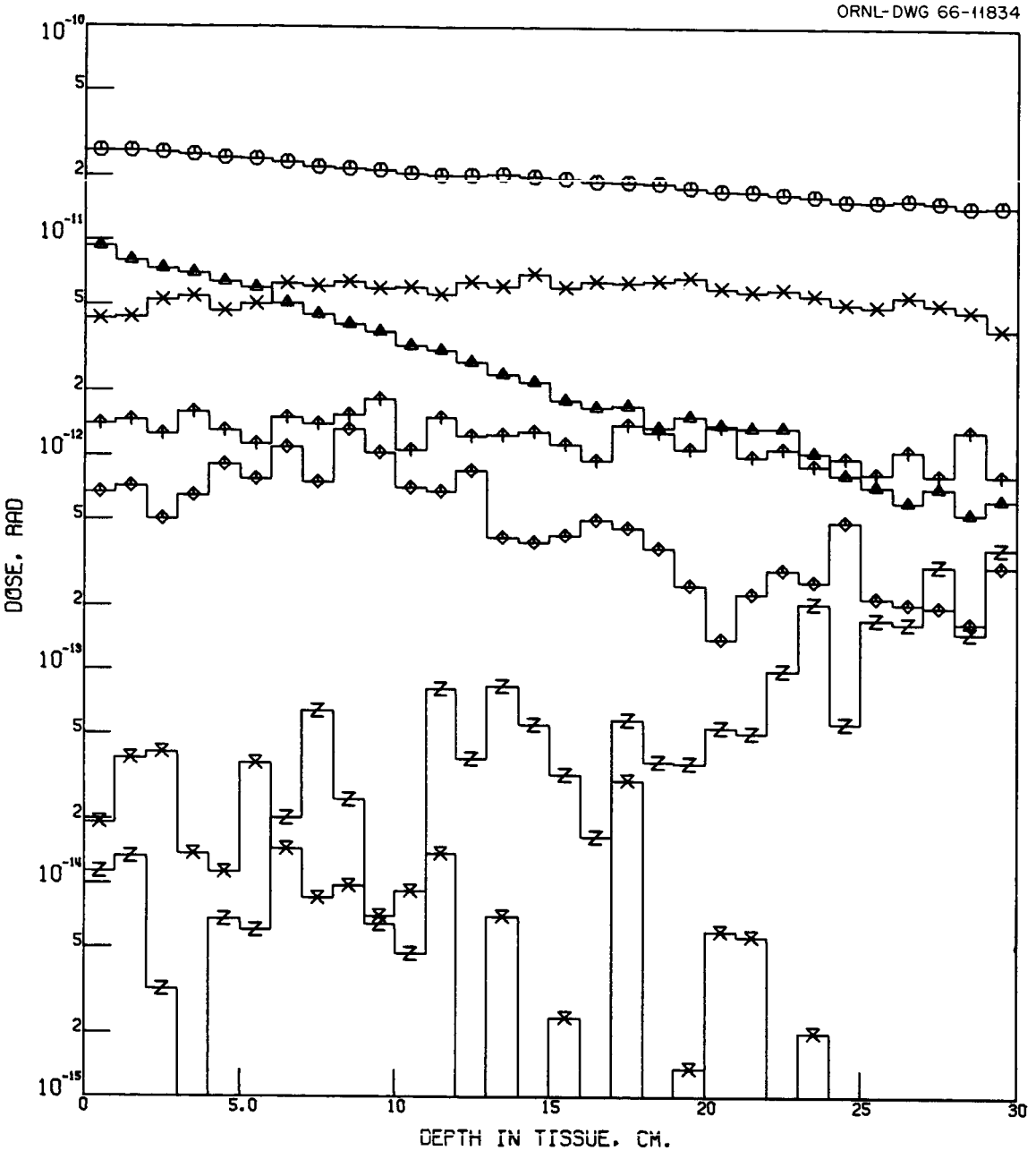

Fig. B7. Rad Dose Due to 350- to 400-MeV Incident Protons as a Function of Depth in Tissue for Z_A = 22 g/cm^2 and Z_{Fe} = 1 g/cm^2.

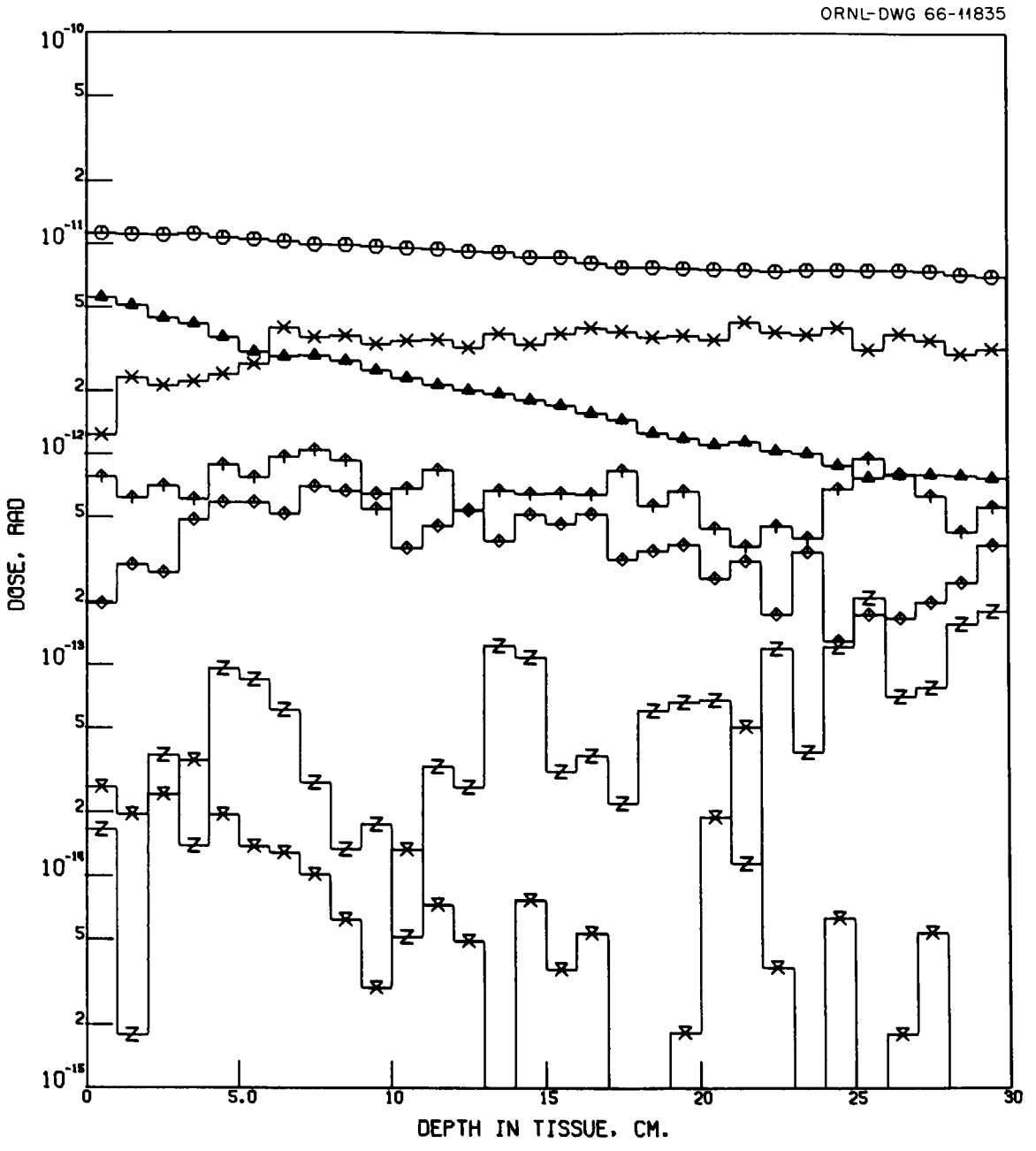

Fig. B8. Rad Dose Due to 400- to 450-MeV Incident Protons as a Function of Depth in Tissue for Z_A = 22 g/cm^2 and Z_{Fe} = 1 g/cm^2.

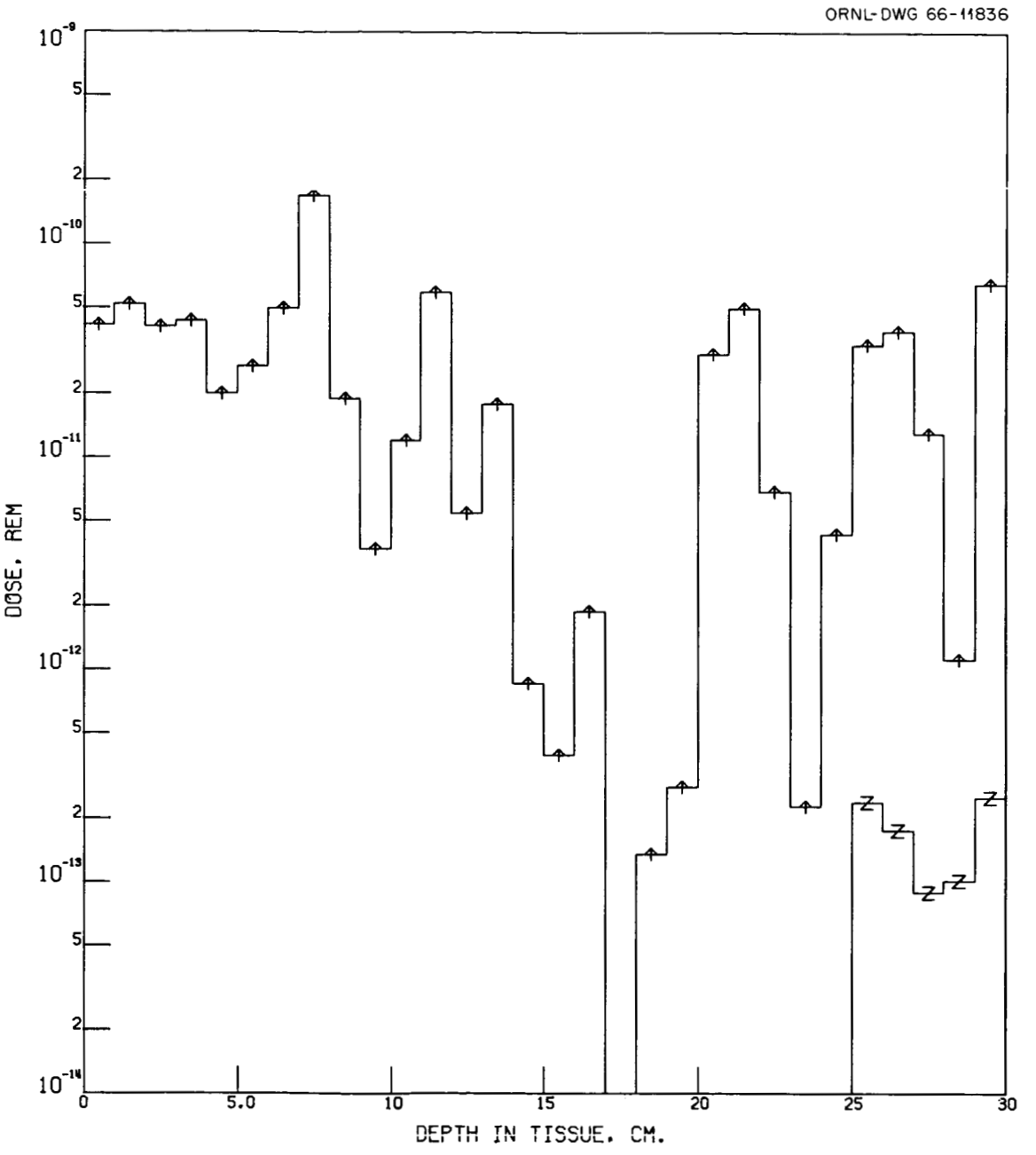

Fig. B9. Rem Dose Due to 50- to 100-MeV Incident Protons as a Function of Depth in Tissue for Z_A = 22 g/cm^2 and Z_{Fe} = 1 g/cm^2.

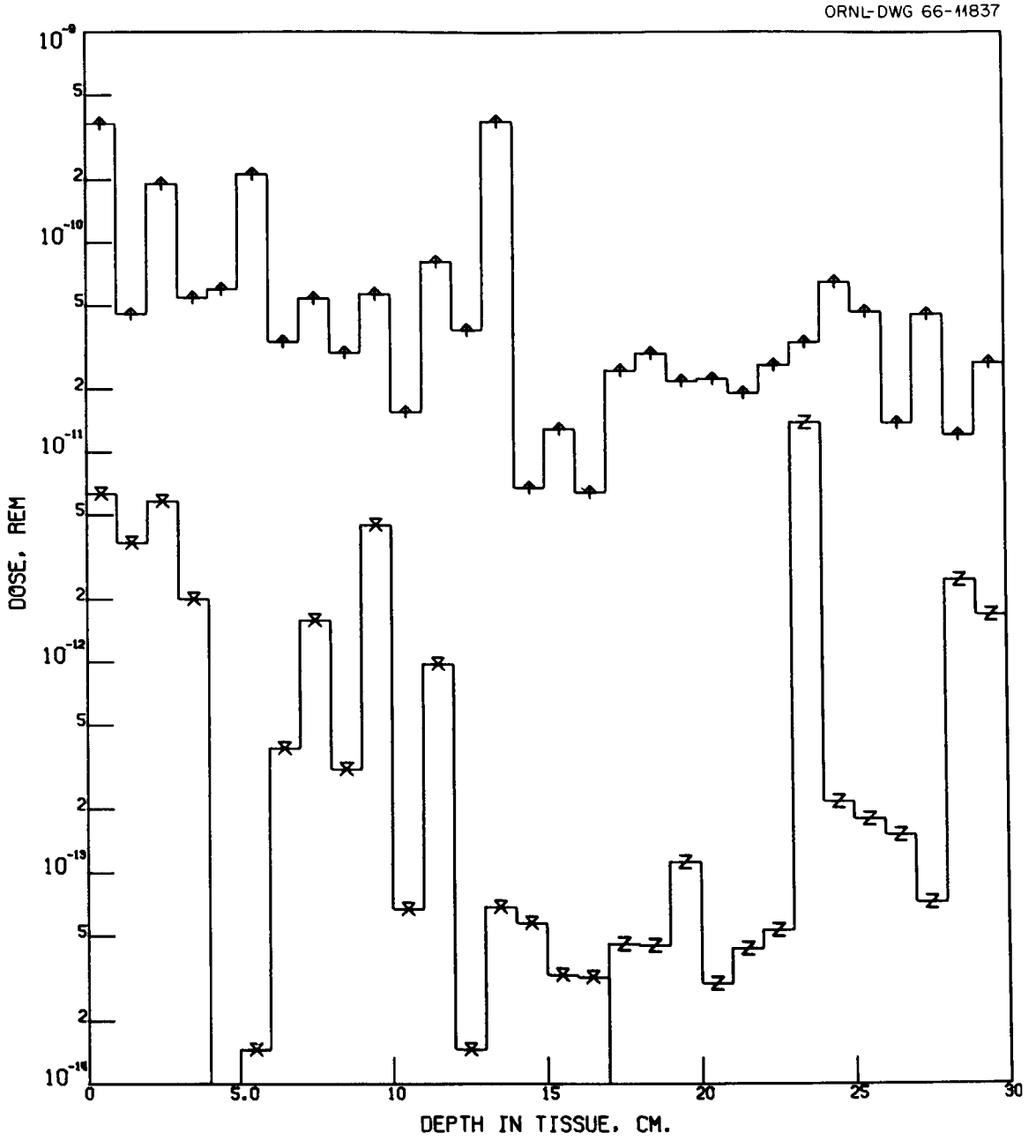

Fig. B10. Rem Dose Due to 100- to 150-MeV Incident Protons as a Function of Depth in Tissue for Z_A = 22 g/cm^2 and Z_{Fe} = 1 g/cm^2.

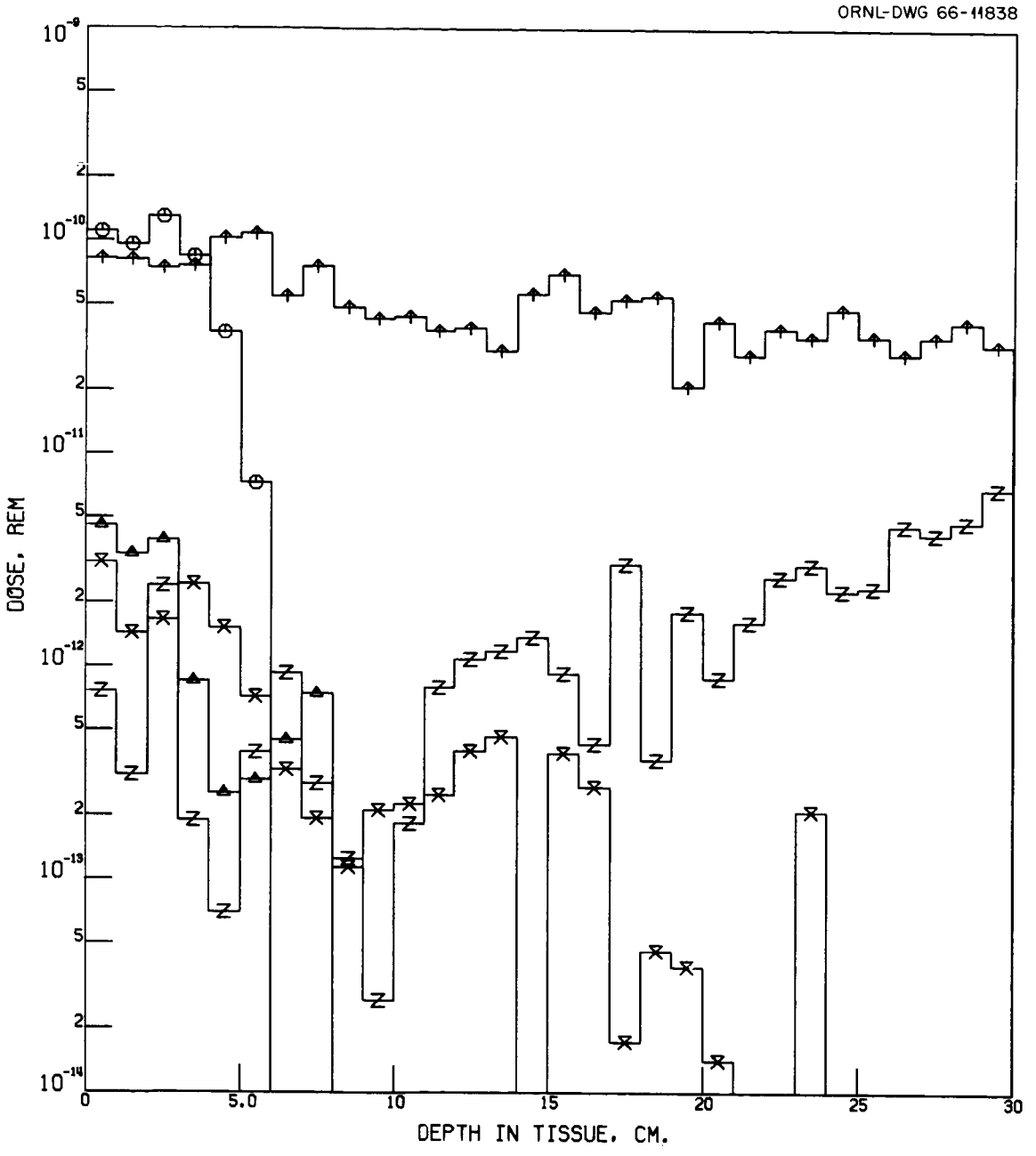

Fig. B11. Rem Dose Due to 150- to 200-MeV Incident Protons as a Function of Depth in Tissue for Z_A = 22 g/cm^2 and Z_{Fe} = 1 g/cm^2.

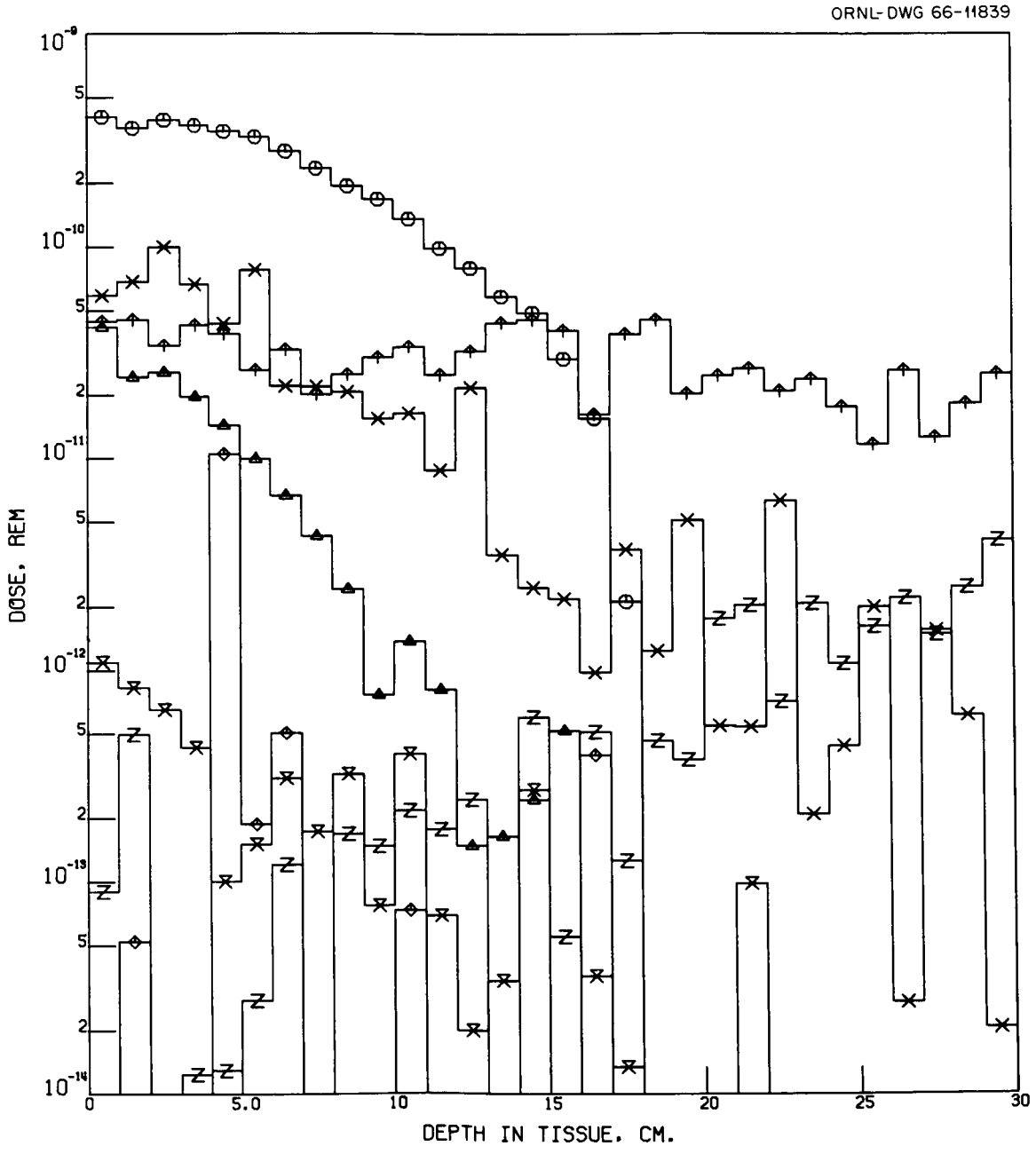

Fig. B12. Rem Dose Due to 200- to 250-MeV Incident Protons as a Function of Depth in Tissue for Z_A = 22 g/cm^2 and Z_{Fe} = 1 g/cm^2.

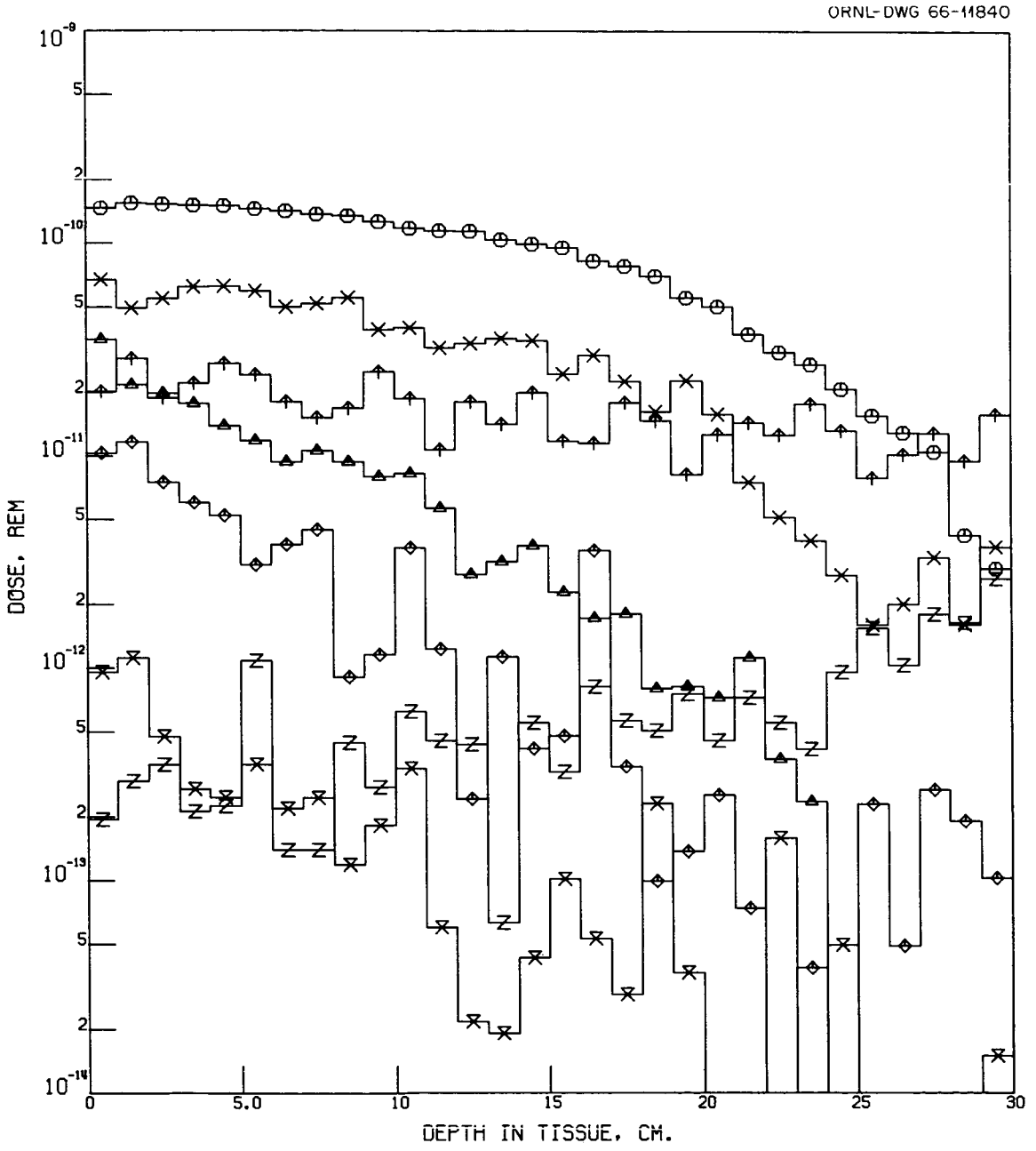

Fig. B13. Rem Dose Due to 250- to 300-MeV Incident Protons as a Function of Depth in Tissue for Z_A = 22 g/cm^2 and Z_{Fe} = 1 g/cm^2.

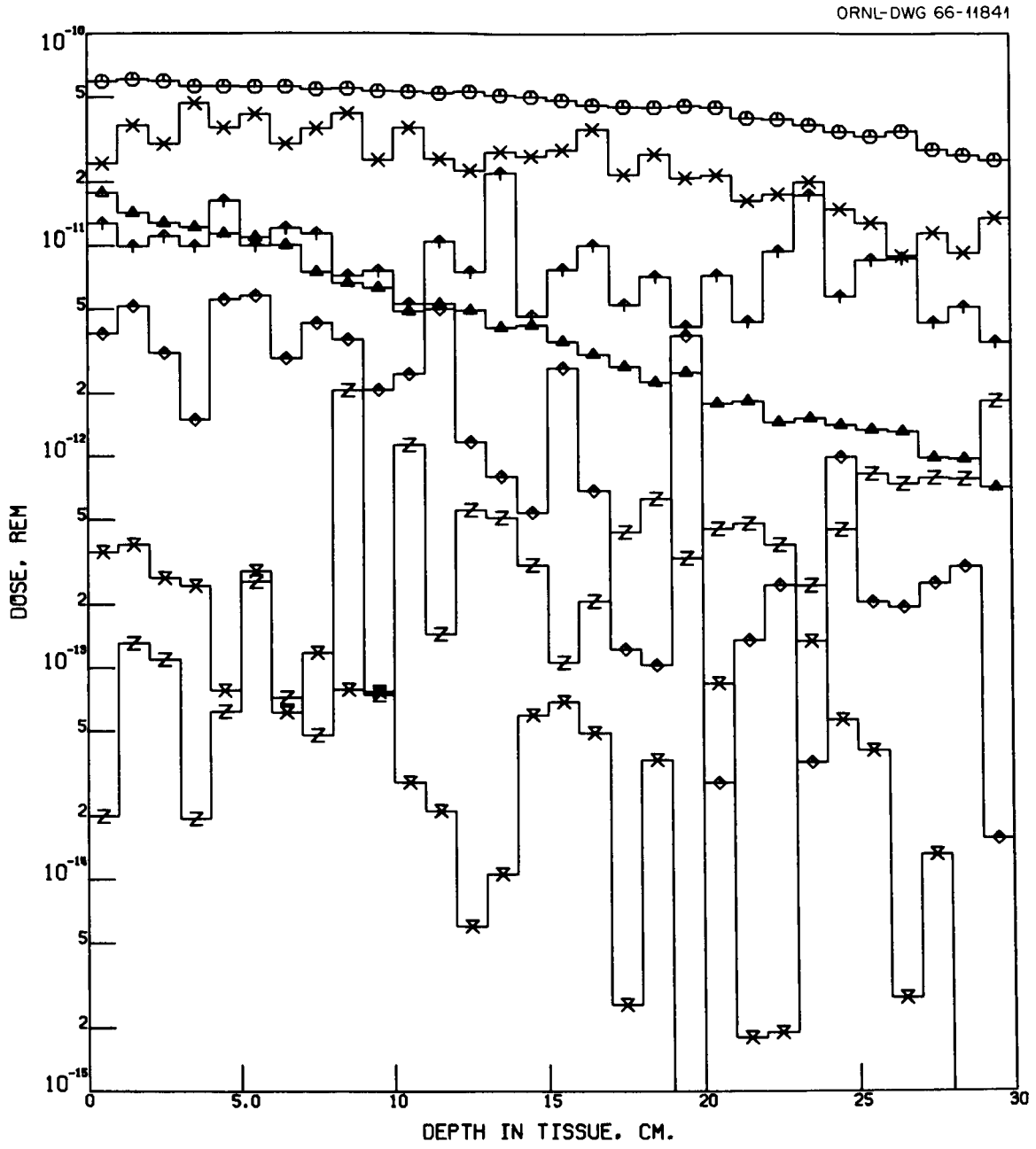

Fig. B14. Rem Dose Due to 300- to 350-MeV Incident Protons as a Function of Depth in Tissue for Z_A = 22 g/cm^2 and Z_{Fe} = 1 g/cm^2.

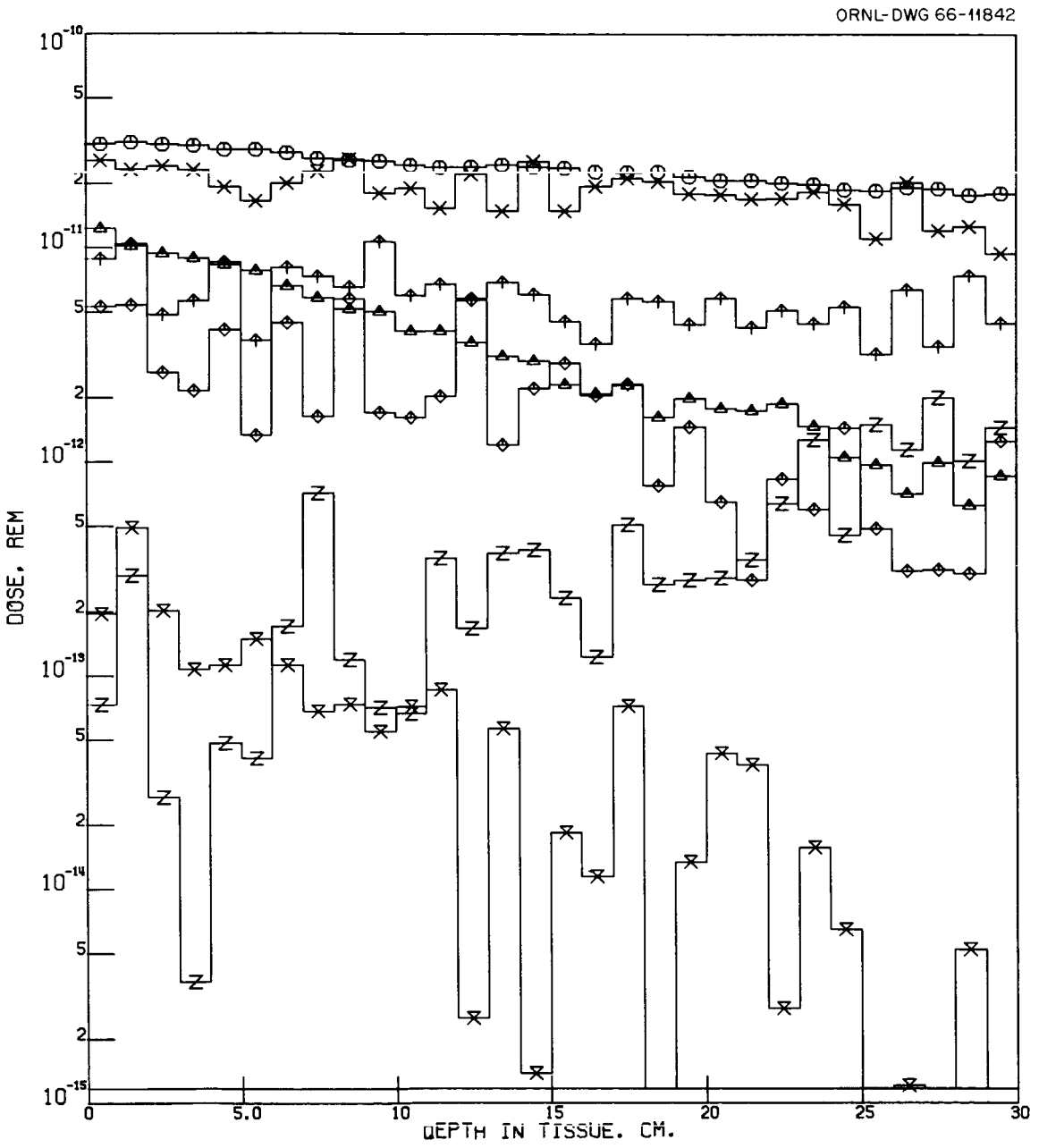

Fig. B15. Rem Dose Due to 350- to 400-MeV Incident Protons as a Function of Depth in Tissue for Z_A = 22 g/cm^2 and Z_{Fe} = 1 g/cm^2.

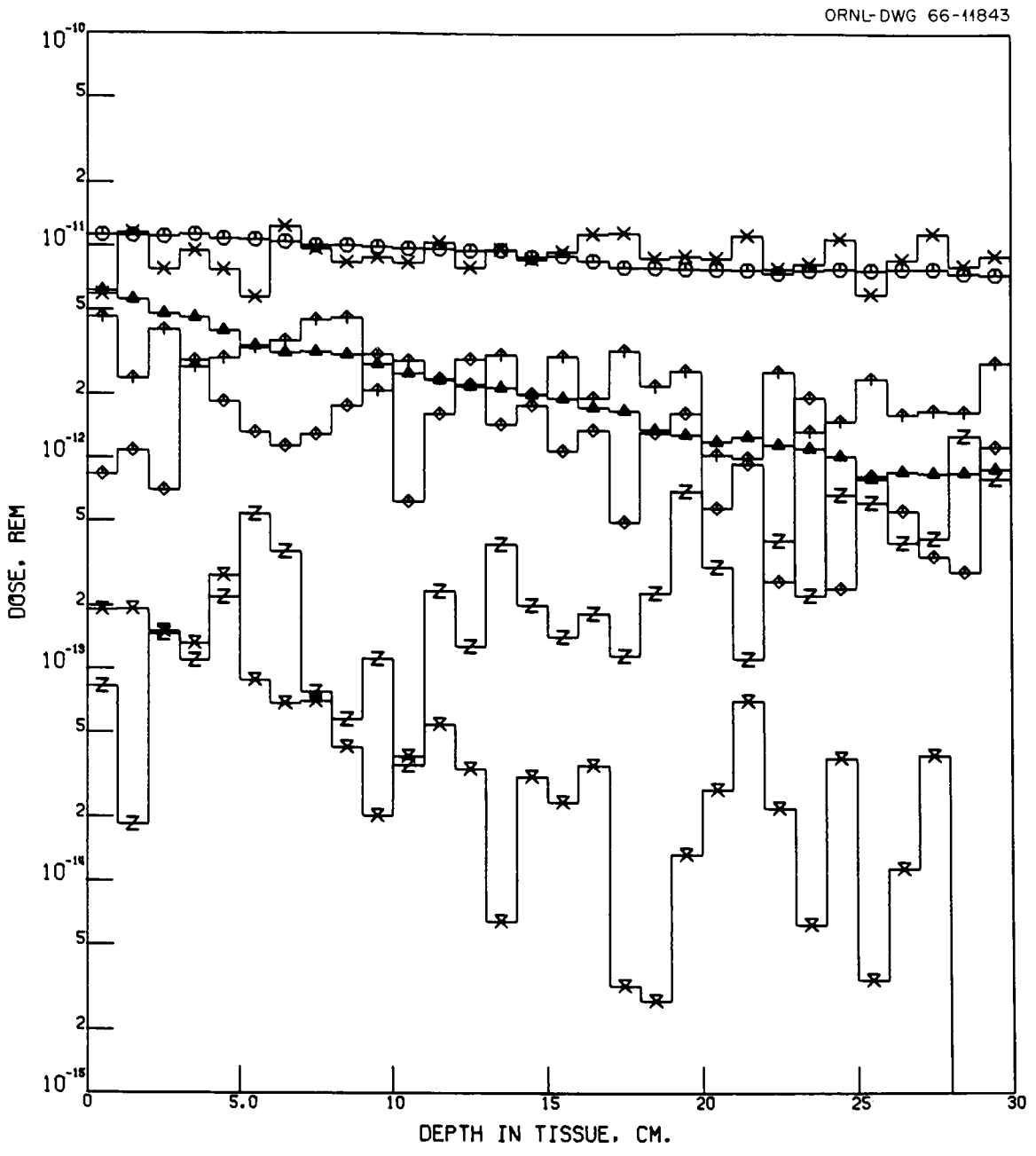

Fig. B16. Rem Dose Due to 400- to 450-MeV Incident Protons as a Function of Depth in Tissue for Z_A = 22 g/cm^2 and Z_{Fe} = 1 g/cm^2.

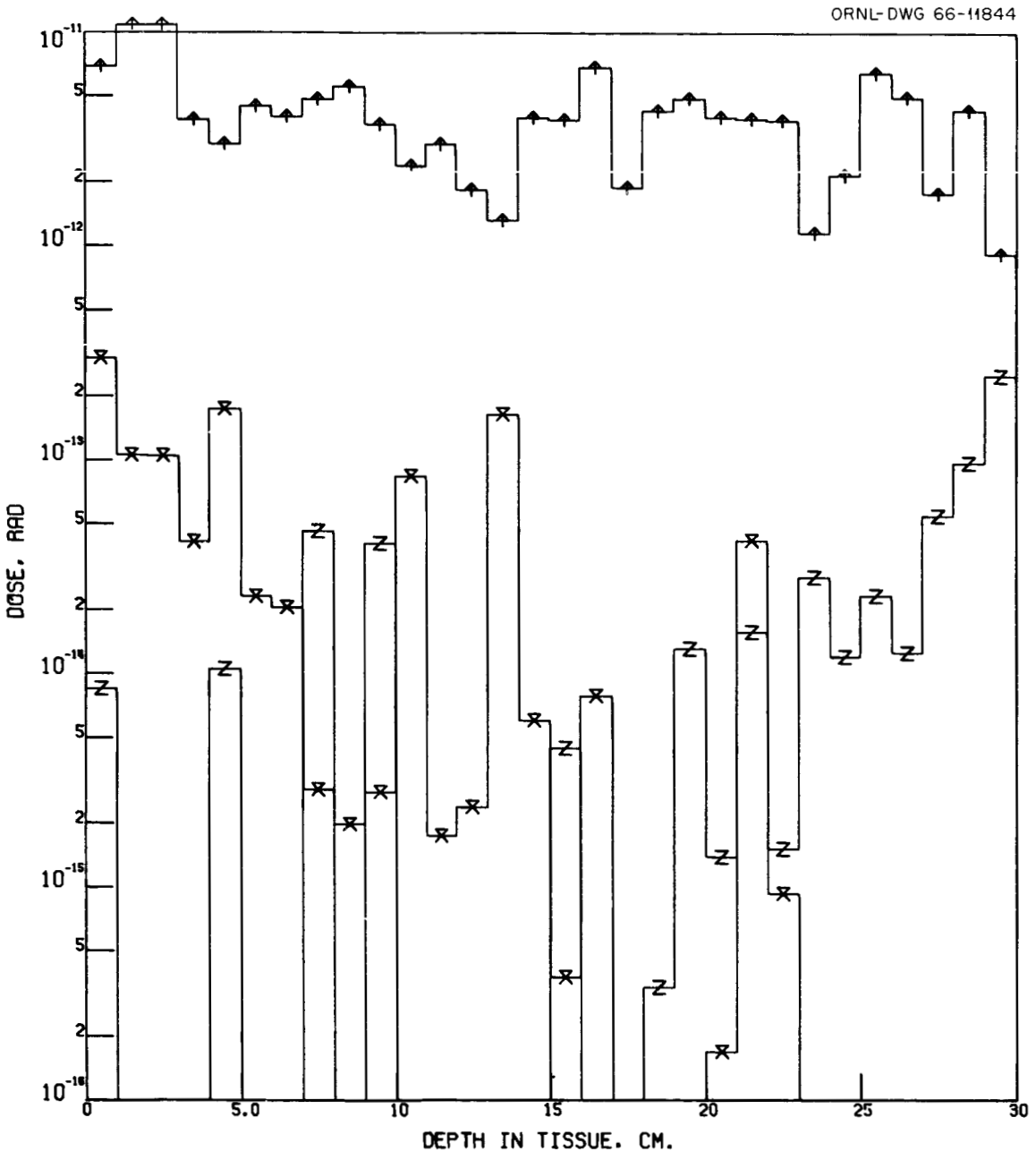

Fig. B17. Rad Dose Due to 50- to 100-MeV Incident Protons as a Function of Depth in Tissue for Z_A = 36 g/cm^2 and Z_{Fe} = 1 g/cm^2.

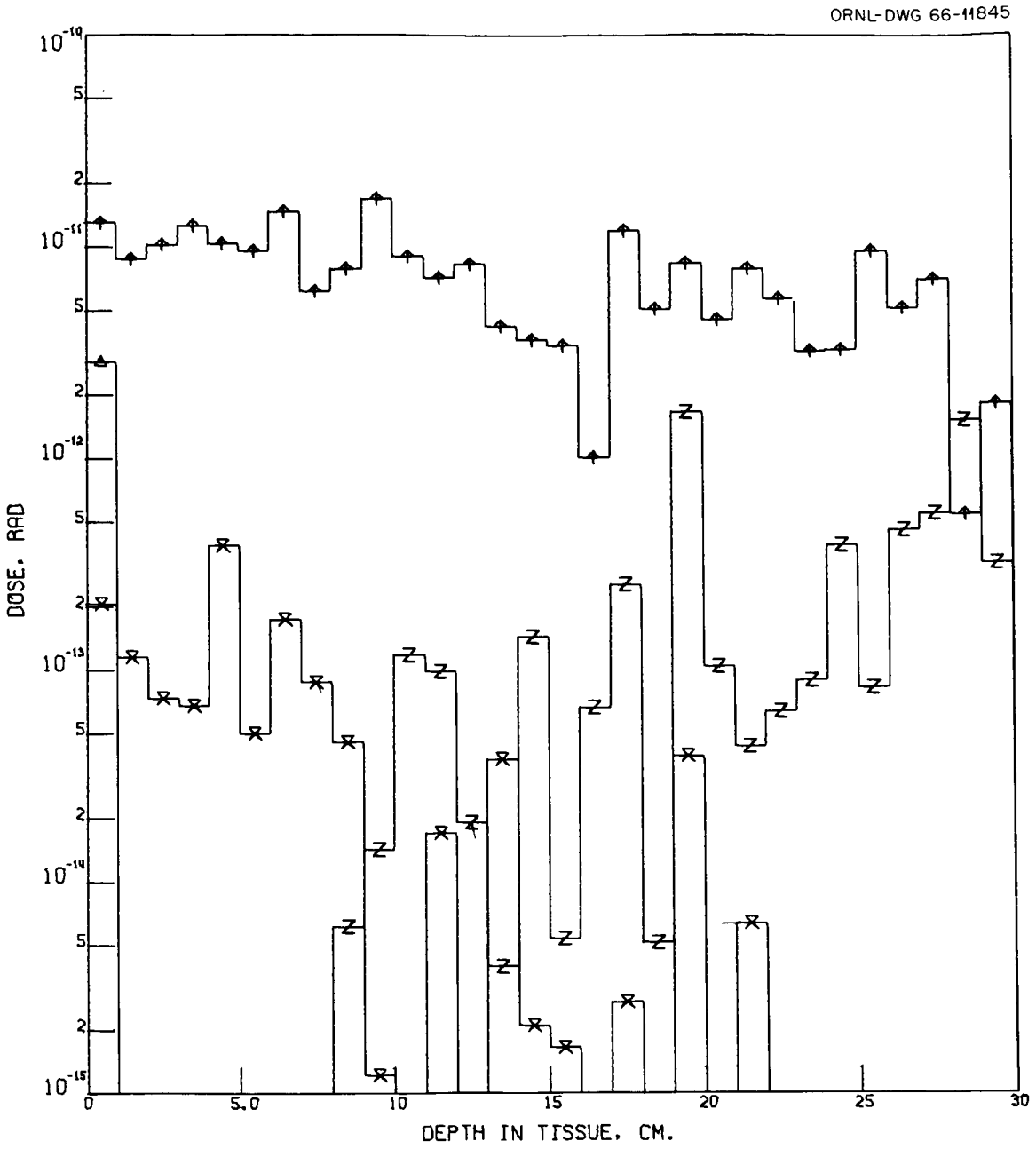

Fig. B18. Rad Dose Due to 100- to 150-MeV Incident Protons as a Function of Depth in Tissue for Z_A = 36 g/cm^2 and Z_{Fe} = 1 g/cm^2.

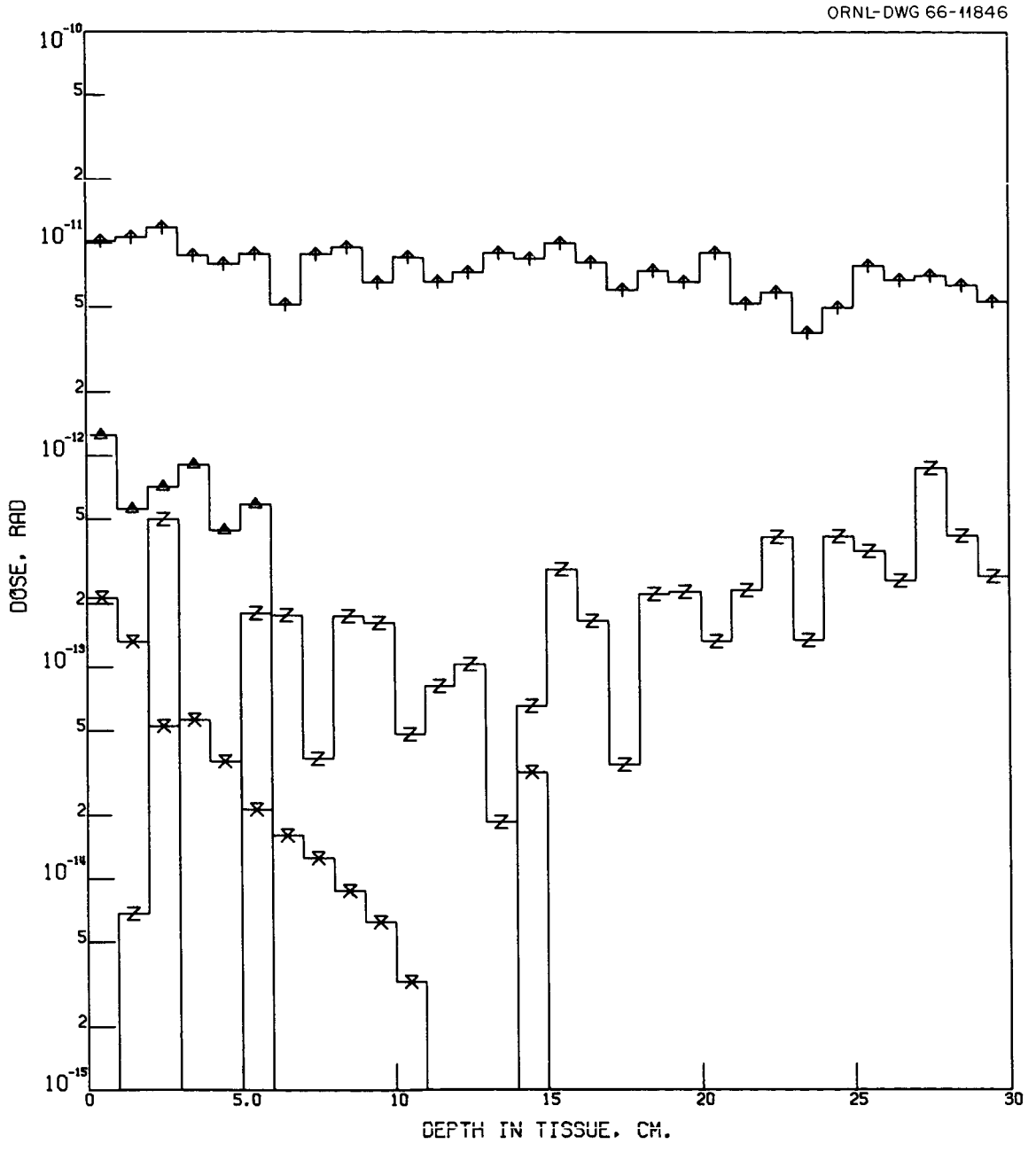

Fig. B19. Rad Dose Due to 150- to 200-MeV Incident Protons as a Function of Depth in Tissue for Z_A = 36 g/cm^2 and Z_{Fe} = 1 g/cm^2.

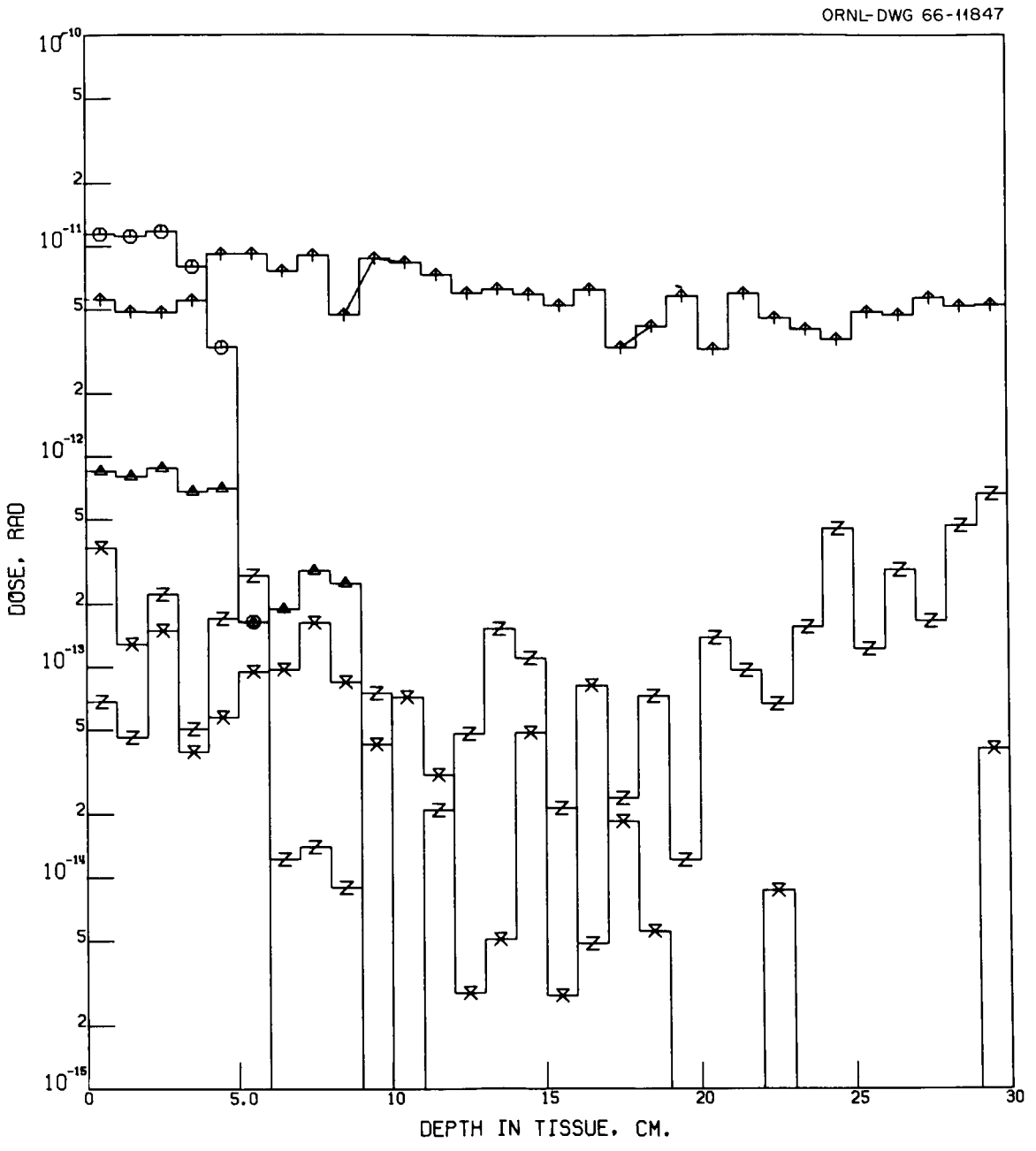

Fig. B20. Rad Dose Due to 200- to 250-MeV Incident Protons as a Function of Depth in Tissue for Z_A = 36 g/cm^2 and Z_{Fe} = 1 g/cm^2.

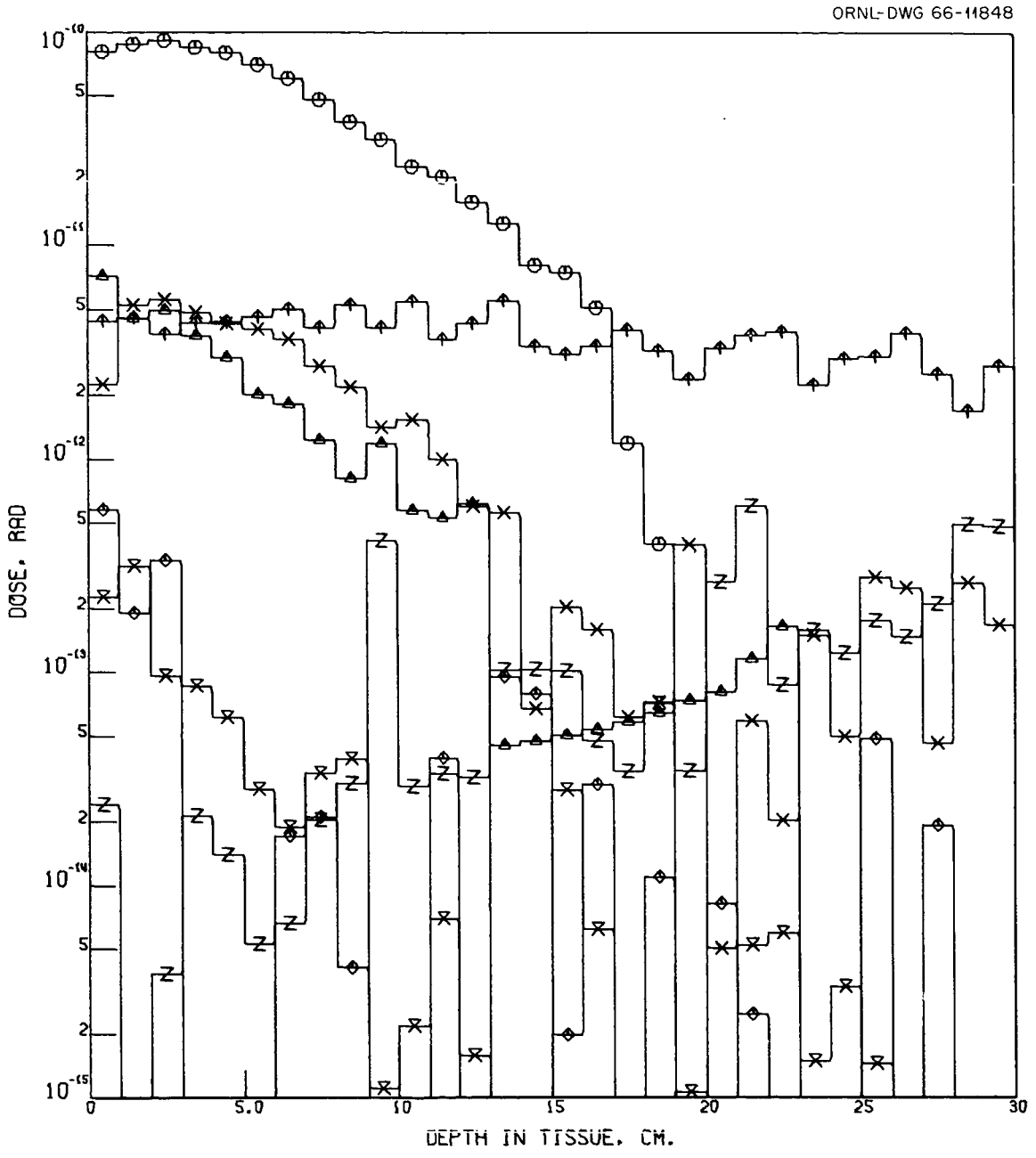

Fig. B21. Rad Dose Due to 250- to 300-MeV Incident Protons as a Function of Depth in Tissue for Z_A = 36 g/cm^2 and Z_{Fe} = 1 g/cm^2.

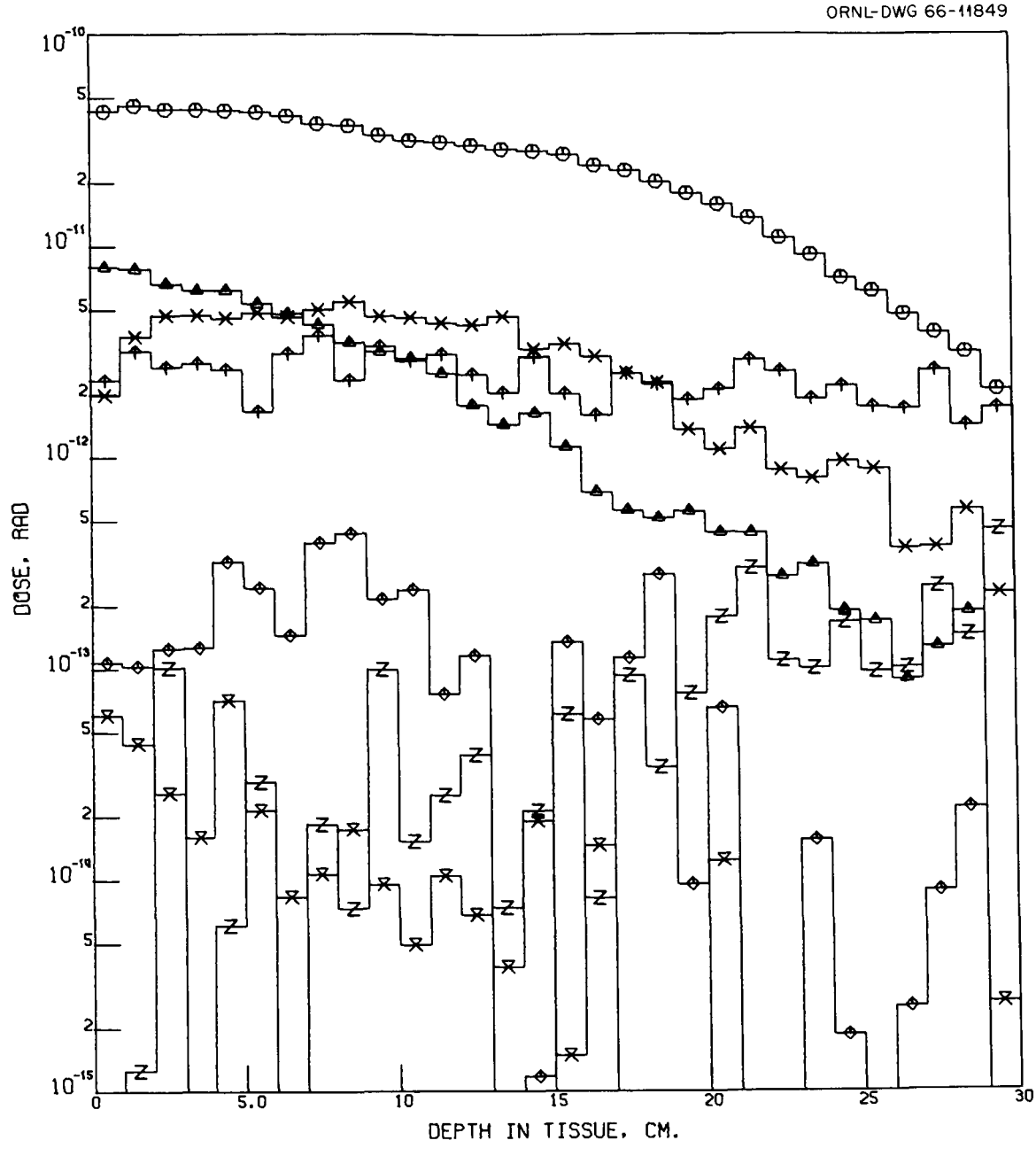

Fig. B22. Rad Dose Due to 300- to 350-MeV Incident Protons as a Function of Depth in Tissue for Z_A = 36 g/cm^2 and Z_{Fe} = 1 g/cm^2.

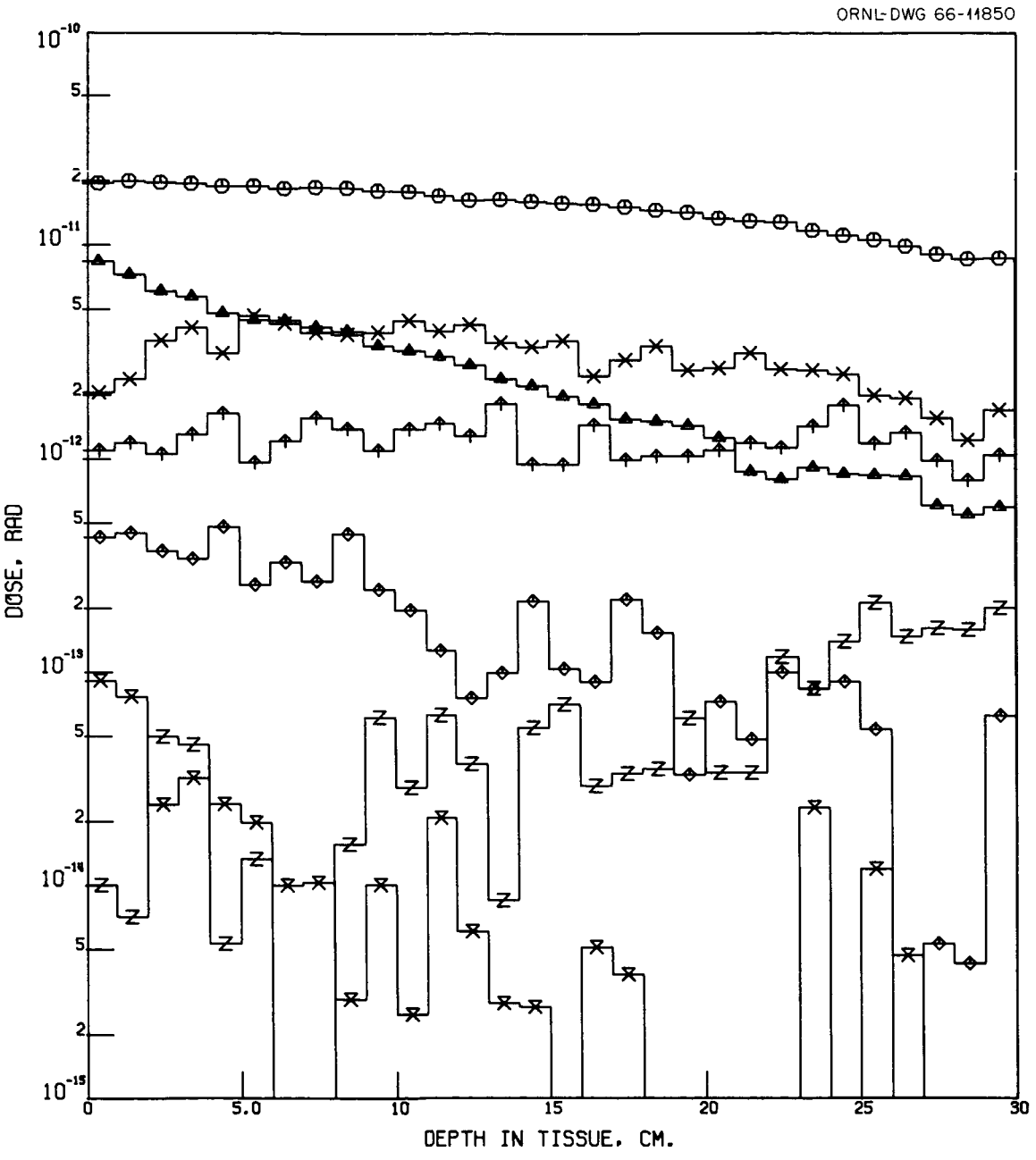

Fig. B23. Rad Dose Due to 350- to 400-MeV Incident Protons as a Function of Depth in Tissue for Z_A = 36 g/cm^2 and Z_{Fe} = 1 g/cm^2.

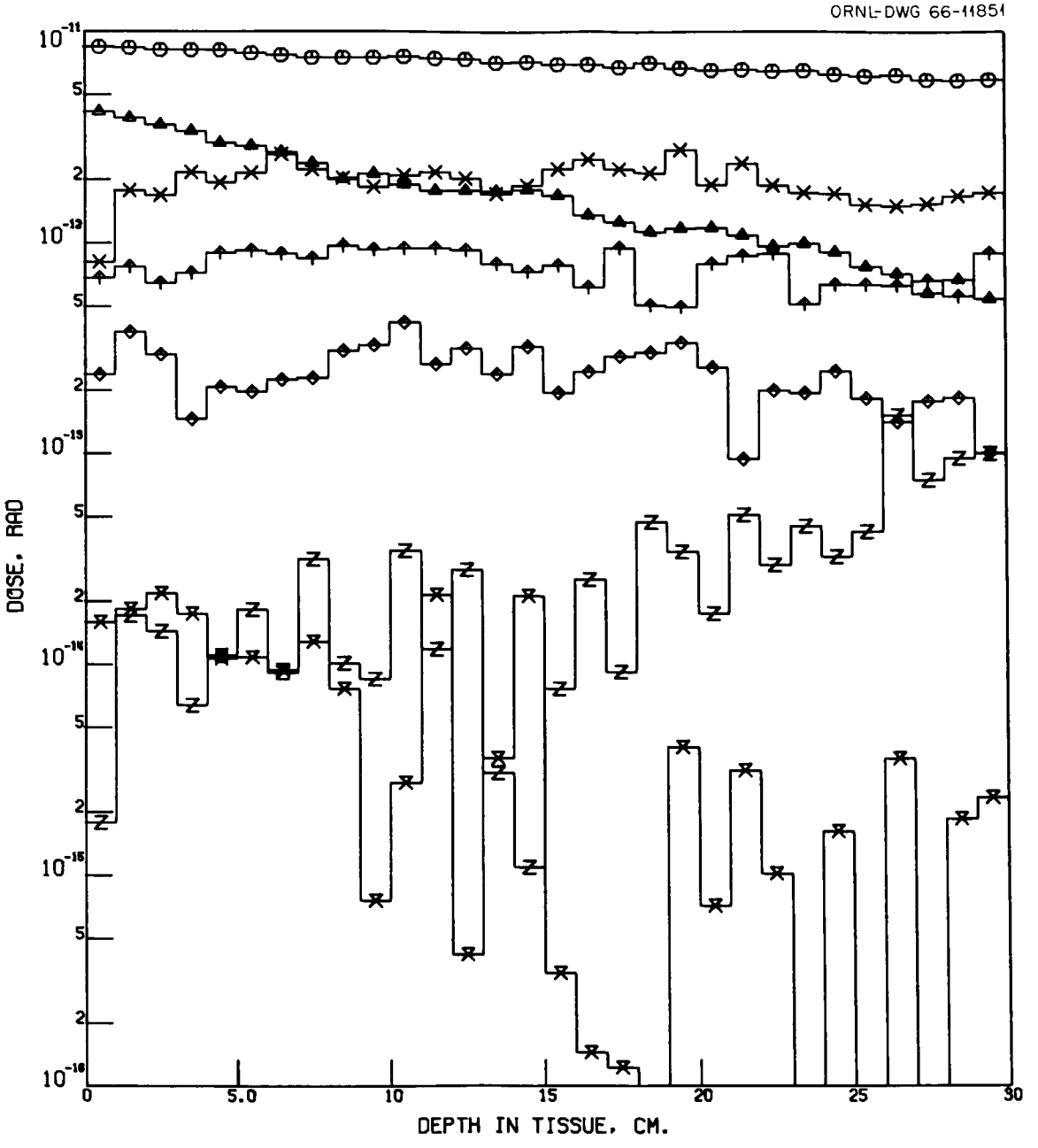

Fig. B24. Rad Dose Due to 400- to 450-MeV Incident Protons as a Function of Depth in Tissue for $Z = 36$ g/cm^2 and $Z_{Fe} = 1$ g/cm

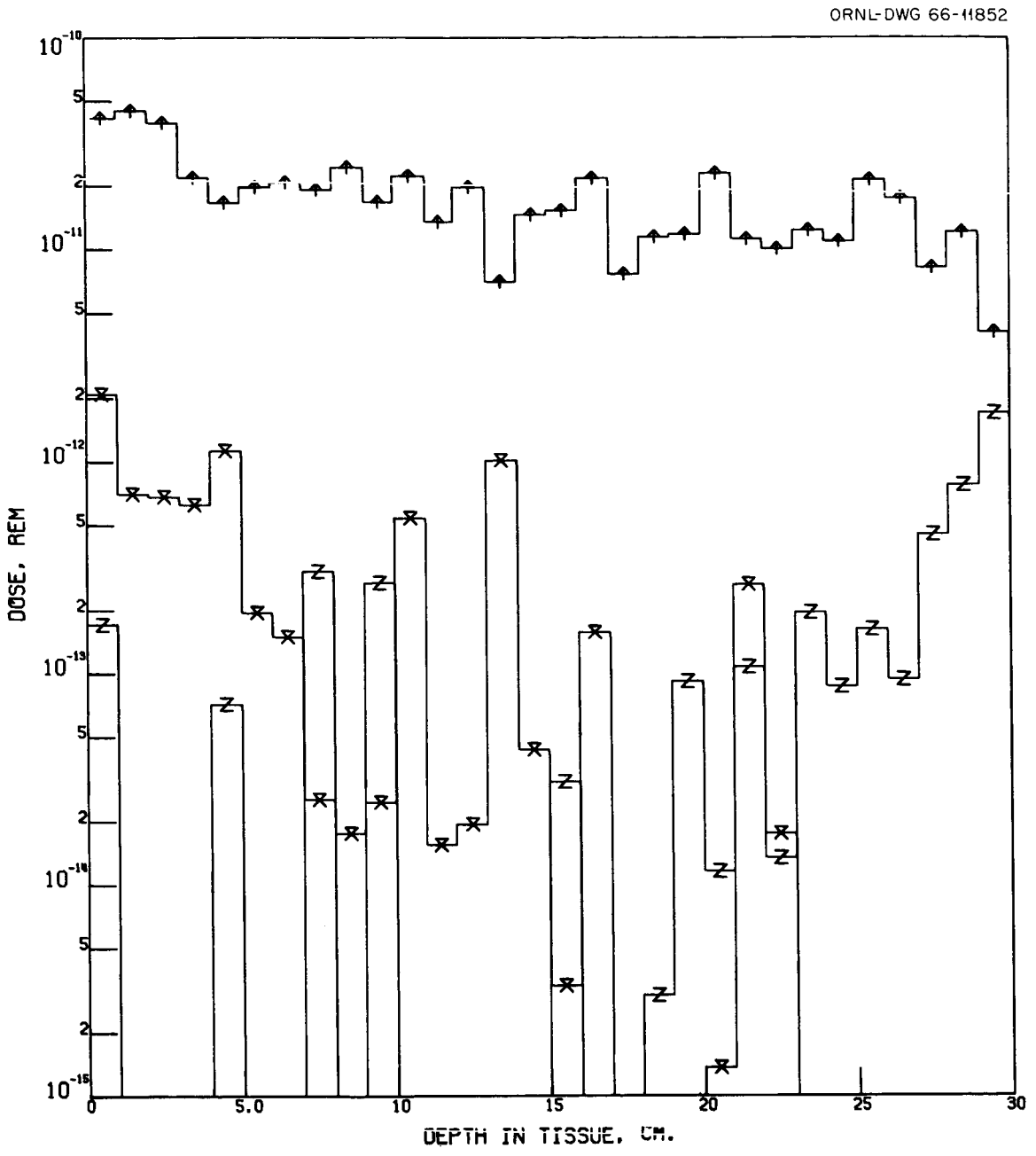

Fig. B25. Rem Dose Due to 50- to 100-MeV Incident Protons as a Function of Depth in Tissue for Z_A = 36 g/cm^2 and Z_{Fe} = 1 g/cm^2.

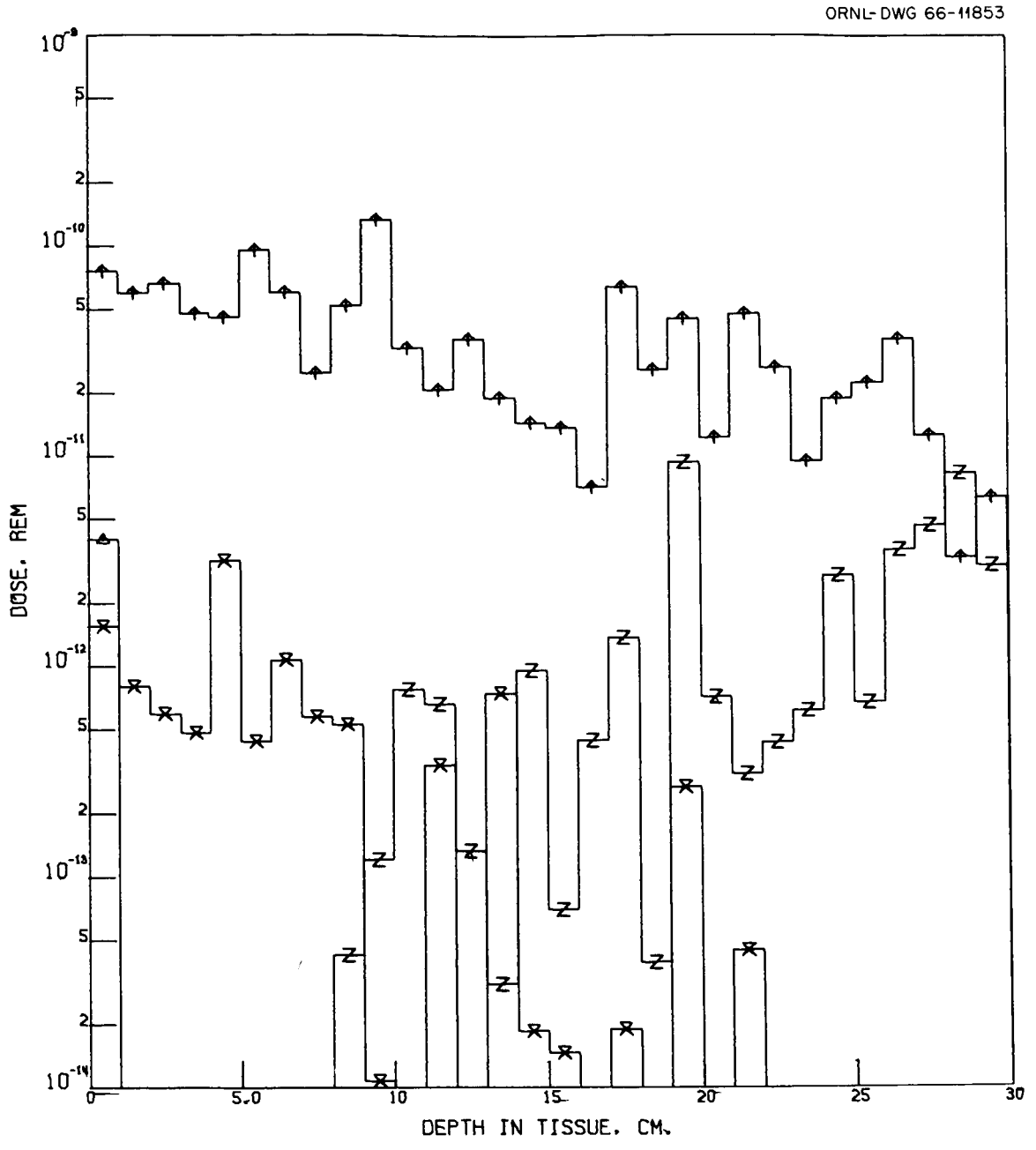

Fig. B26. Rem Dose Due to 100- to 150-MeV Incident Protons as a Function of Depth in Tissue for Z_A = 36 g/cm^2 and Z_{Fe} = 1 g/cm^2.

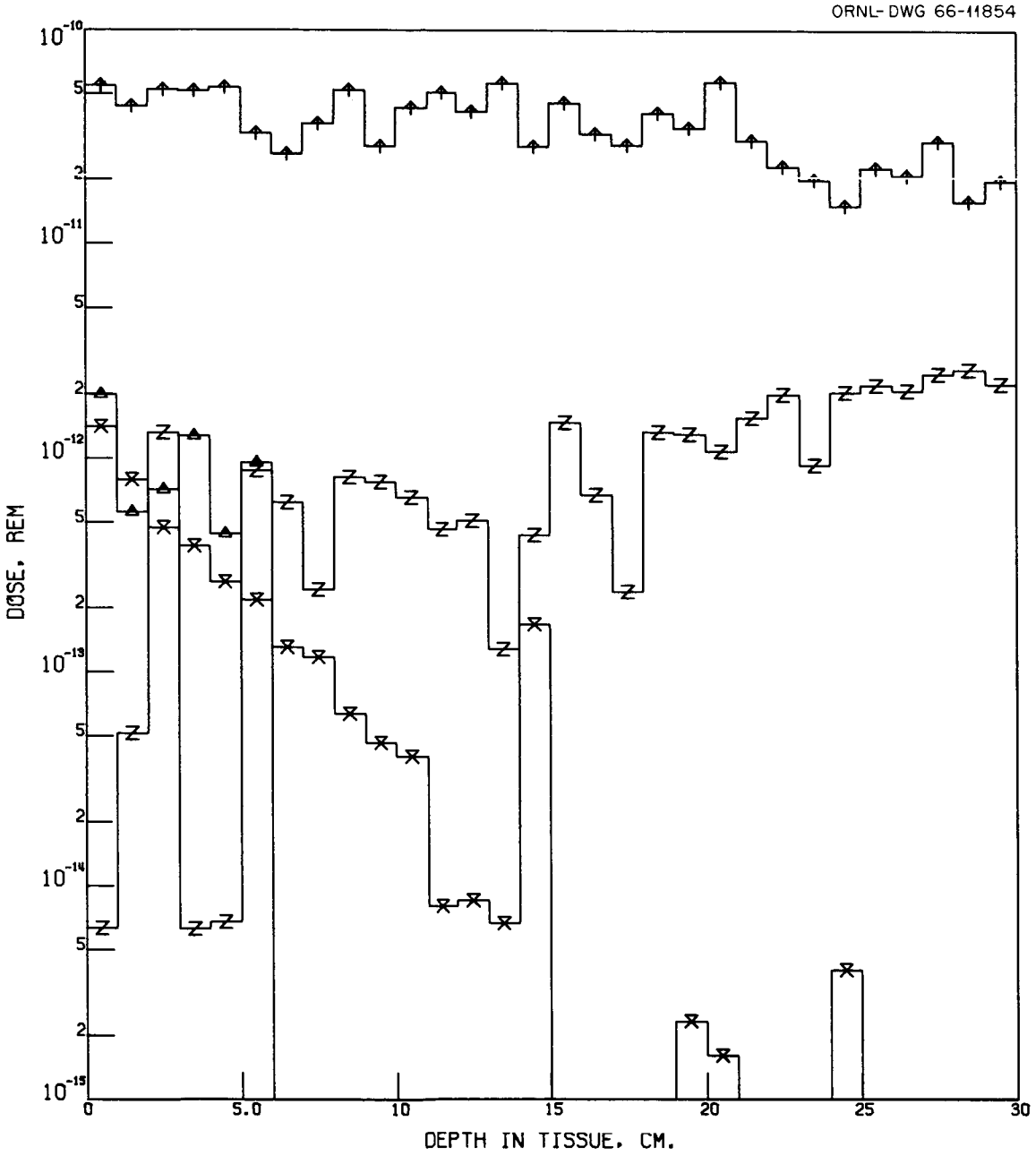

Fig. B27. Rem Dose Due to 150- to 200-MeV Incident Protons as a Function of Depth in Tissue for Z_A = 36 g/cm^2 and Z_{Fe} = 1 g/cm^2.

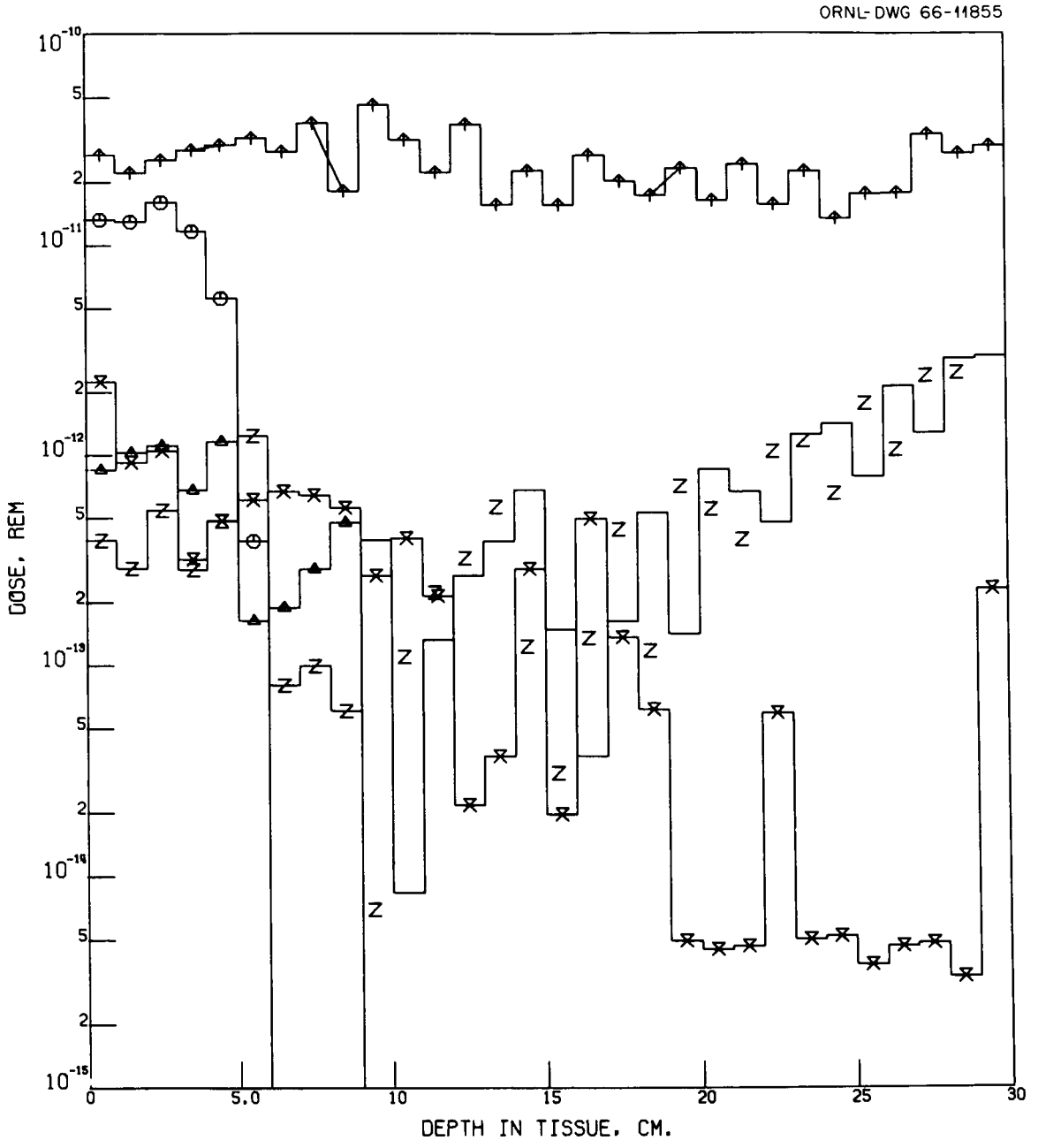

Fig. B28. Rem Dose Due to 200- to 250-MeV Incident Protons as a Function of Depth in Tissue for Z_A = 36 g/cm^2 and Z_{Fe} = 1 g/cm^2.

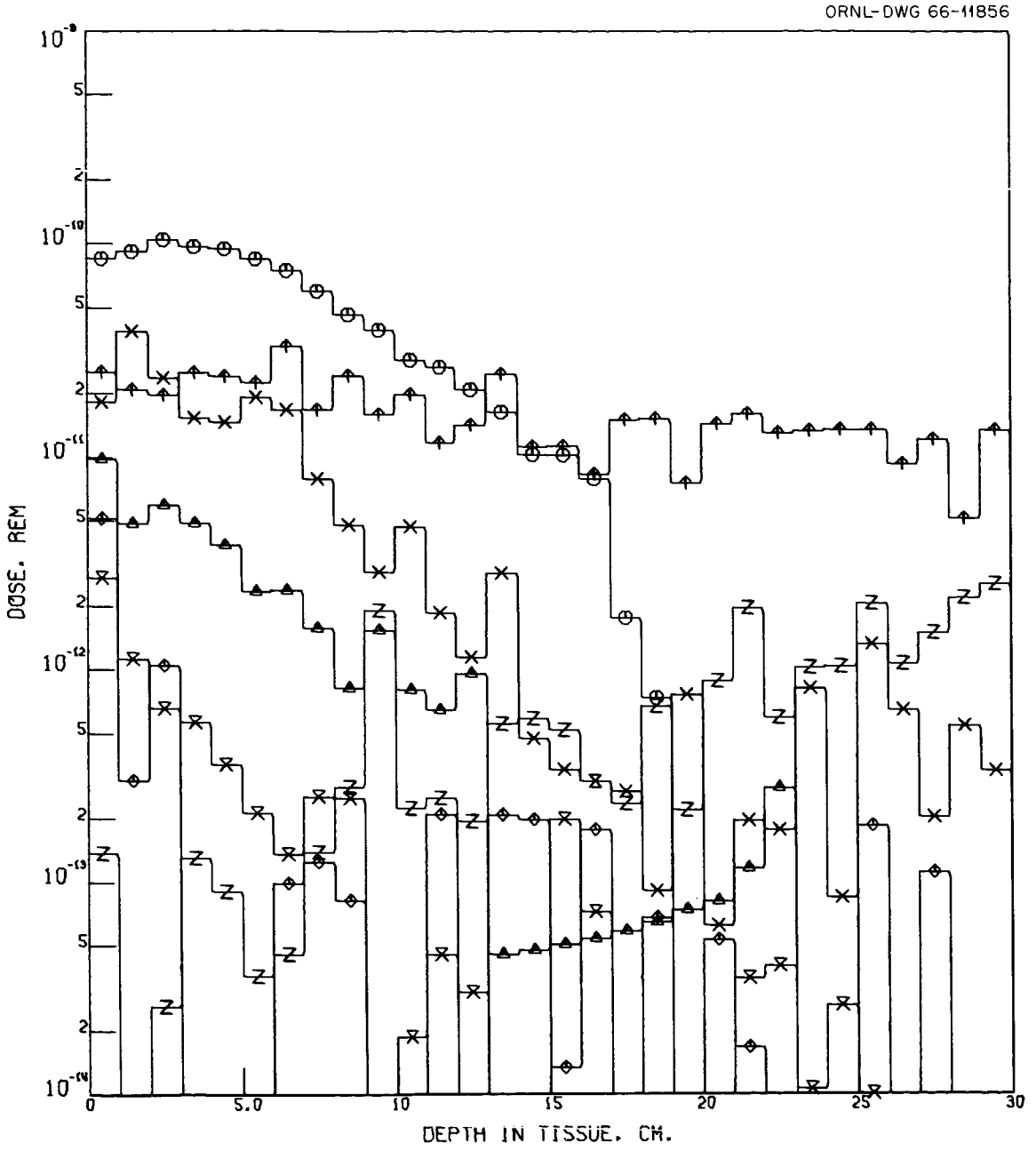

Fig. B29. Rem Dose Due to 250- to 300-MeV Incident Protons as a Function of Depth in Tissue for Z_A = 36 g/cm^2 and Z_{Fe} = 1 g/cm^2.

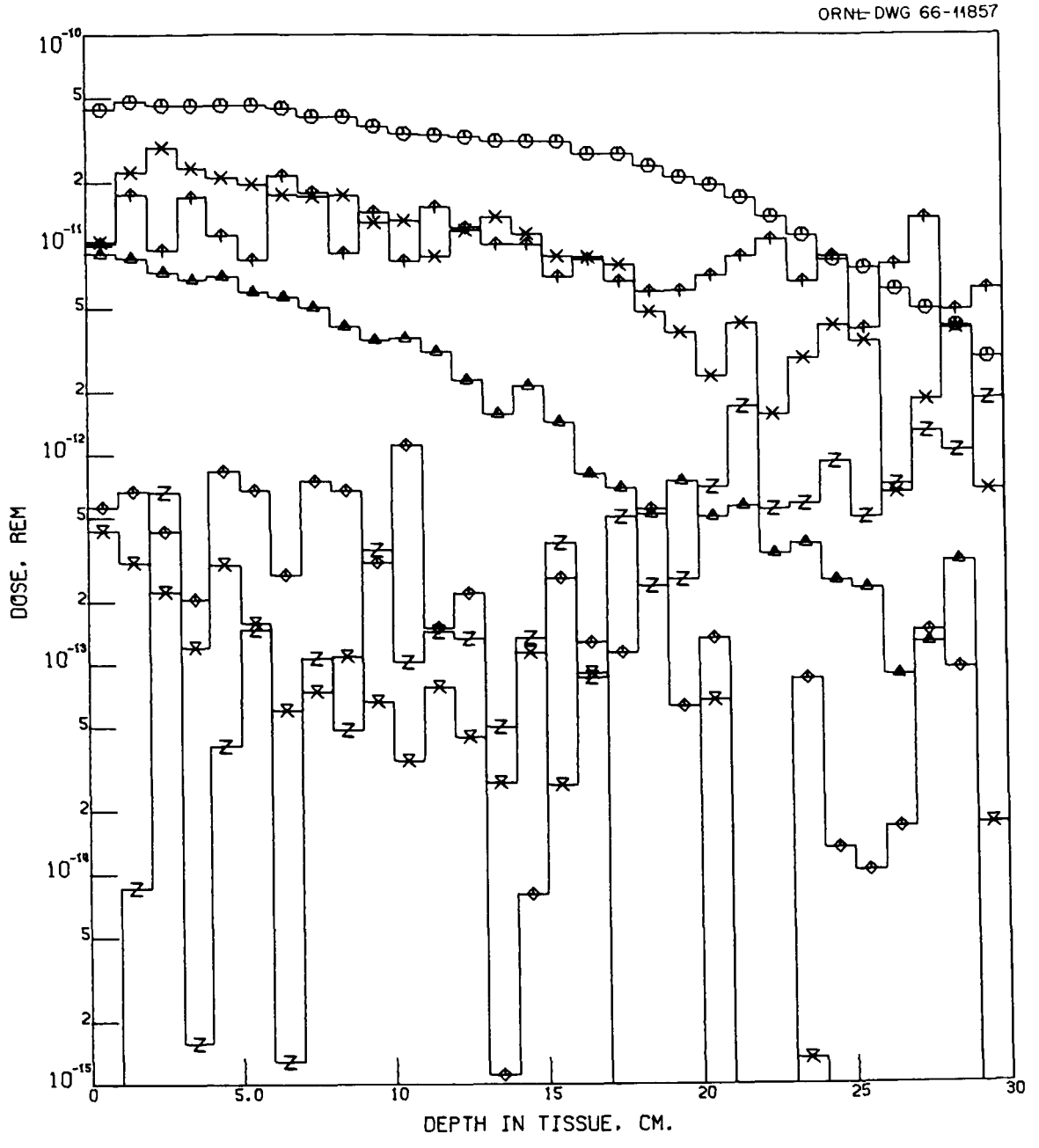

Fig. B30. Rem Dose Due to 300- to 350-MeV Incident Protons as a Function of Depth in Tissue for Z_A = 36 g/cm^2 and Z_{Fe} = 1 g/cm^2.

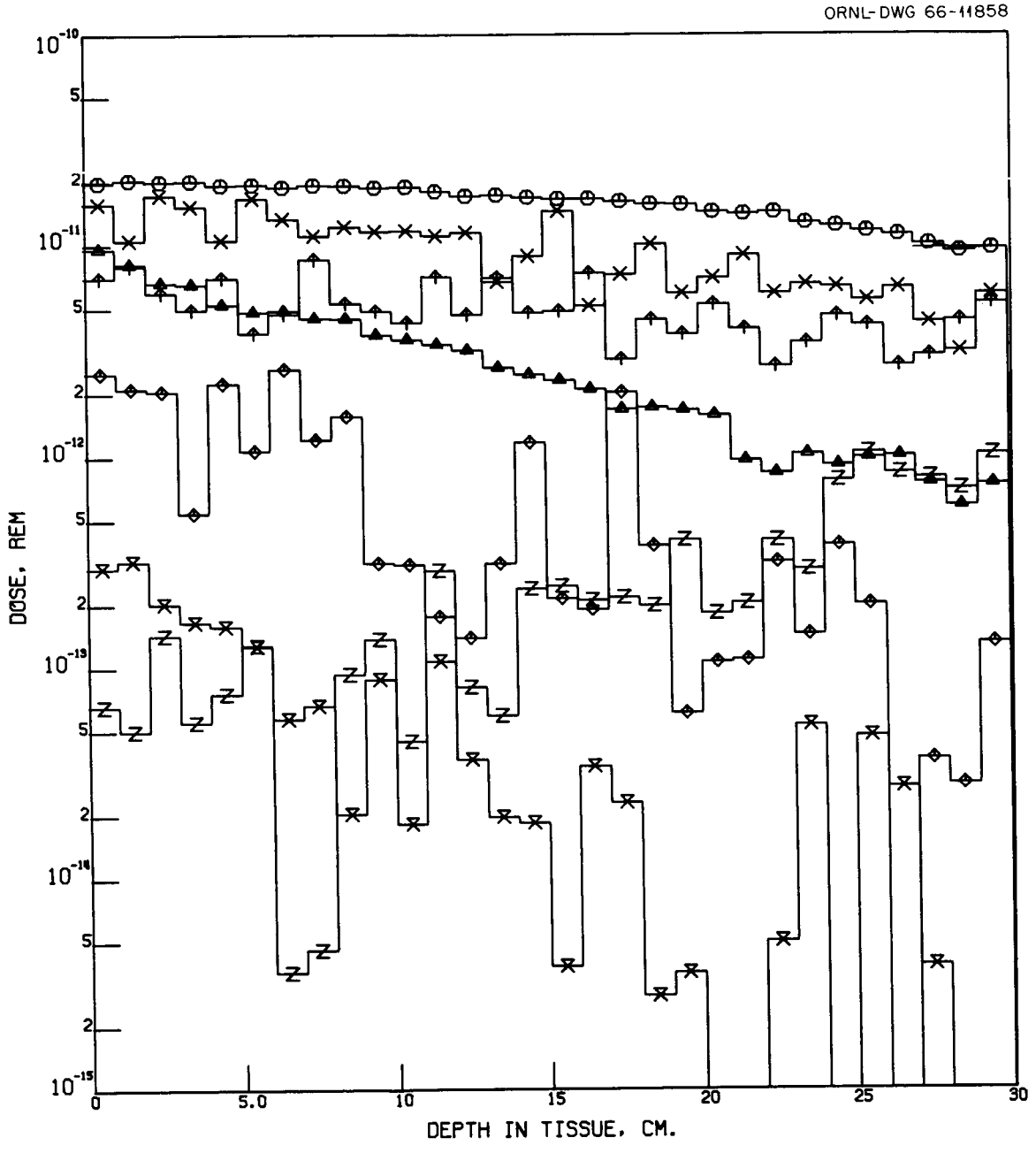

Fig. B31. Rem Dose Due to 350- to 400-MeV Incident Protons as a Function of Depth in Tissue for Z_A = 36 g/cm^2 and Z_{Fe} = 1 g/cm^2.

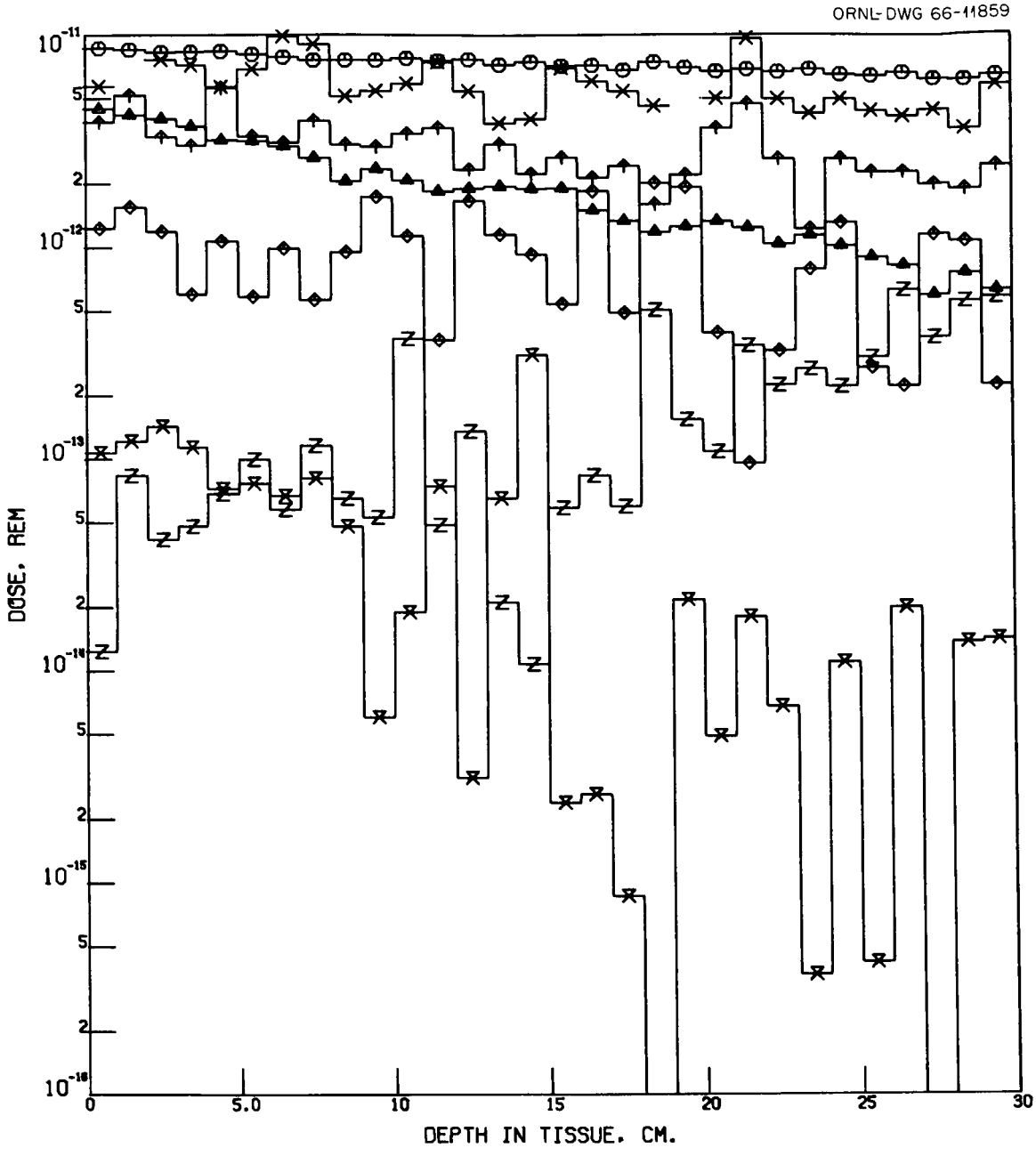

Fig. B32. Rem Dose Due to 400- to 450-MeV Incident Protons as a Function of Depth in Tissue for Z_A = 36 g/cm^2 and Z_{Fe} = 1 g/cm^2.

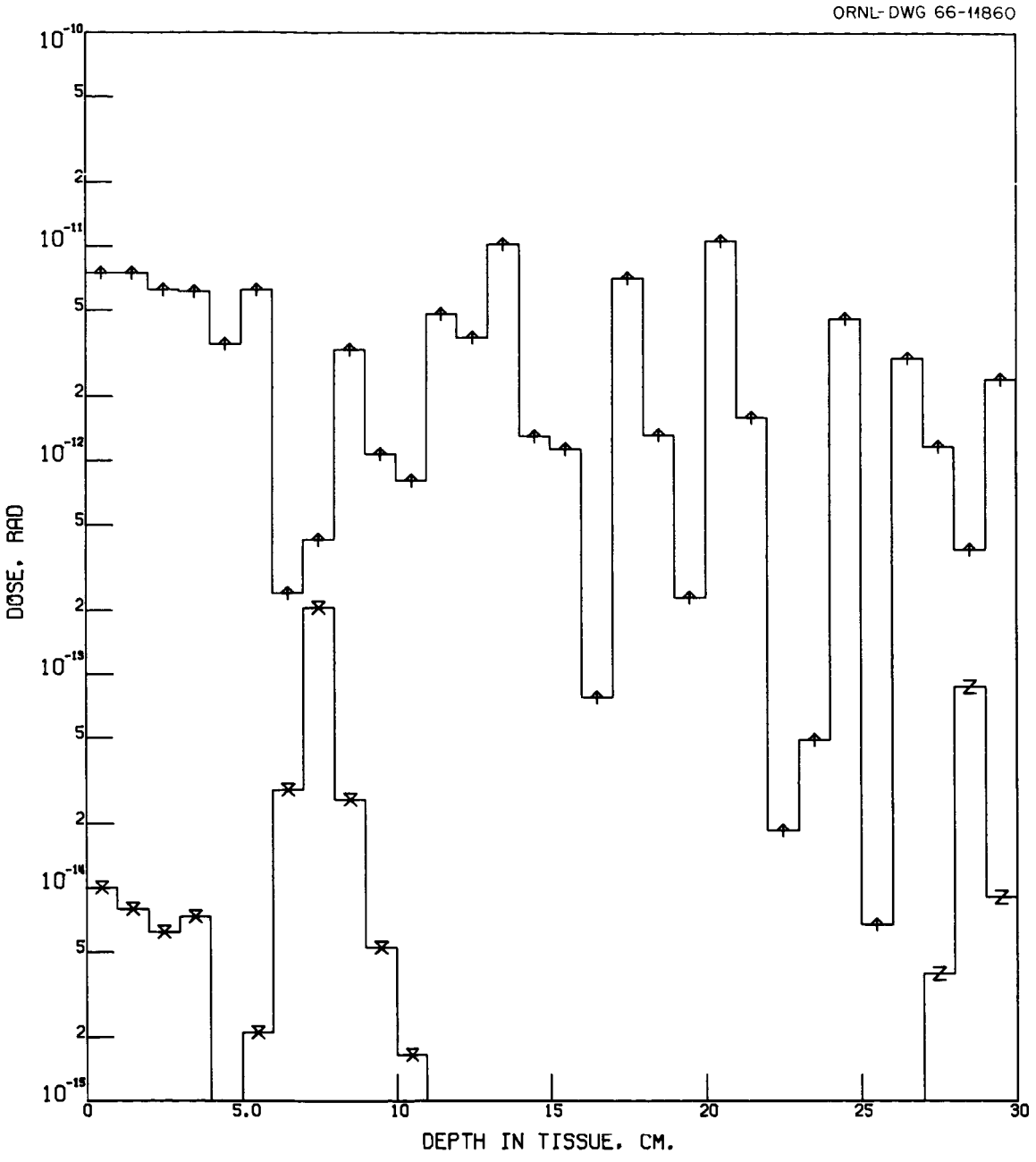

Fig. B33. Rad Dose Due to 50- to 100-MeV Incident Protons as a Function of Depth in Tissue for Z_A = 58 g/cm^2 and Z_{Fe} = 1 g/cm^2.

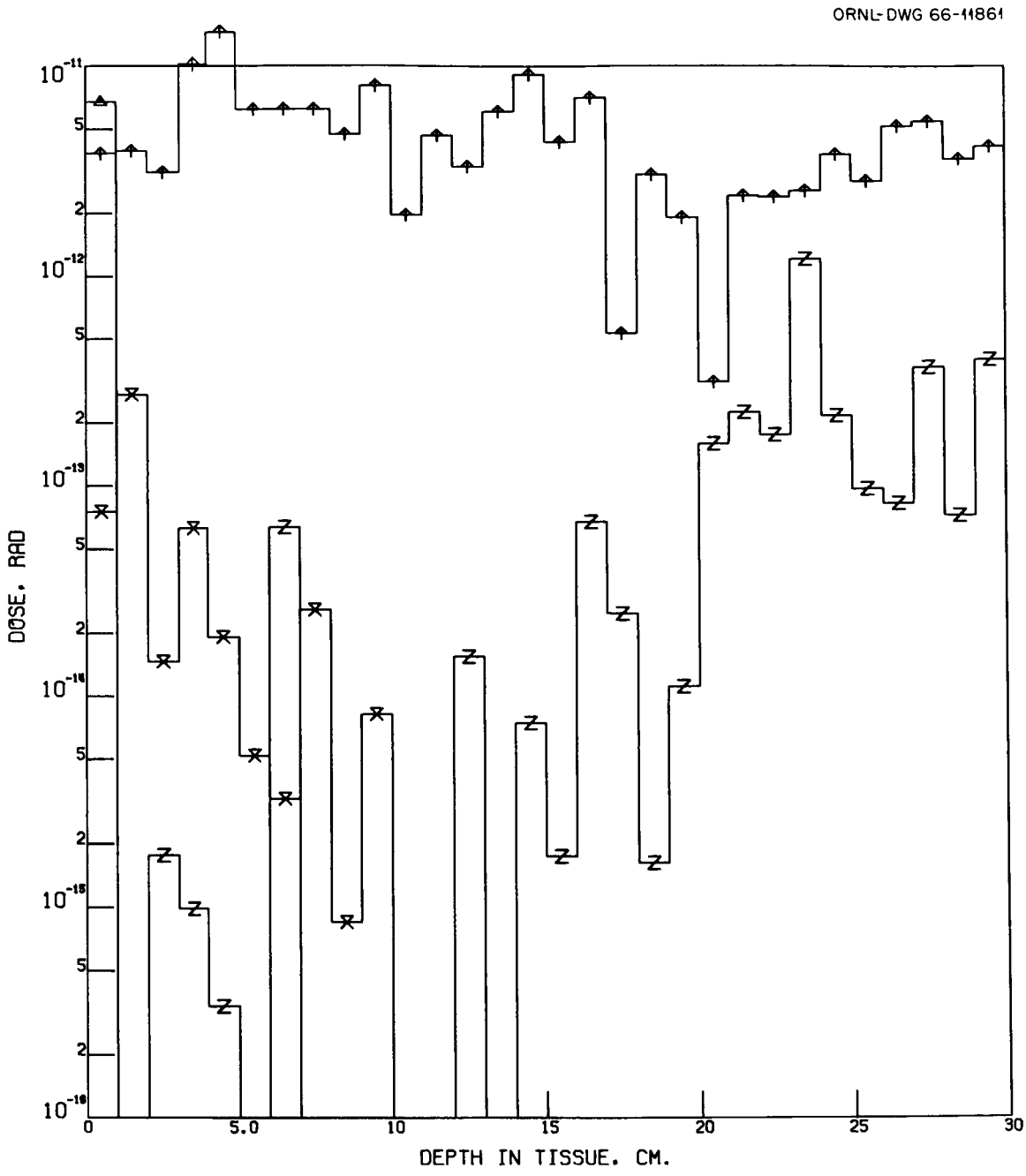

Fig. B34. Rad Dose Due to 100- to 150-MeV Incident Protons as a Function of Depth in Tissue for Z_A = 58 g/cm^2 and Z_{Fe} = 1 g/cm^2.

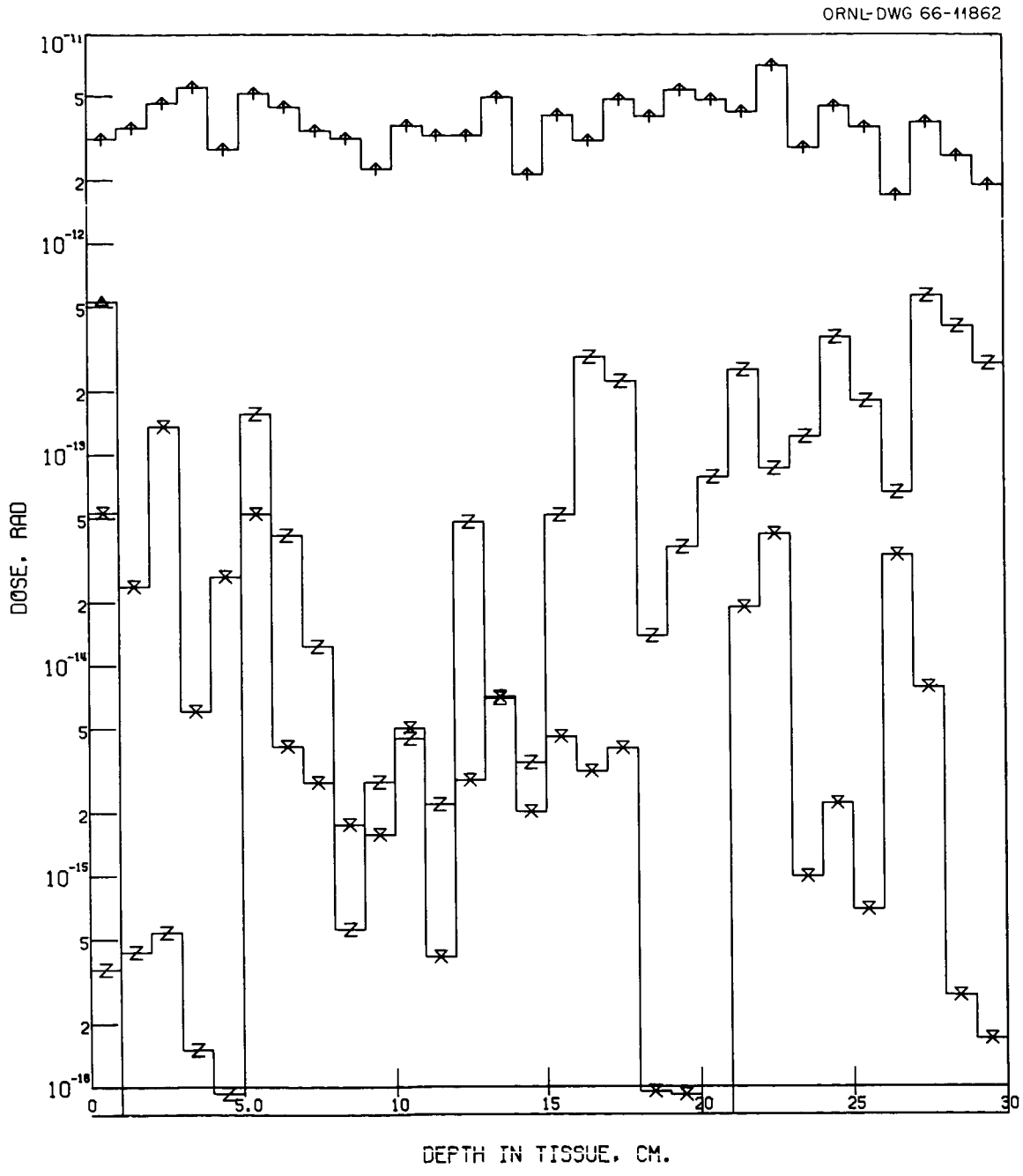

Fig. B35. Rad Dose Due to 150- to 200-MeV Incident Protons as a Function of Depth in Tissue for Z_A = 58 g/cm^2 and Z_{Fe} = 1 g/cm^2.

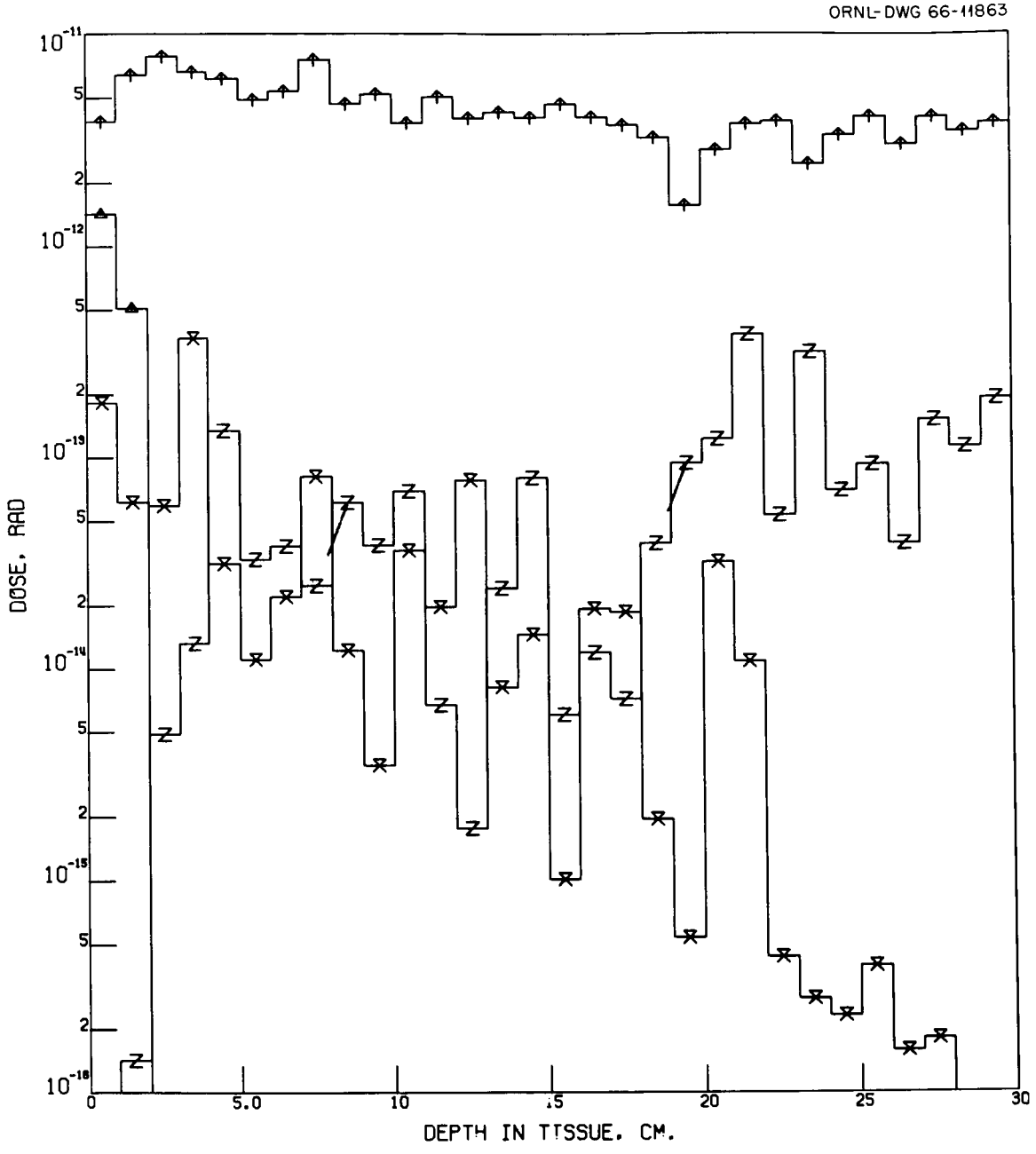

Fig. B36. Rad Dose Due to 200- to 250-MeV Incident Protons as a Function of Depth in Tissue for Z_A = 58 g/cm^2 and Z_{Fe} = 1 g/cm^2.

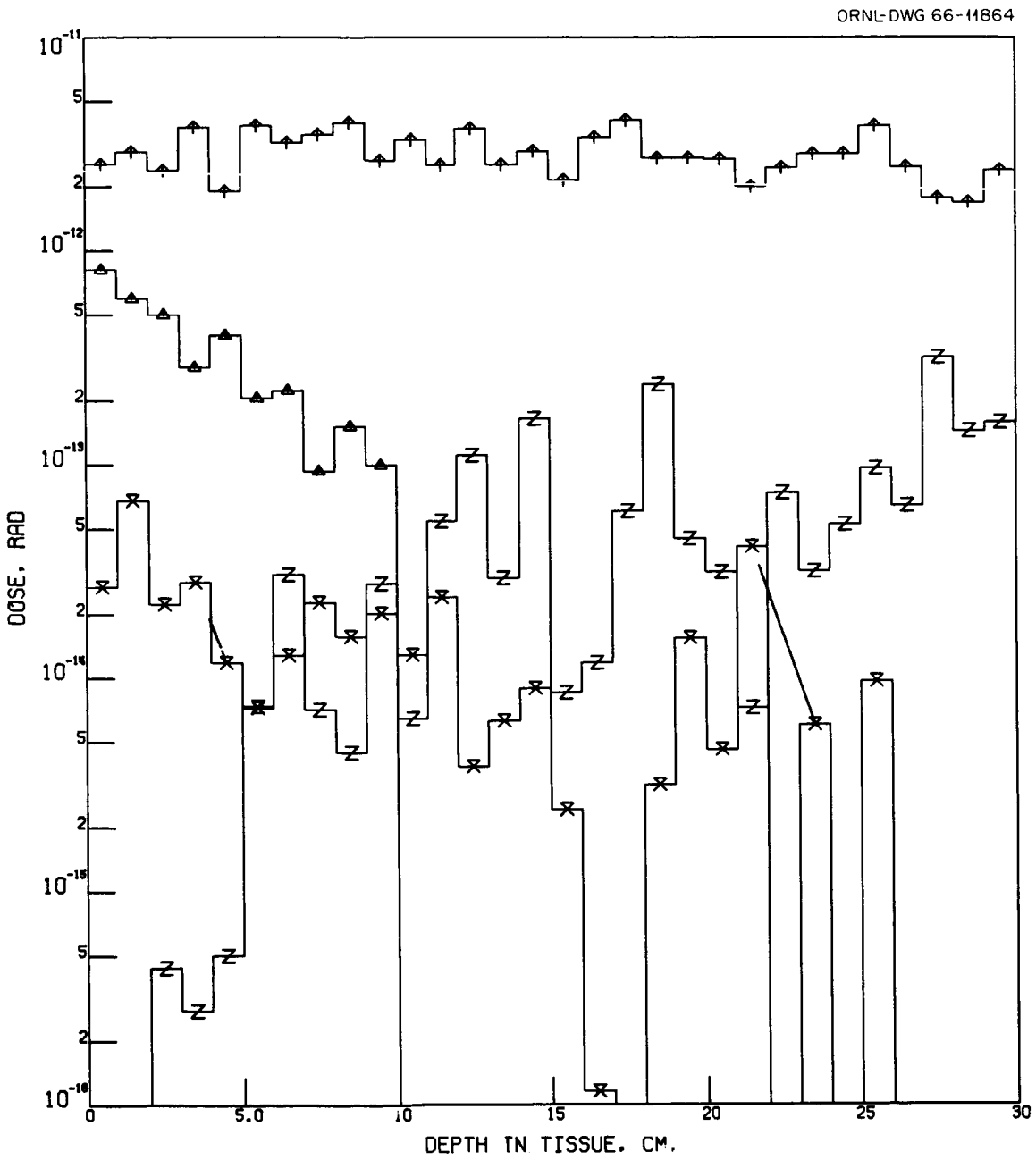

Fig. B37. Rad Dose Due to 250- to 300-MeV Incident Protons as a Function of Depth in Tissue for Z_A = 58 g/cm^2 and Z_{Fe} = 1 g/cm^2.

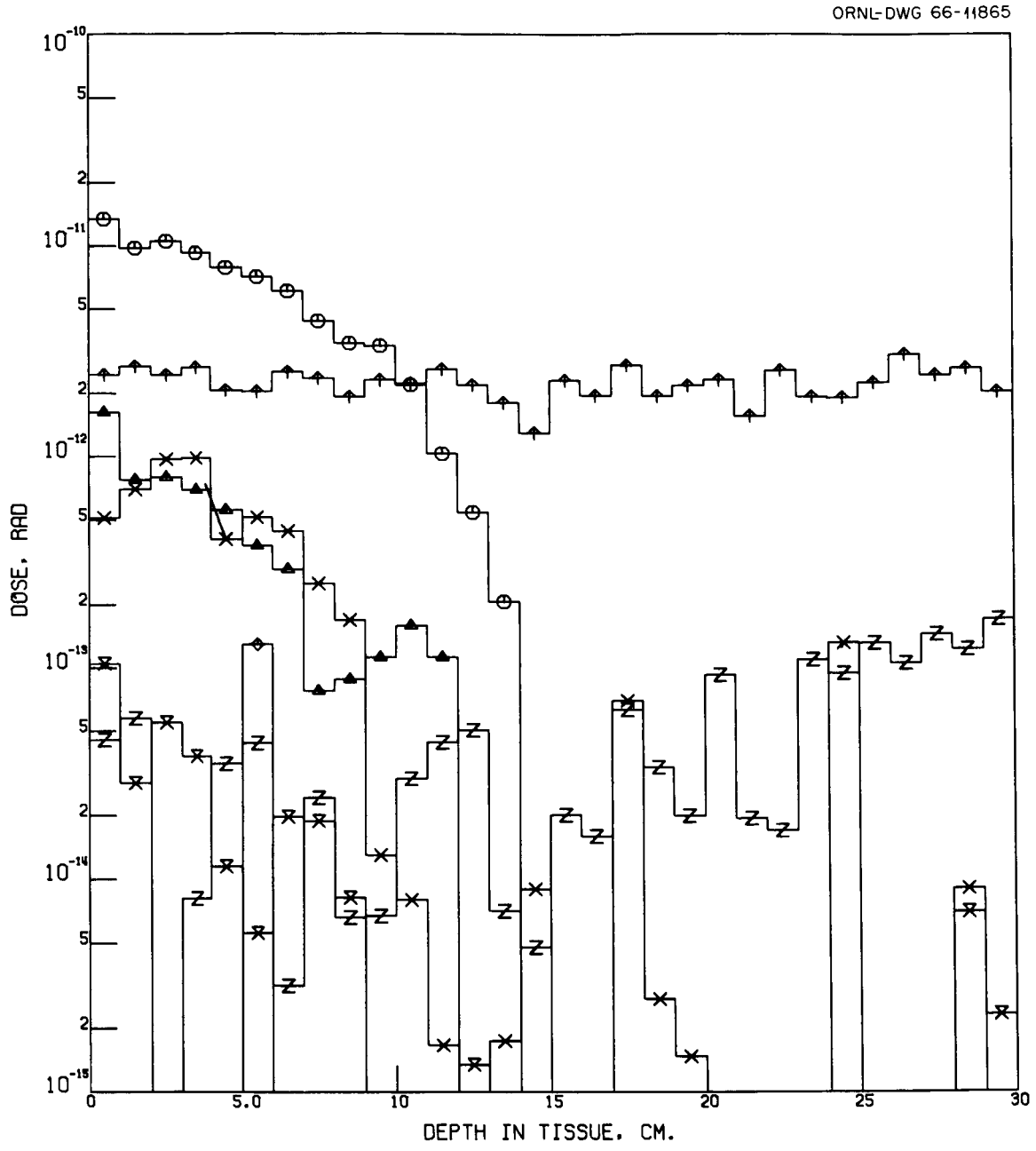

Fig. B38. Rad Dose Due to 300- to 350-MeV Incident Protons as a Function of Depth in Tissue for Z_A = 58 g/cm^2 and Z_{Fe} = 1 g/cm^2.

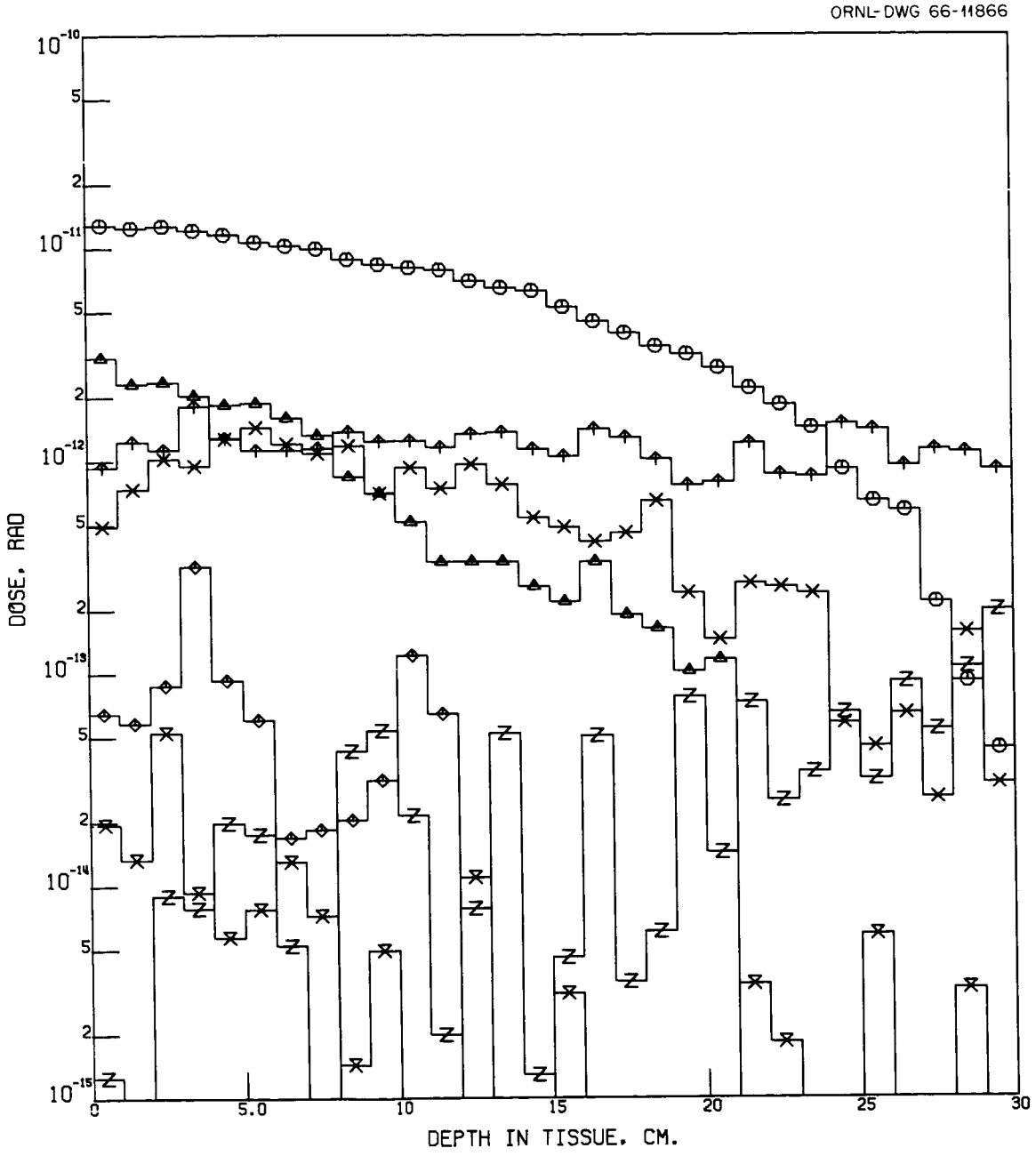

Fig. B39. Rad Dose Due to 350- to 400-MeV Incident Protons as a Function of Depth in Tissue for Z_A = 58 g/cm^2 and Z_{Fe} = 1 g/cm^2.

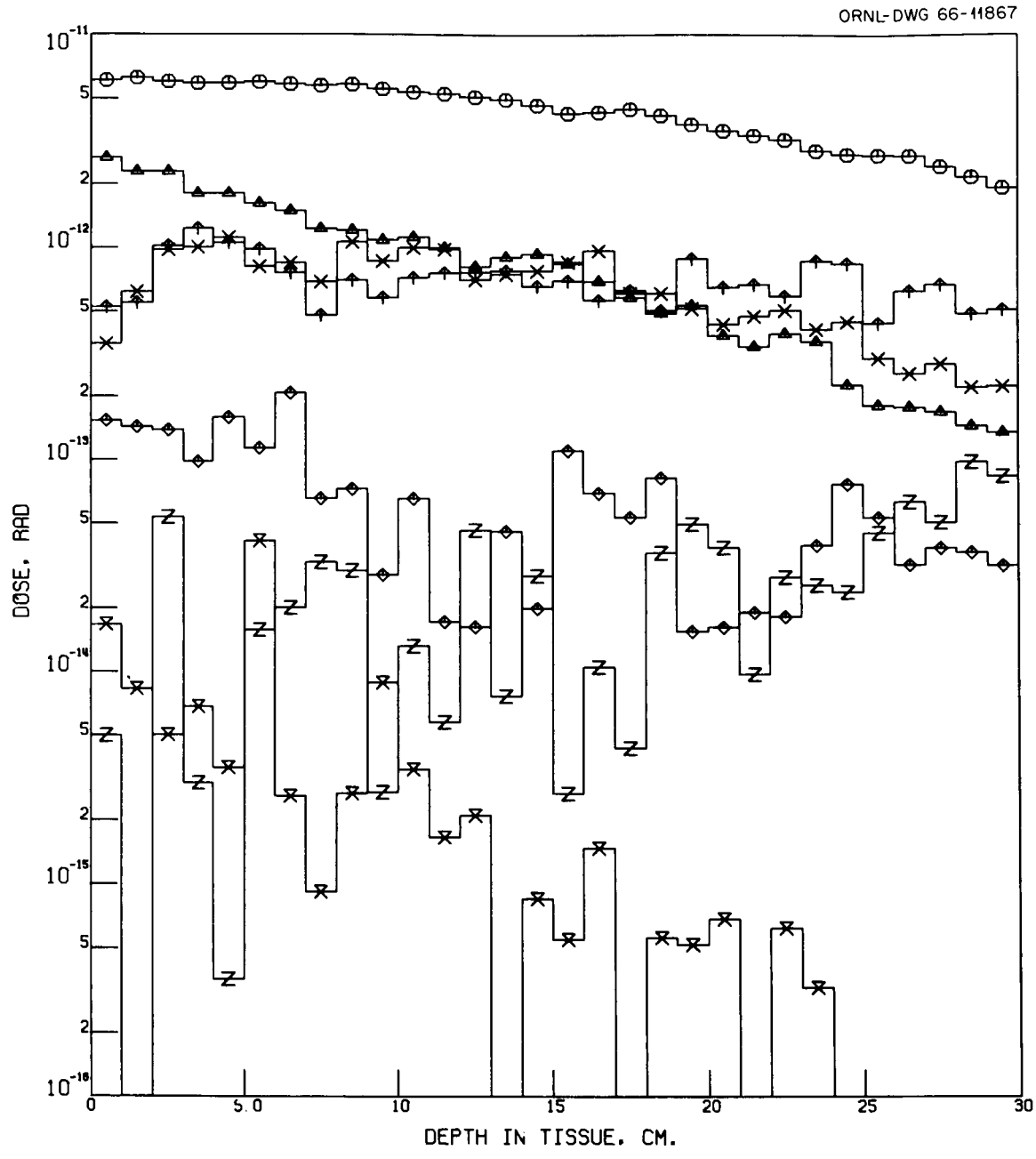

Fig. B40. Rad Dose Due to 400- to 450-MeV Incident Protons as a Function of Depth in Tissue for Z_A = 58 g/cm^2 and Z_{Fe} = 1 g/cm^2.

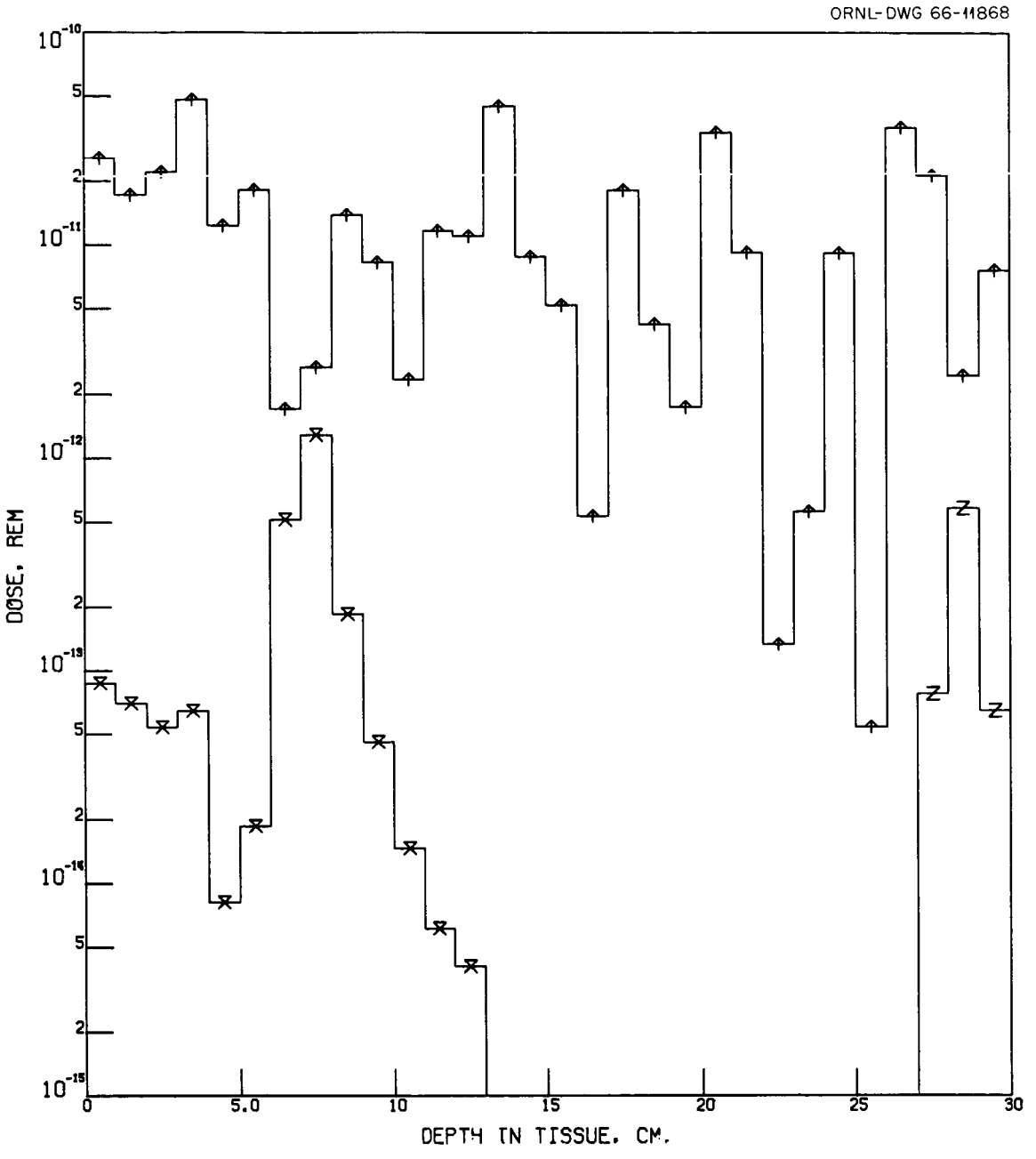

Fig. B41. Rem Dose Due to 50- to 100-MeV Incident Protons as a Function of Depth in Tissue for Z_A = 58 g/cm^2 and Z_{Fe} = 1 g/cm^2.

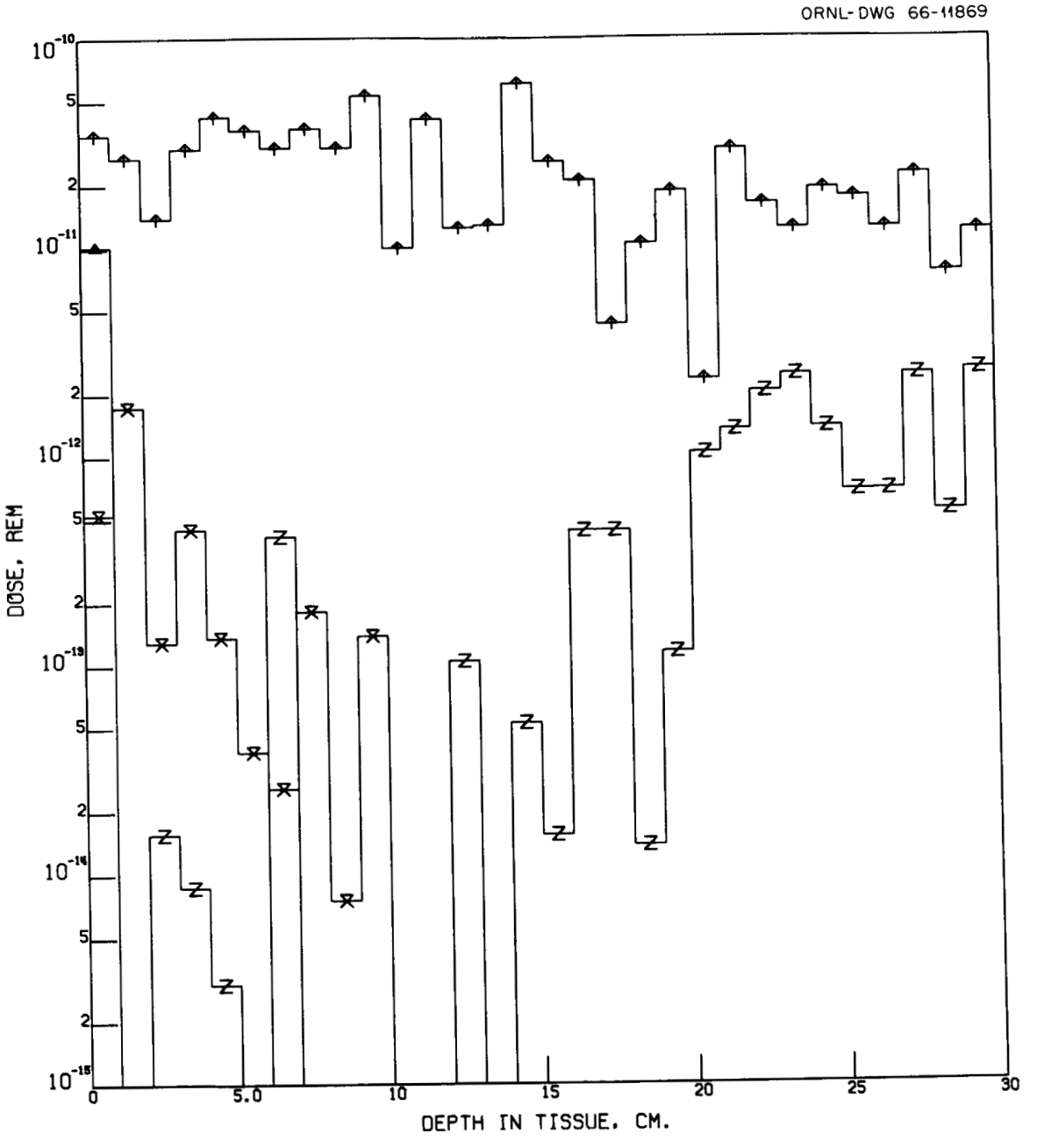

Fig. B42. Rem Dose Due to 100- to 150-MeV Incident Protons as a Function of Depth in Tissue for Z_A = 58 g/cm^2 and Z_{Fe} = 1 g/cm^2.

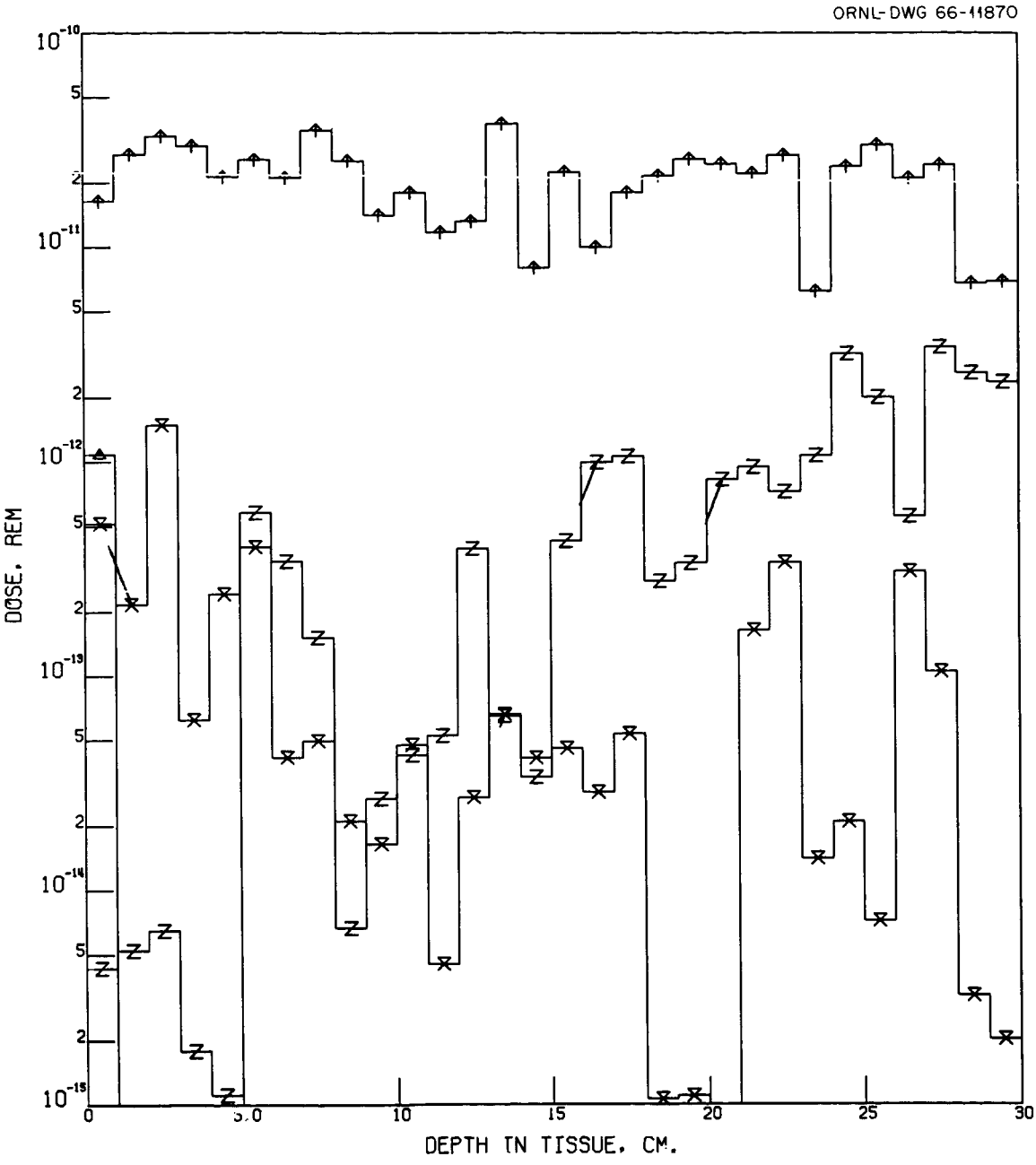

Fig. B43. Rem Dose Due to 150- to 200-MeV Incident Protons as a Function of Depth in Tissue for Z_A = 58 g/cm^2 and Z_{Fe} = 1 g/cm^2.

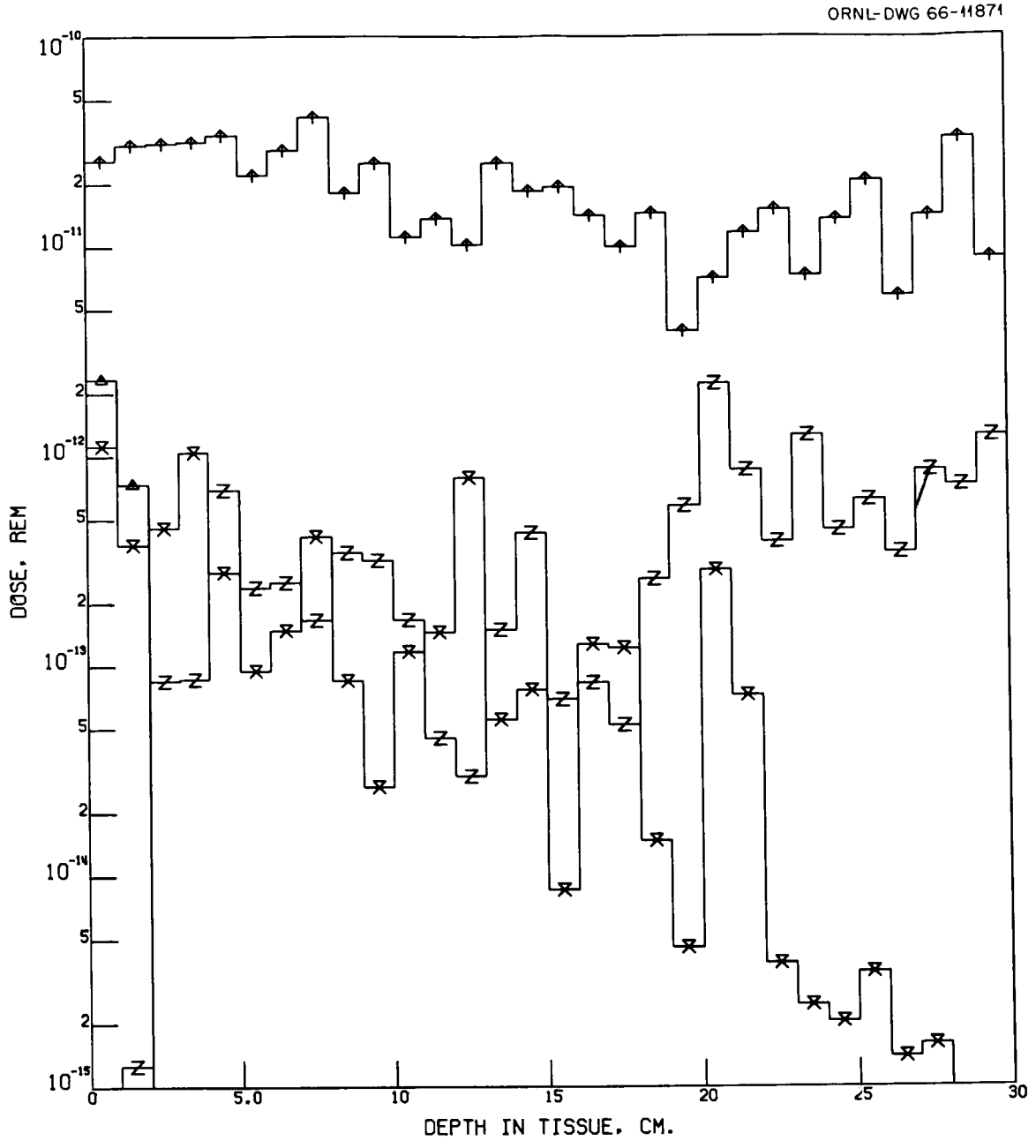

Fig. B44. Rem Dose Due to 200- to 250-MeV Incident Protons as a Function of Depth in Tissue for Z_A = 58 g/cm^2 and Z_{Fe} = 1 g/cm^2.

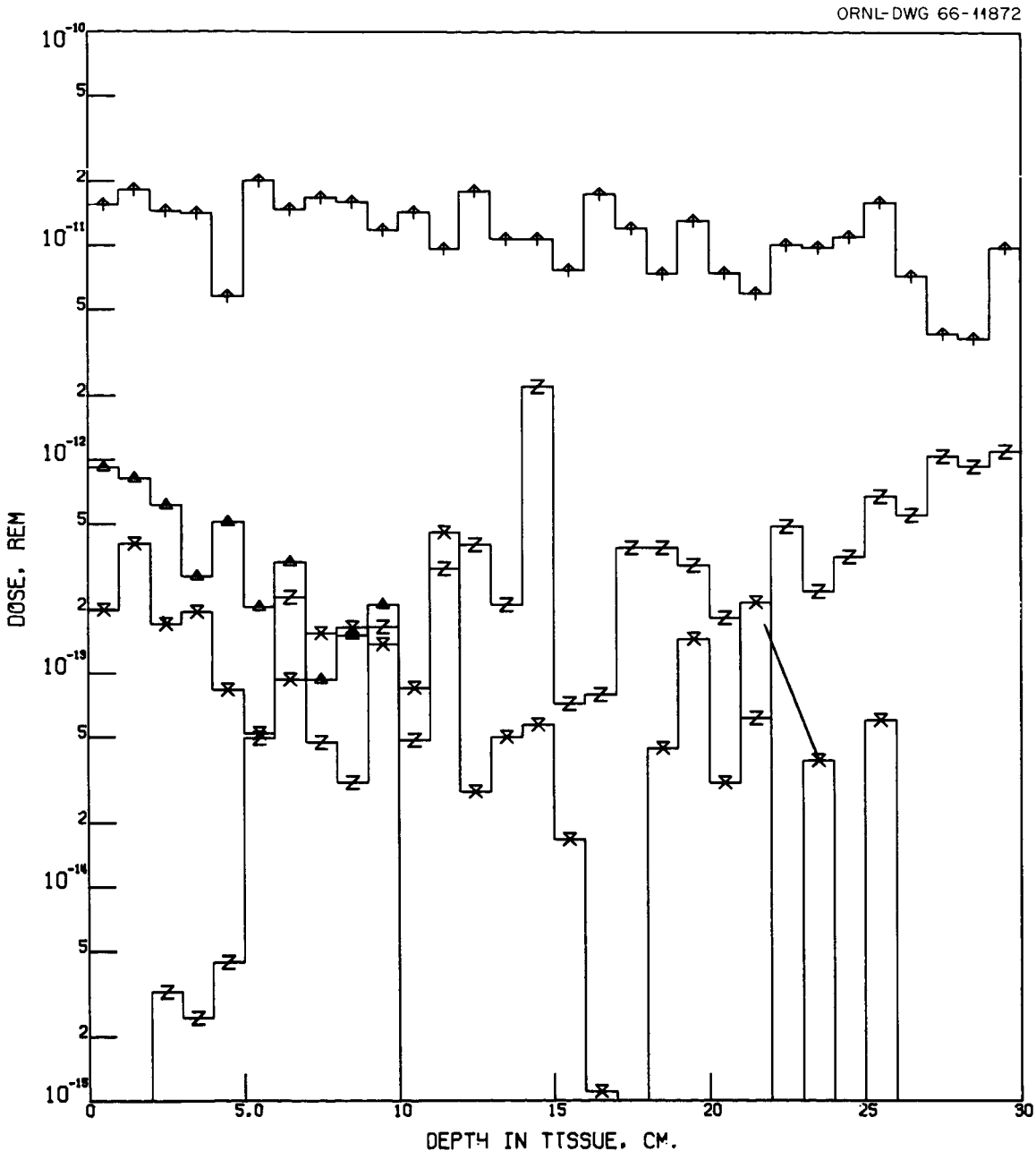

Fig.B45. Rem Dose Due to 250- to 300-MeV Incident Protons as a Function of Depth in Tissue for Z_A = 58 g/cm^2 and Z_{Fe} = 1 g/cm^2.

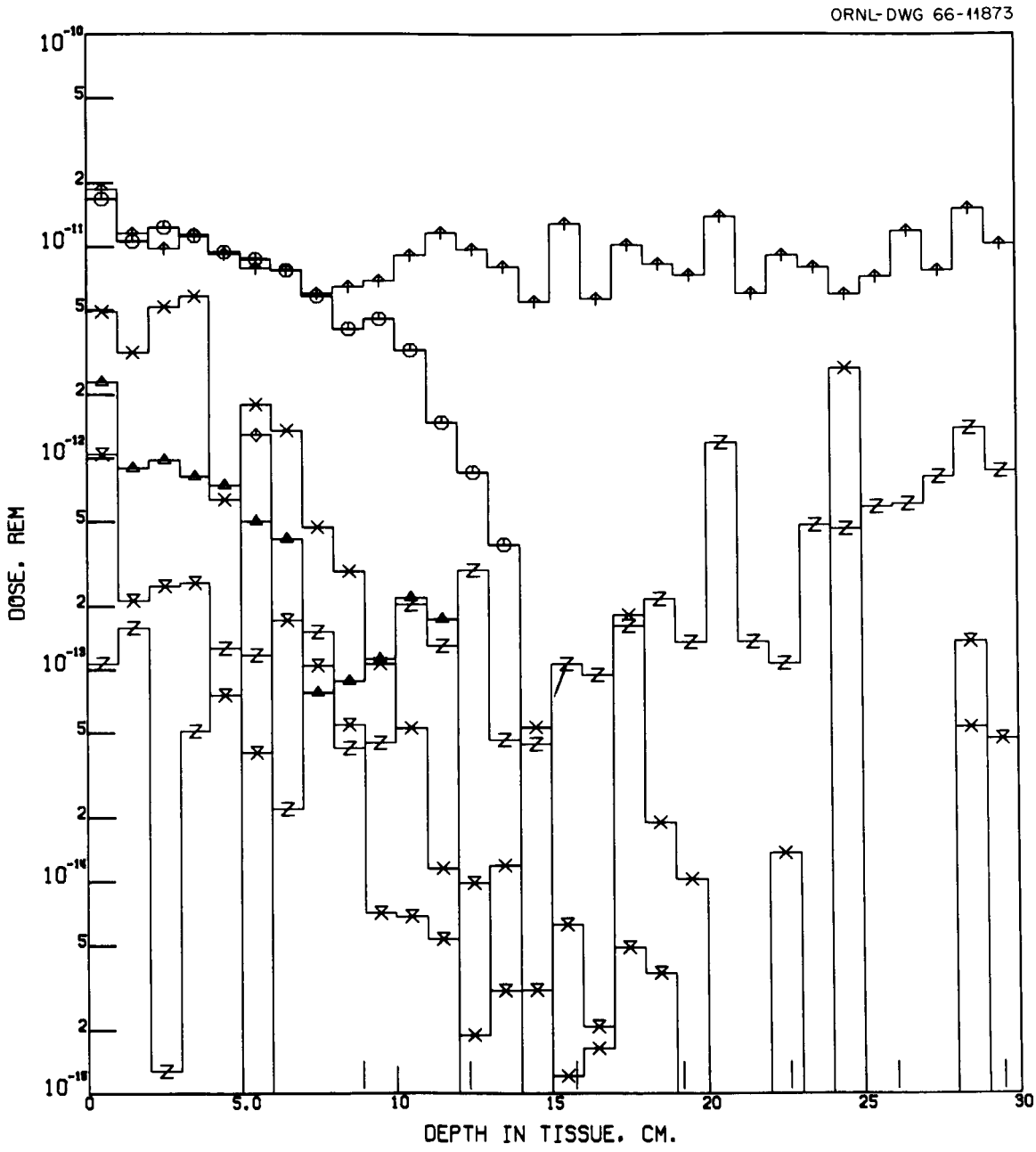

Fig. B46. Rem Dose Due to 300- to 350-MeV Incident Protons as a Function of Depth in Tissue for Z_A = 58 g/cm^2 and Z_{Fe} = 1 g/cm^2.

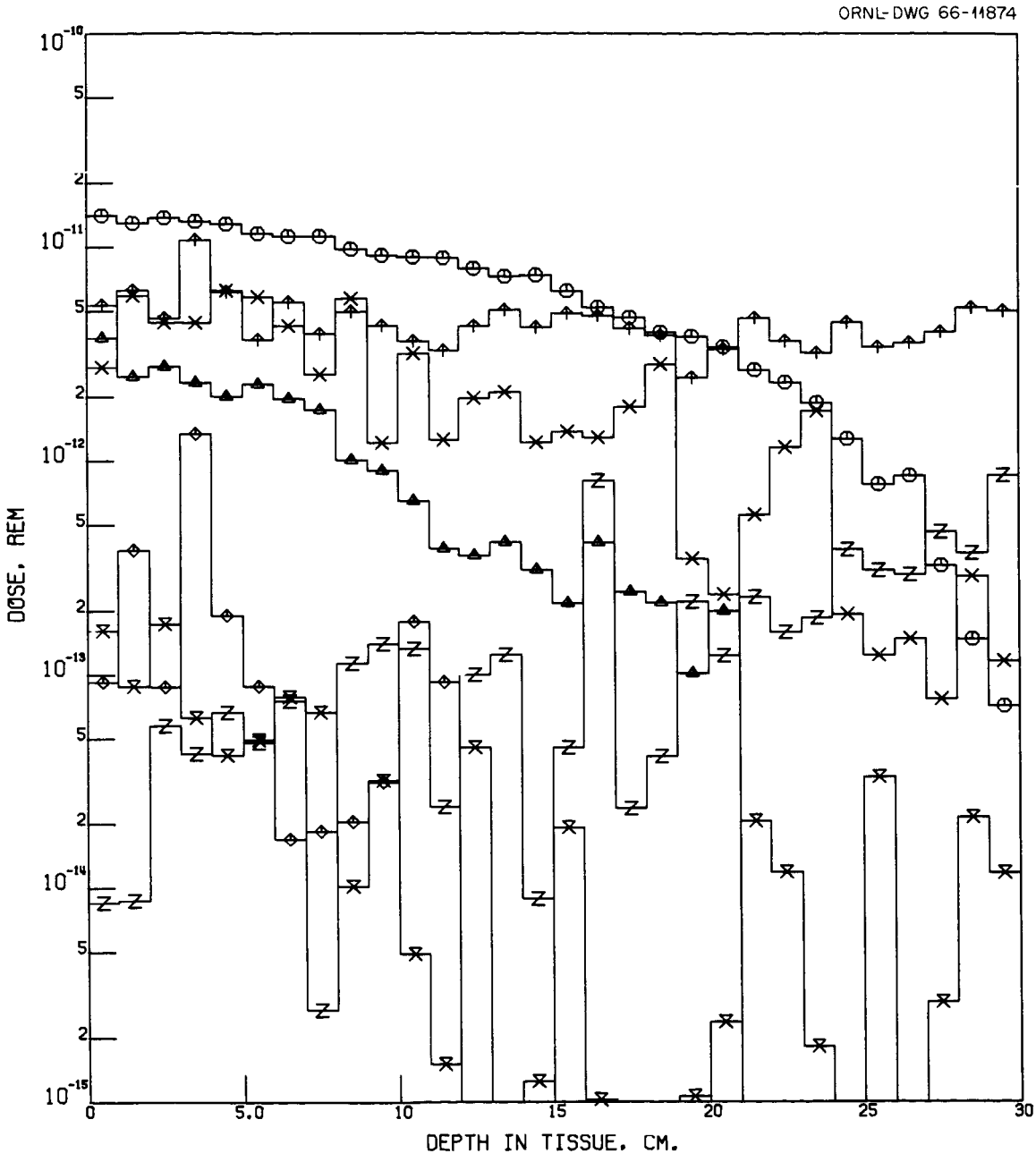

Fig. B47. Rem Dose Due to 350- to 400-MeV Incident Protons as a Function of Depth in Tissue for Z_A = 58 g/cm^2 and Z_{Fe} = 1 g/cm^2.

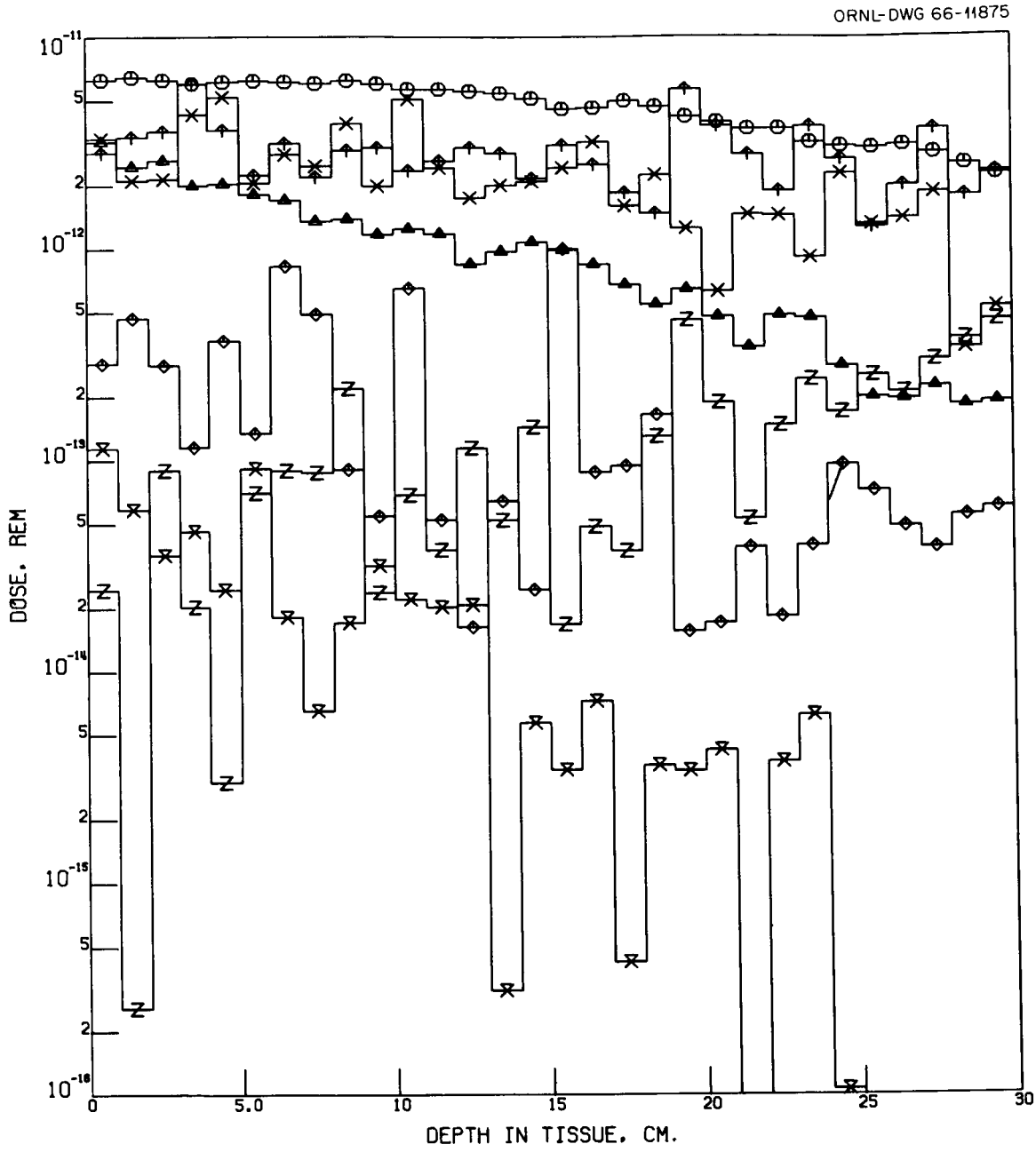

Fig. B48. Rem Dose Due to 400- to 450-MeV Incident Protons as a Function of Depth in Tissue for Z_A = 58 g/cm^2 and Z_B = 1 g/cm^2.

ORNL TM-1594

INTERNAL DISTRIBUTION

1-3. L. S. Abbott
4. F. S. Alsmiller
5-30. R. G. Alsmiller, Jr.
31. H. W. Bertini
32-36. R. T. Boughner
37. W. R. Burrus
38. G. T. Chapman
39. C. E. Clifford
40. W. A. Gibson
41. M. P. Guthrie
42. D. C. Irving
43. D. T. King
44. F. C. Maienschein
45. H. S. Moran
46. R. W. Peelle
47. R. T. Santoro
48. D. K. Trubey
49. V. V. Verbinski
50. J. W. Wachter
51. W. Zobel
52. G. Dessauer (Consultant)
53. B. C. Diven (Consultant)
54. M. L. Goldberger (Consultant)
55. M. H. Kalos (Consultant)
56. L. V. Spencer (Consultant)
57-58. Central Research Library
59. Document Reference Section
60-277. Laboratory Records Department
278. Laboratory Records ORNL RC
279. ORNL Patent Office

EXTERNAL DISTRIBUTION

280-299. Division of Technical Information Extension (DTIE)
300. Division of Research and Development (ORO)